4-1997

The Design and Experimental Optimization of a Wingtip Vortex Turbine for General Aviation Use

Andrew Roberts
Embry-Riddle Aeronautical University - Daytona Beach

THE DESIGN AND EXPERIMENTAL OPTIMIZATION

OF A WINGTIP VORTEX TURBINE FOR GENERAL AVIATION USE

by

Andrew Roberts

A Thesis Submitted to the
Office of Graduate Programs
in Partial Fulfillment of the Requirements for the Degree of
Master of Science in Aerospace Engineering

Embry-Riddle Aeronautical University
Daytona Beach, Florida
April 1997

THE DESIGN AND EXPERIMENTAL OPTIMIZATION

OF A WINGTIP VORTEX TURBINE FOR GENERAL AVIATION USE

by

Andrew Roberts

This thesis was prepared under the direction of the candidate's thesis committee advisor, Prof. Charles N. Eastlake, P.E., Department of Aerospace Engineering, and has been approved by the members of his thesis committee. It was submitted to the Office of Graduate Studies and was accepted in partial fulfillment of the requirements for the degree of Master of Science in Aerospace Engineering.

THESIS COMMITTEE:

Prof. Charles N. Eastlake, P.E.
Advisor

Dr. David Kim
Member

Dr. Vicki Johnson
Member

Dr. David Kim
MSAE Graduate Program Chair

Dr. Allen Ormsbee
Department Chair, Aerospace Engineering

4/15/97
Date

ACKNOWLEDGEMENTS

I would like to express special thanks to my thesis advisor, Prof. Charles Eastlake for his unwavering guidance and advice, good-natured experiential storytelling, and his Piper Cherokee as the subject basis in the preparation and research for this thesis. Appreciation and thanks go out as well to Committee Members Dr. David Kim and Dr. Vicki Johnson, Shop Technician Don Bouvier, Electronics Wizard Mike Potash, and KOMO CNC Milling Machine Operator Extraordinaire Alfred Stanley for their superior technical support and assistance.

A special thank-you is also expressed to the late Dr. Ernest Jones, my initial thesis advisor, for without his initial support and enthusiasm this project would never have gotten off the ground.

I would especially like to thank my family for putting up with my moodiness this semester and always being there to give me words of encouragement at all hours of the day and night.

Finally, I want to thank my friends David, Eric, Richard, and Michelle, and all of my fellow students for their e-mail, jokes, late-night mayhem, sound files of questionable content, kindness, and constant support and interest in my work. I couldn't have done it without you.

ABSTRACT

Author: Andrew Roberts

Title: The Design and Experimental Optimization of a Wingtip Vortex Turbine for General Aviation Use

Institution: Embry-Riddle Aeronautical University

Degree: Master of Science in Aerospace Engineering

Year: 1997

A wingtip vortex turbine (WVT) is an induced drag reduction device that straightens the vortex flow (reducing induced drag and wake turbulence) and also produces a thrust force component. The WVT also has the advantage of extracting the rotational energy of the vortex to turn a generator, which could be used to power onboard applications during normal or emergency flight operations. A 1/4-scale model of a thrust-producing WVT has been designed and tested in a wind tunnel for optimal drag reduction and power generation for general aviation aircraft -- specifically, a Piper Cherokee -- in both a stationary and a rotating mode. In addition, 2, 3, 4, 5, and 6-bladed configurations were tested, over a pitch angle range of -35° to 0°. The 6-bladed configuration proved to be the most efficient at both reducing drag and generating maximum power. At cruise, this model was shown to increase the overall drag slightly by 40 to 60 counts. However, at lift coefficients greater than 0.8, the overall drag was reduced by 20 to 40 counts, depending on whether it was stationary or rotating. At cruise, it generated a power coefficient of 0.004, and a maximum of 0.0059 at a C_L=0.85. These coefficients corresponded to full-scale power outputs of 4.5 hp and 6.7 hp, respectively.

TABLE OF CONTENTS

LIST OF TABLES

LIST OF FIGURES

CHAPTER 1

INTRODUCTION

1.1 OVERVIEW

In aircraft design, it is of great interest to minimize the drag force that results from skin friction, adverse pressure gradients, flow interference between major component surfaces, and induced drag. The first three sources are functions of aircraft surface smoothness, geometry, and manufacturing techniques that are in turn dependent upon the aircraft mission requirements. The latter source, induced drag, is a function of the lift required to keep the airplane aloft, and varies with such parameters as aircraft weight, wing area, altitude, and forward velocity -- that is, all of the factors that affect the required lift coefficient for a given flight condition.

When a wing creates lift, the pressure differential between the upper and lower surfaces causes the air to flow in a spanwise manner around the tip. This motion forms a swirling pattern, or vortex, at the wingtip that continues to circulate downstream. These tip vortices create a significant downwash behind the wing which effectively decreases the angle of attack, thereby tilting the lift vector rearward relative to the flight path. The lift vector can then be resolved into vector components of effective lift and induced drag. For a typical transport category aircraft, the induced drag constitutes approximately 10 to

15 percent of the total drag in cruising flight, and as much as 35 to 40 percent when operating at higher lift coefficients [1].

In addition, wingtip vortices are also a cause for concern in terms of air safety, especially in high-traffic areas where aircraft are taking off or landing in short time intervals. Vortices can be extremely powerful, especially when produced by a heavy transport operating at a high lift coefficient as is the case during takeoff and landing. Moreover, in the case of heavy transport aircraft, vortices often linger downstream of the flight path for distances of 2 miles before they begin to undergo serious viscous breakdown [2]. Research has shown that smaller aircraft following a heavy transport can be subjected to rolling moments which exceed the aircraft roll control authority, and result in dangerous loss of altitude, and/or possible structural failure.

In order for an aircraft to generate lift, these vortices are necessary to complete the total circulation pattern formed by the bound vortex of the wing and the starting vortex downstream. The case often illustrated in inviscid fluid concepts is that in which vorticity cannot begin or end, which is also true in the viscous, relative near-field flow of an aircraft. Therefore, in practice wingtip vortices cannot be eliminated completely, but can be reduced in size and strength after their formation by various means.

One device, developed by NASA's Richard Whitcomb that has been used extensively to do this is the winglet -- a small, stationary wing-like surface that extends into the vortex flow near the wing trailing edge. The winglet was designed solely to increase efficiency by two means. First, it simply acts as a stator, or flow straightener to suppress the vortex swirl, thus reducing the downwash, and consequently induced drag.

Secondly, as the air flows over the winglet at some angle of attack (due to the combination of the aircraft's forward velocity and the vortex's rotational velocity), it produces a lift vector perpendicular to the local flow, forming a significant thrust component while its own contribution to the total drag is rather negligible. Initial high subsonic wind tunnel tests of winglets on a jet transport resulted in a total ΔC_D=-0.0015 at the design condition of Mach 0.80 and a lift coefficient of 0.53. A comparison of this increment with the estimated induced drag coefficient of the wing suggested that the winglets reduced the induced drag by about 13 percent [3]. The development of many other drag-reducing devices followed, such as endplates, tip sails, splines, and so on with varying degrees of success.

Wingtip vortices represent not only the cause of induced drag, but more generally a loss of lift energy that would otherwise be present in the case of an infinite aspect ratio wing. For these reasons, the wingtip vortex turbine (WVT), the subject of this research, deserves at least as much attention as the winglet. The WVT (see Figure 1.1) operates on the same principle as the winglet as a stationary device in straightening the vortex flow (thereby reducing induced drag and wake turbulence) and also in producing a thrust force component. However, unlike winglets and other fixed devices, the WVT can operate in a rotating mode where the rotational energy from the vortex is extracted to turn a generator, which could be used to power avionics, electric flight control systems, or other onboard applications during normal or emergency flight operations. Interestingly, it has also been thought that the WVT could be used to drive pumps for a boundary layer control system [1].

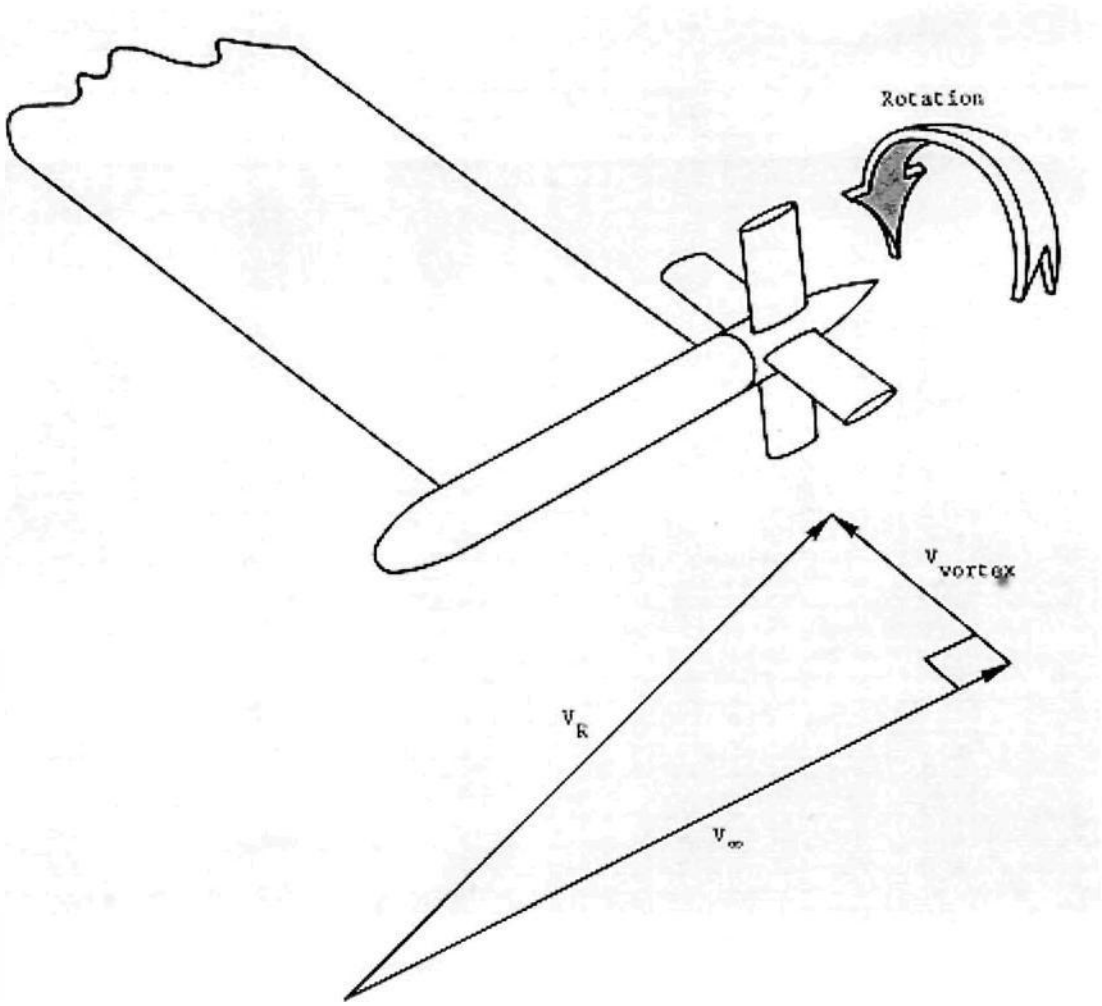

Figure 1 1 General Configuration of a Wingtip Vortex Turbine [1]

1.2 PREVIOUS RESEARCH

In the mid 1980's and early 90's, engineers led by Claude Patterson of NASA's Langley Research Center conducted basic, proof-of-concept research on the use of WVT's through wind tunnel and flight tests. In short, all of the test results proved that the WVT accomplished what it was designed to do -- reduce induced drag and generate rotational shaft energy

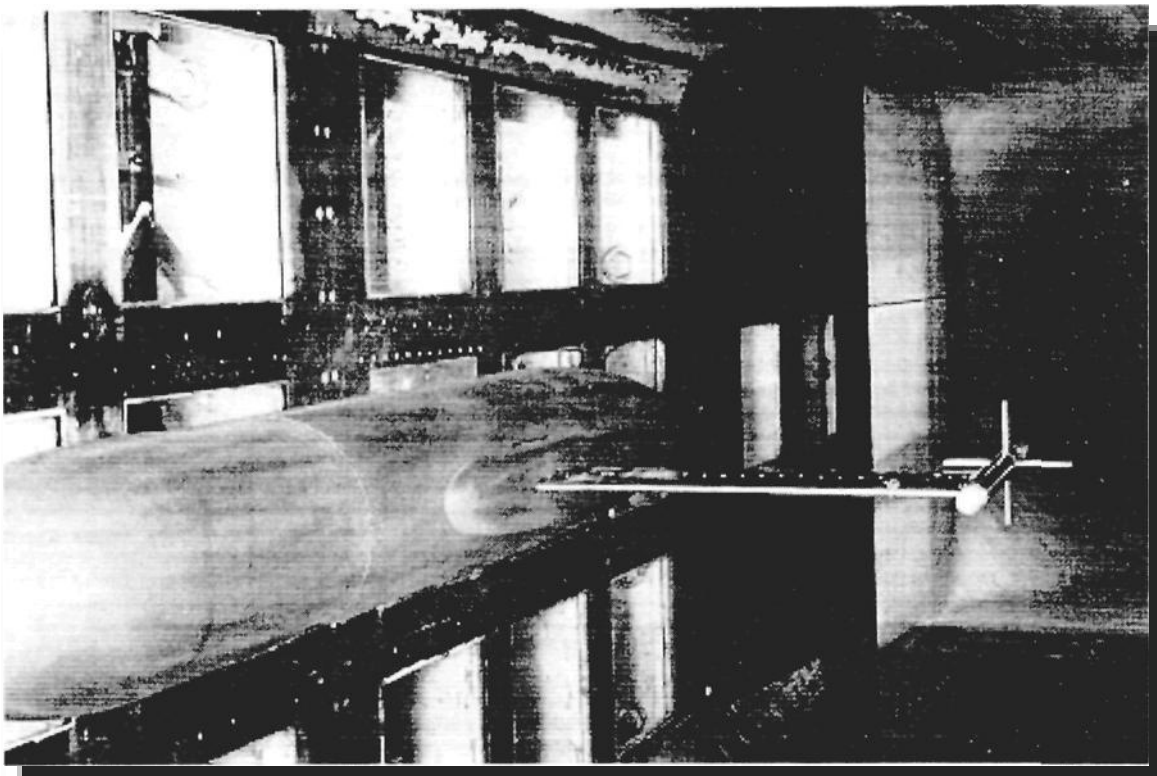

Figure 1.2 NASA Langley Wind Tunnel Test of a Wingtip Vortex Turbine [1]

1.2.1 WIND TUNNEL TESTING OF THE WVT

Wind tunnel tests were conducted at the Langley 8-Foot Transonic Pressure Wind Tunnel, at Mach 0.70. The model was a semi-span airplane with an unswept, untapered wing using a NACA 64_1A012 airfoil, with and without a WVT attached (see Figure 1.2). The WVT itself consisted of a non-rotating nacelle mounted on the wingtip, and a rotating hub holding four blades. The nacelle also housed a variable-load clutch mechanism to impose a torque load on the turbine so that power output could be measured while it rotated. The WVT was tested in both rotating and non-rotating modes.

Three sets of turbine blades were tested to determine the effects of airfoil shape and planform: cambered/untapered, symmetrical/untapered, and symmetrical/tapered. Turbulent boundary layer conditions were simulated by applying 0.125" wide, No. 120 carborundum grains at the 5.4 percent chord position on the upper and lower surfaces of the wing, and at the 5.5 percent chord position of the WVT blades.

In terms of induced drag reduction, the symmetrical/tapered WVT configuration showed the greatest reduction from the baseline wing, ranging from ΔC_D=-0.002 at C_L=0.3 and C_{Dtot}=0.018, to ΔC_D=-0.005 at C_L=0.4 and C_{Dtot}=0.022. Neither of the untapered WVT configurations showed any significant drag reduction until C_L=0.3, with the maximum reduction of ΔC_D=-0.002 occurring at C_L=0.4 and C_{Dtot}=0.0235. This was a significant result which meant that most of the vortex straightening came from the inboard portions of the blades where the vortex's angular velocities are always the highest. In addition, the added outboard blade area on the untapered blades appeared to have a negative effect on drag reduction. In all cases however, the non-rotating WVT reduced drag additionally by approximately 3 drag counts (1 drag count = ΔC_D of 0.0001) compared to the rotating WVT [1]. This was presumably due to the lower relative angular velocities between the vortex and the rotating blades, thus resulting in less vortex flow straightening and slightly higher induced drag. Notably, the blades tested were all untwisted, and were all oriented with zero incidence relative to the WVT nacelle centerline. This would further imply that the WVT's tested reduced the induced drag more from the standpoint of flow straightening, rather than production of a thrust component.

In terms of rotational power generated, the choice of airfoil for the blades was the governing factor. The cambered/untapered WVT configuration produced significantly higher output with the power coefficient C_P varying between 0.00035 and 0.00085 for C_L=0.18 to 0.45, respectively. Both of the symmetrical airfoil blade configurations produced a much lower C_P varying between approximately 0.00008 and 0.0005 for the same range of lift coefficients. The untapered/symmetrical configuration did have a slight power edge over the tapered/symmetrical configuration with a ΔC_P of +0.000025 at all lift coefficients. This would imply that the extra outboard blade area does aid slightly in power provision owing to the greater moment arm distance from the WVT axis of rotation [1].

Figure 1.3 Flight Test of Wingtip Vortex Turbines on a Piper Turbo Arrow IV [4]

1.2.2 FLIGHT TESTING OF THE WVT

Flight tests of WVT's were conducted on a Piper PA-28 Turbo Arrow IV (see Figure 1.3) at typical cruising conditions of 140 mph and C_L=0.325. The overall WVT

configuration used was very similar to that used in the wind tunnel tests. However, two sets of variable-pitch blades were used -- both with planform taper and cambered airfoil sections, but one with zero twist and the other with $+15^{o}$ of twist (root at 0^{o} incidence, tip at $+15^{o}$ incidence) to compensate for the lower vortex angular velocities outboard near the blade tips [4]. Both were tested in the rotating mode, but only the untwisted blades were tested in the non-rotating mode since it was likely that the twisted blades would have stalled if not allowed to rotate.

In both the rotating and non-rotating modes, there was a reduction in total drag for blade pitch angles of less than 2.5^{o}. The ΔC_D reached a maximum at -4.5^{o} pitch of -0.0022 for the non-rotating mode, and -0.0016 at -4^{o} pitch for the rotating mode. An increase or decrease in pitch angle from these optimum angles led to a decrease in magnitude of ΔC_D, indicating that the vortex flow was still being straightened but that perhaps the inboard or outboard portions of the blades had stalled and were not turning the flow at peak efficiency.

In the free-rotating condition (no load applied), the twisted-blade WVT rotated at a maximum of 500 to 600 RPM. However, it was tested for power output at one-half of this maximum rotational speed (300 RPM) since previous analysis had shown that the WVT develops nearly maximum power under this loading [1]. Interestingly, the WVT developed a minimum of 2 horsepower at -4^{o} pitch, but a maximum of 6 horsepower at $+4^{o}$ pitch. This would imply that the blades operated at higher lift coefficients to generate greater torque and horsepower, but might also have at least partially stalled, and/or were

generating a significant amount of induced drag of their own, resulting in the increase in total drag at the higher pitch angles.

1.3 CURRENT RESEARCH

Although the previous research on WVT's has been quite comprehensive in itself, they have only been tested on a rather simple, proof-of-concept basis. The aforementioned test results indicate that induced drag can certainly be reduced and significant shaft power generated, but only as trade-offs to one another. The question then arises, can WVT blades be designed such that these two objectives are met for a given incidence angle and set of flight conditions? In this author's opinion, the blades tested to date have been designed somewhat arbitrarily with little detailed regard for the complexities of vortex flow.

Therefore, the goal of this research was to experimentally and analytically develop, design, and wind tunnel test a 1/4-scale WVT model that would be optimized for drag reduction as the primary objective and power generation as a secondary objective. It should be noted that in previous research, the emphasis for drag reduction was placed on straightening the vortex flow. Since this concept was already proven to be effective, the research for this thesis was instead focused on maximizing the thrust force component from the WVT blades assumed that some flow straightening would result anyway. This was decided simply because an analysis of flow straightening would be difficult, perhaps impossible, to quantify and predict analytically, and might require the

use of CFD analysis which was determined to be beyond the desired scope of this research.

The WVT in this research was designed around the cruise conditions since most aircraft spend the majority of their airborne life in this mode. Because it was designed to fit on the wingtips of light aircraft, the WVT's overall size and internal volume is small, thus limiting the mechanical complexity to allow only for design and testing of fixed-incidence blades. In practice, the full-scale WVT would probably have manually-adjustable blades so that the aircraft owner could "tweak" the incidence for more thrust or more power, whichever would be more desirable to the user. Fortunately, this inherent mechanical simplicity would also keep the cost of WVT's to a minimum which is an all-important factor for general aviation aircraft owners.

Typically, WVT's would be used on larger transport category aircraft since the potential advantages would be much greater, given the higher vortex strength produced. However, since the Embry-Riddle low-speed wind tunnel is limited to low Reynolds number testing, as well as the fact that the thesis advisor had expressed some interest in testing a full-scale WVT as a follow-on thesis, this research was conducted using a 1/4-scale, semi-span Piper Cherokee wing as the basis for experimentation. This would also allow for very direct performance data comparisons between this WVT model and the full-scale WVT's flight tested previously. The wing model was constructed of a white foam core with a plywood spar, and coated with a single layer of light fiberglass. It had a 15.75" chord, a 27" semi-span, and used a NACA 65_2-415 airfoil with 2^{o} of washout. An endplate was attached to the far end of the wing to simulate connection to the fuselage. A

0.016" thick by 0.125" wide trip strip was applied to the upper and lower surface at the 10% chord point to simulate typical full-scale surface roughness. The entire wing was painted flat gray to aid in flow visualization as well as to provide a matte surface for uniform roughness.

Unless otherwise noted, all testing was completed in the subsonic wind tunnel at Embry-Riddle Aeronautical University at a freestream velocity of 93.5 ft/sec, which corresponds to a chord Reynolds number of approximately 750,000. The cruise lift coefficient for the Piper Cherokee was calculated to be 0.36, based on gross weight (2150 lb) cruise conditions of 130 mph at 5000 ft. This C_L corresponds to a geometric angle of attack of 2° according to the baseline wing lift curve shown in Figure 1.4, and was the angle used for all subsequent WVT analysis and testing.

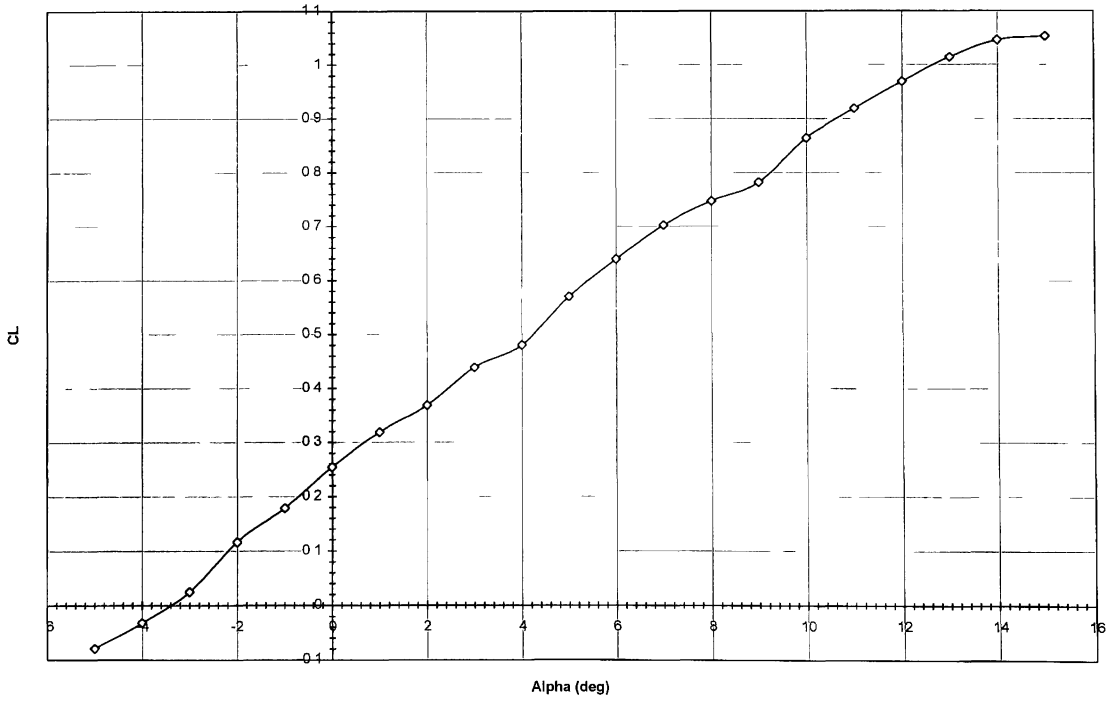

Figure 1.4 Lift Coefficient vs. Angle of Attack for Piper Cherokee Semi-Span Model

CHAPTER 2

BACKGROUND THEORY

2.1 VORTEX THEORY

Early in the WVT design process, it was hypothesized that the blade twist distribution would have to match, or nearly match the vortex flow angle distribution so that each section of the blade would be oriented relative to the flow to produce maximum thrust. This required determination of vortex flow parameters such as flow angle, axial velocity (V_x), tangential velocity (V_z), and the vortex centerline location. All of these parameters were measured experimentally, but initially were predicted by analytical methods.

2.1.1 WINGTIP VORTEX GENERATION

Any finite aspect ratio wing exhibits a non-uniform, spanwise lift distribution that is generally dependent upon wing area, planform shape, and airflow spillage around the tips. In general, the lift per unit span at any given location is described by the Kutta-Joukowski theorem:

$$L' = \rho V_\infty \Gamma'$$

where ρ is the air density, V_∞ is the freestream velocity, and Γ' is the circulation about the wing section. Due to the pressure differential between the upper and lower surfaces,

there is an airflow spillage and mixing that occurs around the tips, which results in a loss of lift Therefore, L' becomes zero at the tip but increases to a maximum at the wing centerline. Similarly, Γ' is a maximum at the centerline (denoted as Γ'_o) and decreases to zero strength about the tip section However, the total vorticity for the entire system must remain constant and is equal in magnitude to Γ'_o. Thus, as the local circulation Γ' decreases from the centerline towards the tip, the residual circulation is shed from the wing as a trailing vortex as shown in Figure 2 1. As a result of convective motion and

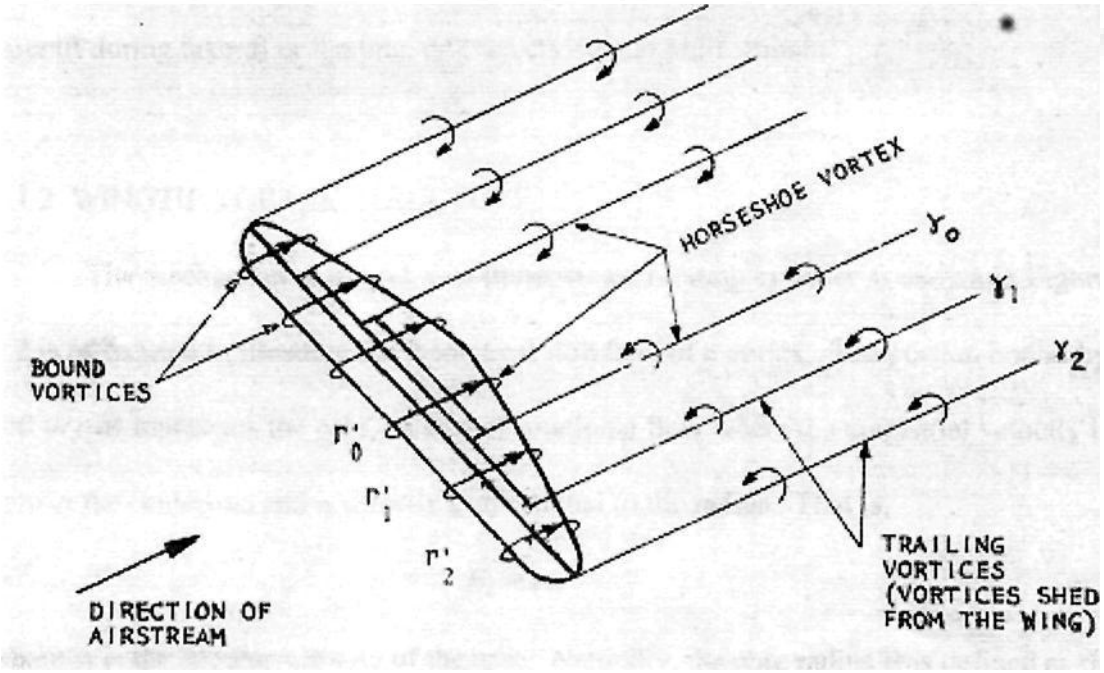

Figure 2.1 System of Bound and Trailing Vortices [2]

regional pressure diffusion toward the wingtips, the trailing vortex sheet undergoes a "roll-up" process in which the tip vortices are formed, each with circulation strength Γ'_o, as shown in conjunction with Figure 2.1 by the relationship:

$$\Gamma = \gamma_0 + \gamma_1 + \gamma_2 = (\Gamma'_0 - \Gamma'_1) + (\Gamma'_1 - \Gamma'_2) + (\Gamma'_2 - 0) = \Gamma'_0 \qquad [2]$$

which again shows that vorticity is conserved for the system.

When the Kutta-Joukowski theorem is rewritten in dimensionless form for a finite wing, it becomes the familiar equation for the lift coefficient:

$$\frac{b\Gamma}{V_\infty S} \propto C_L = \frac{L}{\frac{1}{2}\rho V_\infty^2 S}$$

to which the total wing circulation is proportional. This means that the tip vortex strength increases for an aircraft of higher spanwise wing loading or, if it is flying, at a low speed or at high altitude. This would be the case, for example, of a heavy transport-category aircraft during takeoff or landing, or even cruising at high altitude.

2.1.2 WINGTIP VORTEX STRUCTURE

The mechanism of a rigid, two-dimensional rotating cylinder as shown in Figure 2.2 is often used to illustrate the theoretical flowfield of a vortex. The portion bound by r=0 to r=R represents the core, an area of rotational flow where the tangential velocity is zero at the centerline and is directly proportional to the radius. That is,

$$V_z = r\omega$$

where ω is the angular velocity of the core. Naturally, the core radius R is defined as the radius at which the maximum tangential velocity occurs. The portion from r=R to r=∞ represents the irrotational flow of a potential vortex where the tangential velocity is described by:

$$V_z = \frac{\Gamma}{2\pi r}$$

where Γ is the circulation generated by the core.

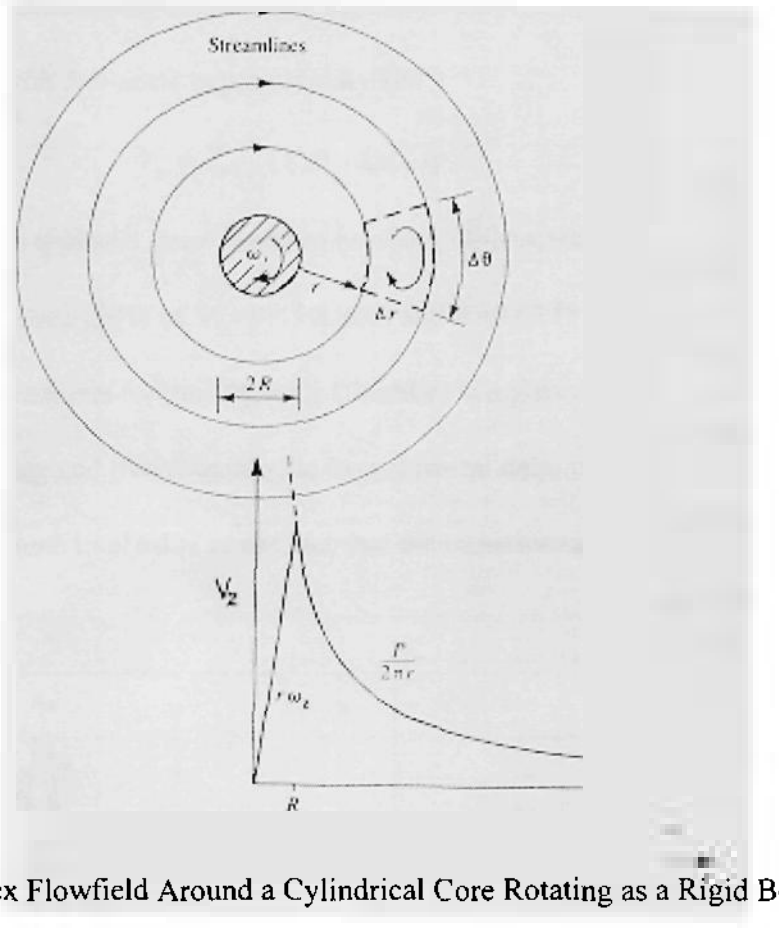

Figure 2.2 Vortex Flowfield Around a Cylindrical Core Rotating as a Rigid Body [5]

These relationships describe flow in an inviscid, potential vortex. There are a number of analytical models that approximate the more realistic viscous tangential velocity distribution, one of which was developed by Rankine that represents a two-dimensional line vortex in a laminar flow:

$$V_z = V_{z\max}\left(\frac{r}{R}\right) \quad \text{for } r<R$$
$$V = V_{z\max}\left(\frac{R}{r}\right) \quad \text{for } r\geq R \qquad [2]$$

Experimental data has shown, however, that portions of a vortex exhibit turbulent flow with greatly increased effective velocity. Another model developed by Kuhn and Nielsen

based on turbulent boundary layer and logarithmic circulation theory has been determined to correspond well with full-scale experimental data:

$$V_z = V_{z\max}(\frac{r}{R})[1 + \ln(\frac{r}{R})] \qquad [2]$$

In practice, V_{zmax} has typically been found to be about 50 percent of the flight speed [2]. Using V_{zmax}=46.75 ft/sec (50% of V_∞=93.5 ft/sec) and R=0.0175 ft based on experimental measurements for the 1/4-scale Cherokee wing model, these analytical methods underestimate and overestimate the experimental data, respectively as shown in Figure 2.3. This is most likely due to the fact that the experimental vortex was taken at a

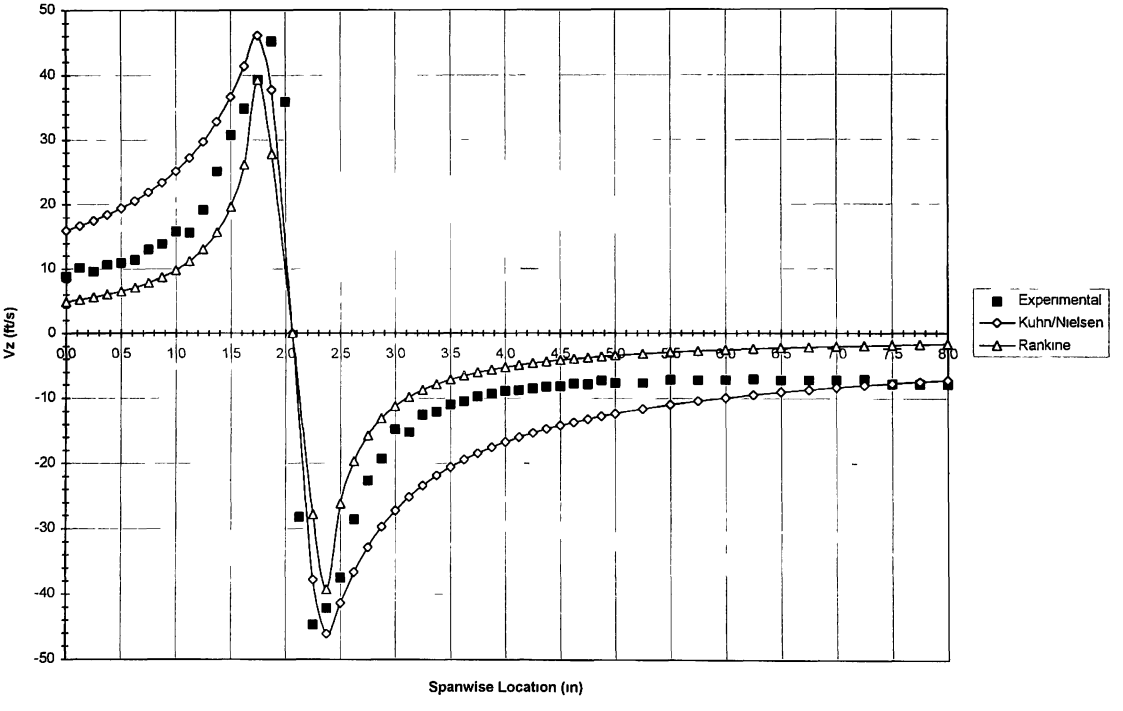

Figure 2.3 Experimental Data and Theoretical Vortex Models Compared

relatively low Reynolds number of 750,000, which might imply that the vortex is made up of flow in transition from a laminar to a turbulent state. Apparently, the average of values from the two methods would likely give a very accurate tangential velocity distribution for aircraft models operating at these conditions. The fact that the vortex core is defined by relatively small radii results in very high tangential velocities, which corresponds to static air pressure and density significantly lower than that of atmospheric as shown in Figure 2.4 for a typical vortex.

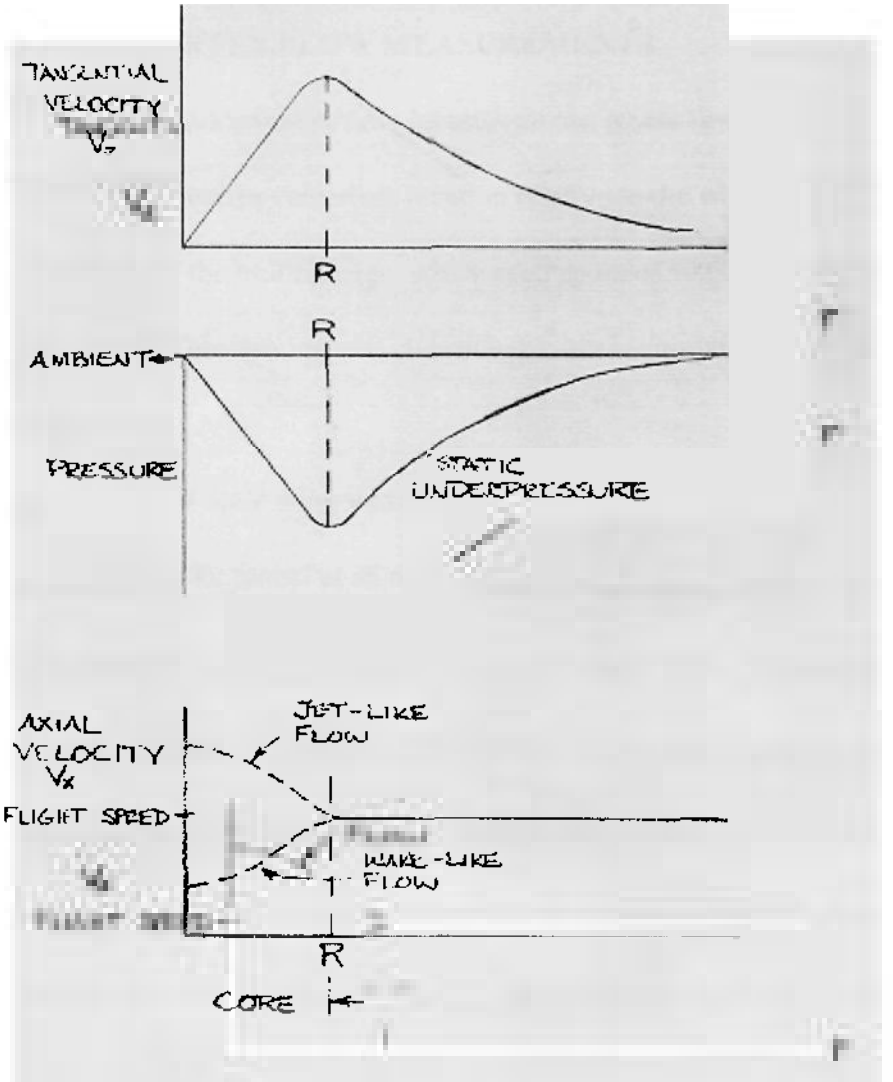

Figure 2.4 Velocity and Pressure Distributions in a Viscous Vortex [2]

In addition, researchers have reported axial perturbations on the order of ±15% of the flight speed. Experimental observations have shown the existence of a jet-like axial flow at high angles of attack and a wake-like flow at lower angles. Apparently, the jet-like flow results from the core underpressure while the wake-like flow is associated with the wing profile drag. Moreover, combinations of the two flows have been shown to occur as well [2].

2.2 EXPERIMENTAL VORTEX FLOW MEASUREMENTS

In order to collect accurate vortex flow measurements, it was first necessary to determine the location of the vortex centerline location relative to the wing model at a point 10% of the chord aft of the trailing edge, which corresponded to the location of the leading edge of the blades. This spacing was chosen to maintain similarity to the NASA Langley model.

A 9" section of the 1/4 scale wing was placed in the test section of the Embry-Riddle three-dimensional smoke tunnel at an angle of attack of 2^{o}. The tunnel speed, although not actually measured, was around 30 ft/sec. Kerosene-vapor smoke was injected into the model and emerged through holes in the tip spaced 1" apart along the chord line. The smoke was observed to roll up into the vortex, with the centerline located 2" inboard of the tip and 0.5" above the trailing edge as illustrated in Figure 2.5.

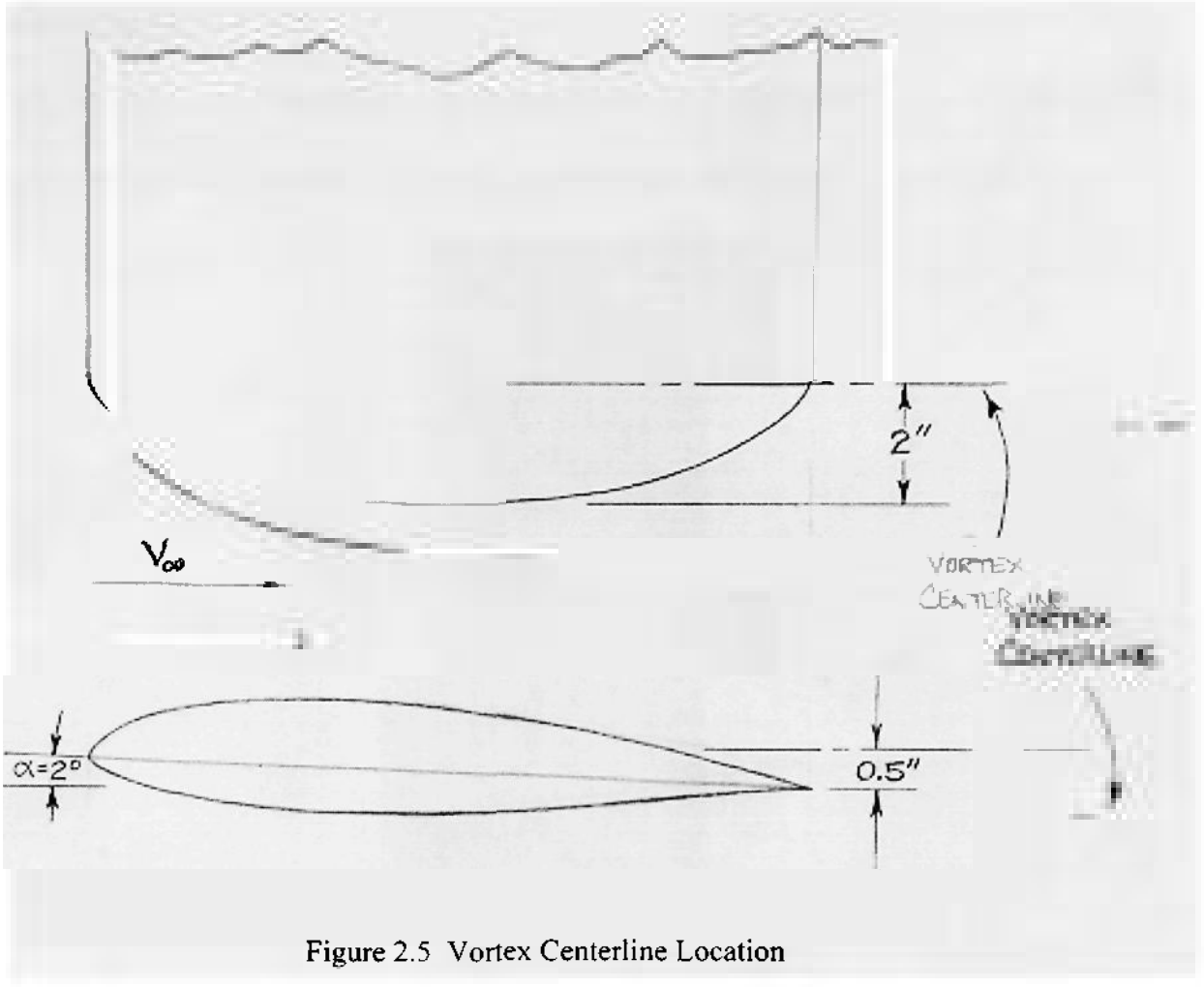

Figure 2.5 Vortex Centerline Location

In addition, the 27" semi-span, 1/4-scale wing model was mounted in the test section of the Embry-Riddle subsonic wind tunnel also at an angle of attack of 2°. In lieu of smoke, 8" tufts of white and black yarn were attached to the wingtip along the chord and around the trailing edge. These tufts rolled up into the vortex flow, verifying the centerline location obtained in the smoke tunnel.

Given this information, vortex flow measurements were initially taken using a United Sensor DC-125-12-CD five-hole flow directionality probe (Figure 2.6) connected to the lab manometer bank. This probe was mounted on a two-axis traversing

mechanism, which was bolted to the wind tunnel test section ceiling as shown in Figure 2.7. The traversing mechanism was adjusted so that the tip of the probe was located at a point 10% of the chord aft of the wing trailing edge. Before the wing model was

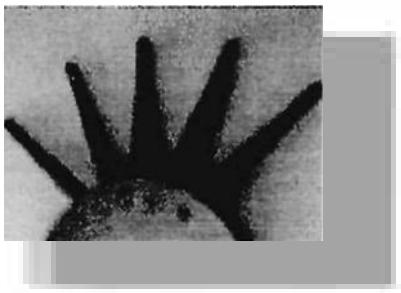

20

mechanism, which was bolted to the wind tunnel test section ceiling as shown in Figure 2.7. The traversing mechanism was adjusted so that the tip of the probe was located at a point 10% of the chord aft of the wing trailing edge. Before the wing model was

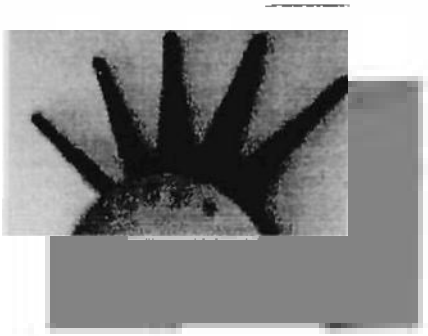

20

mechanism, which was bolted to the wind tunnel test section ceiling as shown in Figure 2.7. The traversing mechanism was adjusted so that the tip of the probe was located at a point 10% of the chord aft of the wing trailing edge. Before the wing model was

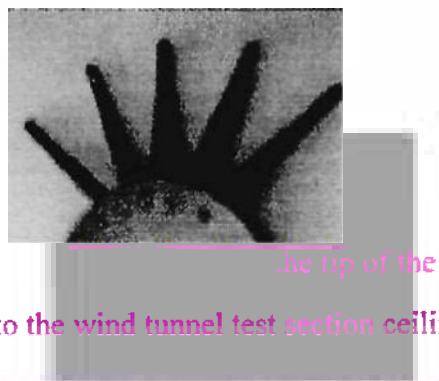

2.7. The traversing mechan.. he tip of the probe was located at a 20

mechanism, which was bolted to the wind tunnel test section ceiling as shown in Figure

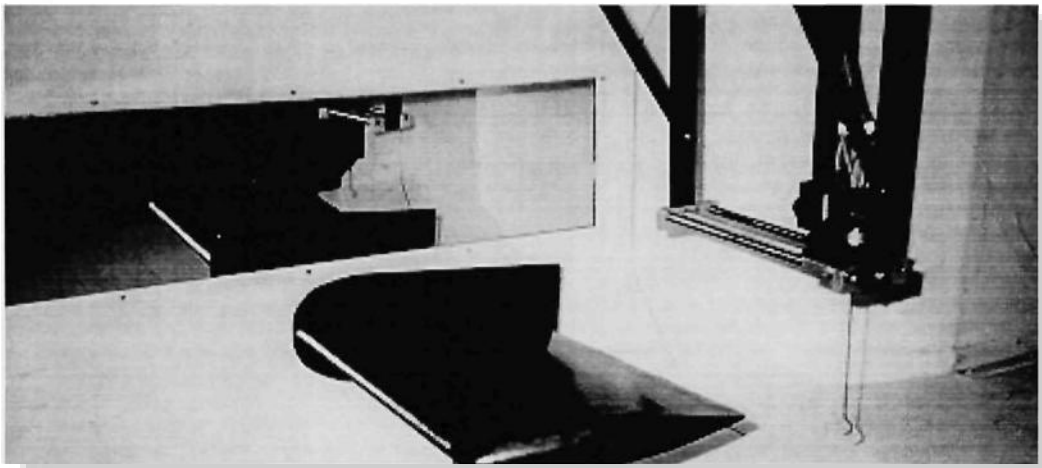

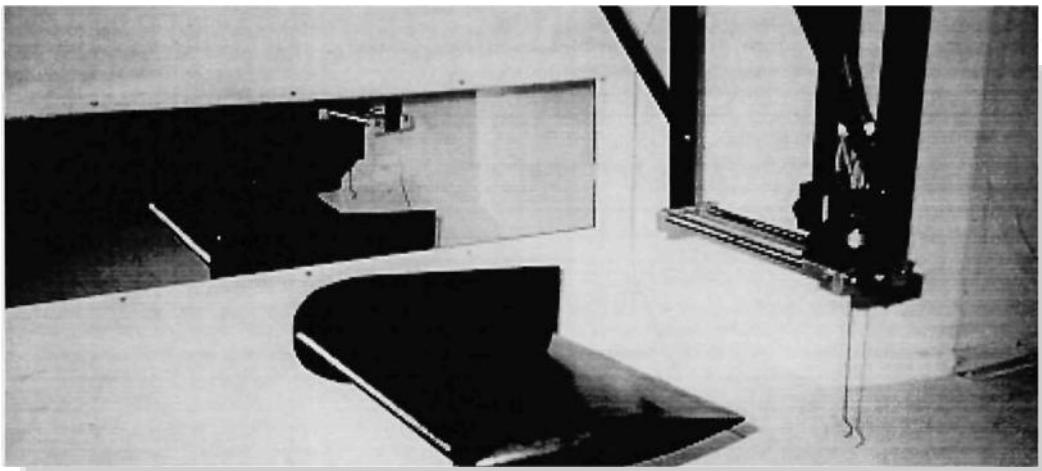

21

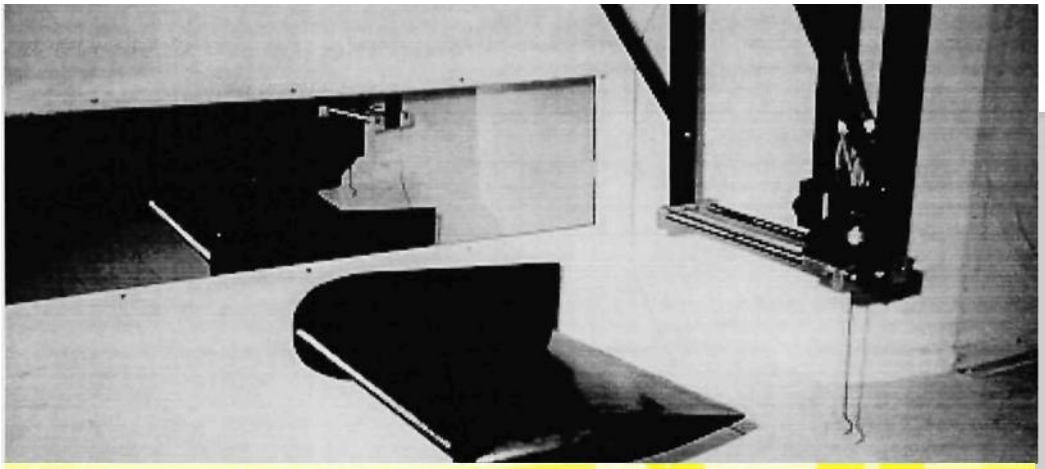

was measured to have a radius of 0.21" These measurements successfully served as baseline data to provide a clear picture of the vortex at hand, to develop a general sizing of the WVT and its blade and nacelle components, and also to verify the results of the aforementioned analytical prediction models.

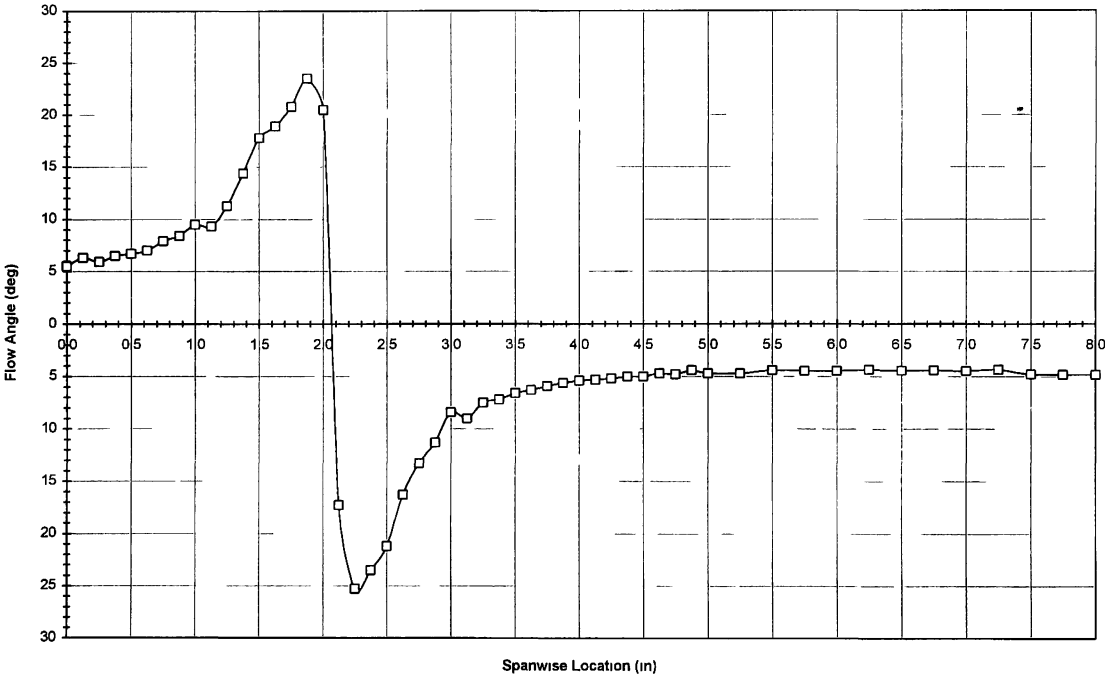

Figure 2.8 Experimental Vortex Flow Angle Measurements

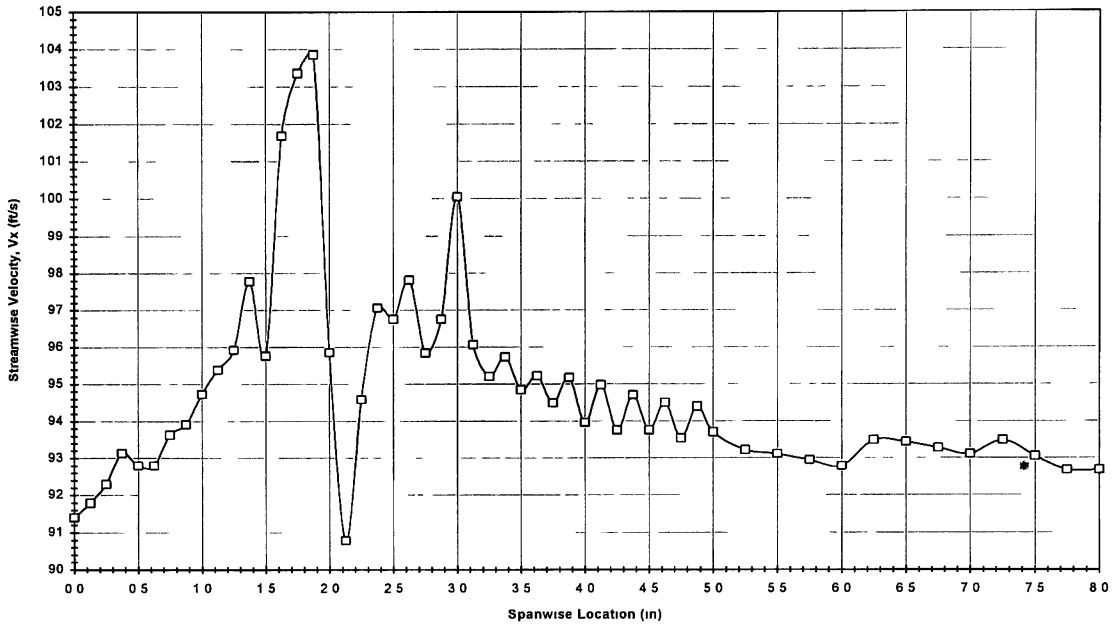

Figure 2.9 Experimental Vortex Streamwise Velocity Measurements

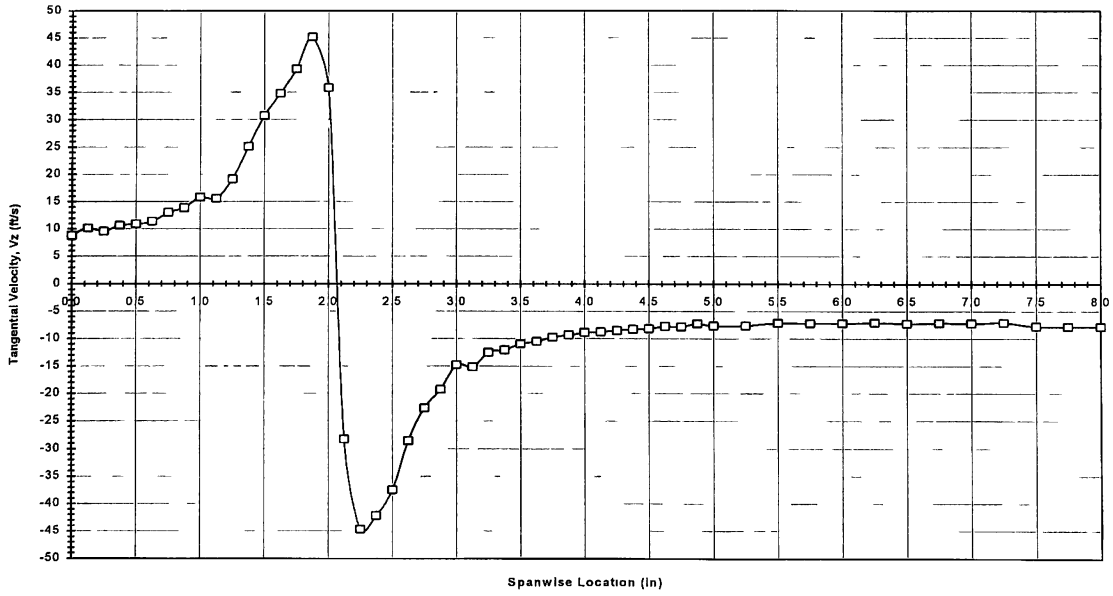

Figure 2.10 Experimental Vortex Tangential Velocity Measurements

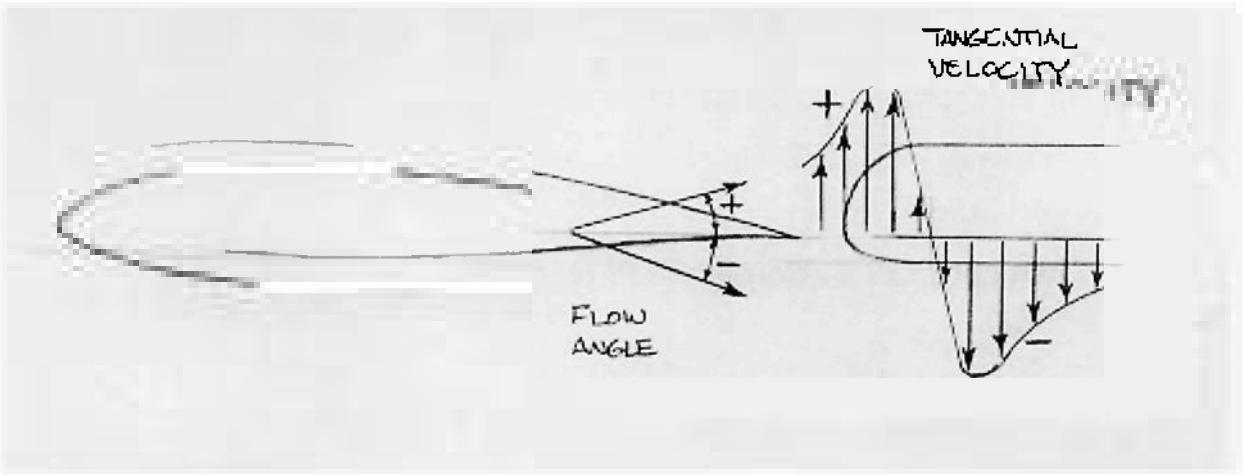

24

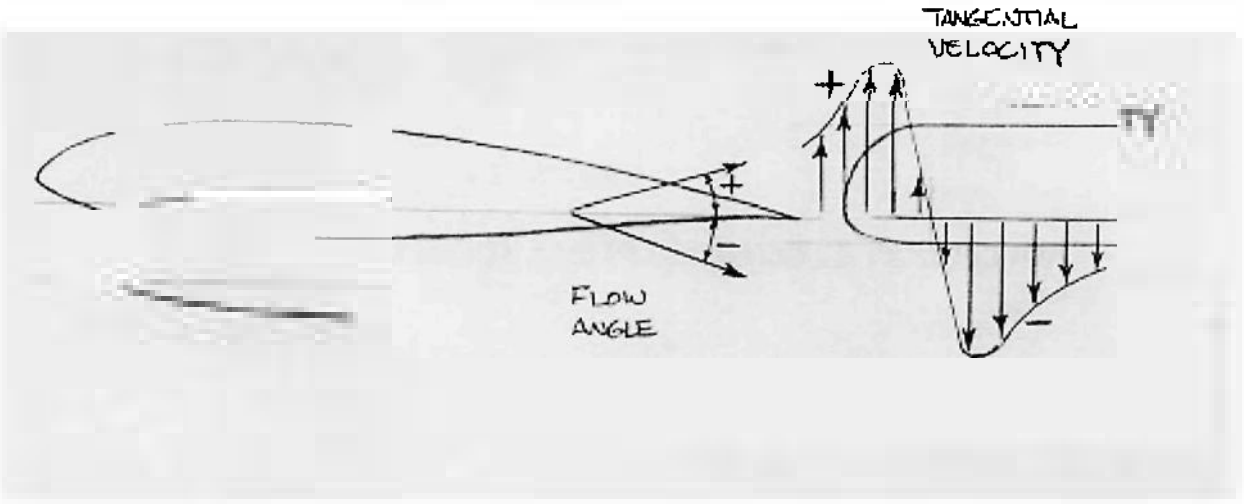

24

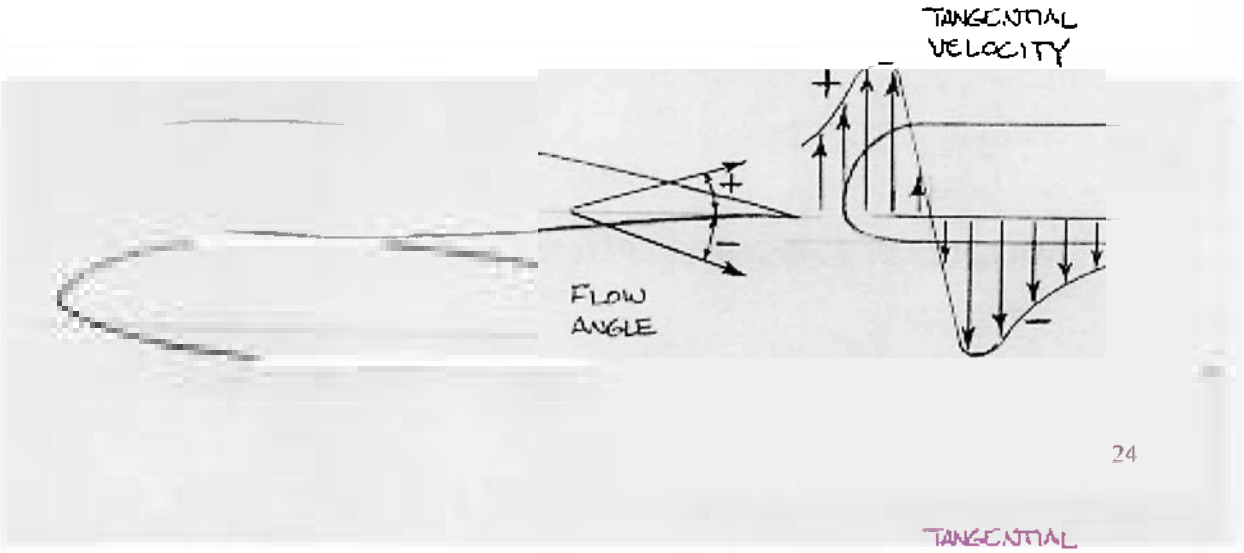

24

TANGENTIAL

CHAPTER 3

WVT DESIGN METHODOLOGY AND PERFORMANCE PREDICTION

3.1 WVT NACELLE

CHAPTER 3

WVT DESIGN METHODOLOGY AND PERFORMANCE PREDICTION

3.1 WVT NACELLE

CHAPTER 3

WVT DESIGN METHODOLOGY AND PERFORMANCE PREDICTION

3.1 WVT NACELLE

stationary section that attached internally to the wing to provide a general support structure and housing for power generation and instrumentation, and a rotating hub that provided a means of attaching the fixed (but adjustable) pitch blades. This hub also incorporated a faired end-cone to reduce trailing flow separation.

26

stationary section that attached internally to the wing to provide a general support structure and housing for power generation and instrumentation, and a rotating hub that provided a means of attaching the fixed (but adjustable) pitch blades. This hub also incorporated a faired end-cone to reduce trailing flow separation.

26

stationary section that attached internally to the wing to provide a general support structure and housing for power generation and instrumentation, and a rotating hub that provided a means of attaching the fixed (but adjustable) pitch blades. This hub also incorporated a faired end-cone to reduce trailing flow separation.

structure and housing for power generation and instrumentation, and a rotating hub that 26

stationary section that attached internally to the wing to provide a general support

designed to be 1" in diameter, which also allowed for a good fit of a 1" diameter miniature slip clutch placed between the hub and the stationary tube. The nacelle dimensions and design can be viewed in more detail in Chapter 4.

In order for the WVT to be most effective in turning the vortex flow and creating thrust, it was necessary for the nacelle centerline to be coincident with that of the vortex. As mentioned in the previous chapter, the vortex centerline was found to be located 2"

27

designed to be 1" in diameter, which also allowed for a good fit of a 1" diameter miniature slip clutch placed between the hub and the stationary tube. The nacelle dimensions and design can be viewed in more detail in Chapter 4.

In order for the WVT to be most effective in turning the vortex flow and creating thrust, it was necessary for the nacelle centerline to be coincident with that of the vortex. As mentioned in the previous chapter, the vortex centerline was found to be located 2"

27

designed to be 1" in diameter, which also allowed for a good fit of a 1" diameter miniature slip clutch placed between the hub and the stationary tube. The nacelle dimensions and design can be viewed in more detail in Chapter 4.

In order for the WVT to be most effective in turning the vortex flow and creating thrust, it was necessary for the nacelle centerline to be coincident with that of the vortex. As mentioned in the previous chapter, the vortex centerline was found to be located 2"

miniature slip clutch placed between the hub and the stationary tube. The nacelle 27

designed to be 1" in diameter, which also allowed for a good fit of a 1" diameter

Although the nacelle's size was kept to a minimum, its presence formed a circular boundary that influenced the vortex velocity distribution. To determine these new distributions, a second set of flowfield measurements around the nacelle were taken in the wind tunnel using the five-hole probe and traversing mechanism as shown in Figure 3.3. Problems had developed with the original probe due to apparent clogging of two of the five holes. An available United Sensor SDC-12-6-15°-.250 conical five-hole probe was calibrated (see Appendix A) for flow angularity and velocity component measurement and was used for these new measurements. Figures 3.4, 3.5, and 3.6 show the flow angle, axial velocity, and tangential velocity distributions, respectively, as a function of spanwise location and around the nacelle.

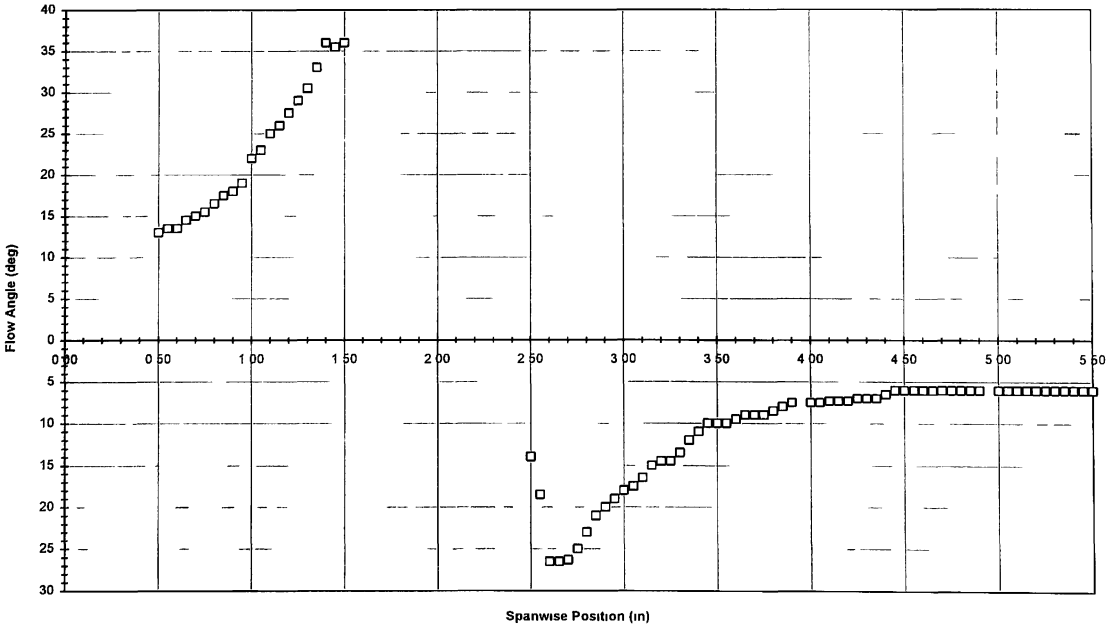

Figure 3.4 Experimental Vortex Flow Angle Measurements Around Nacelle

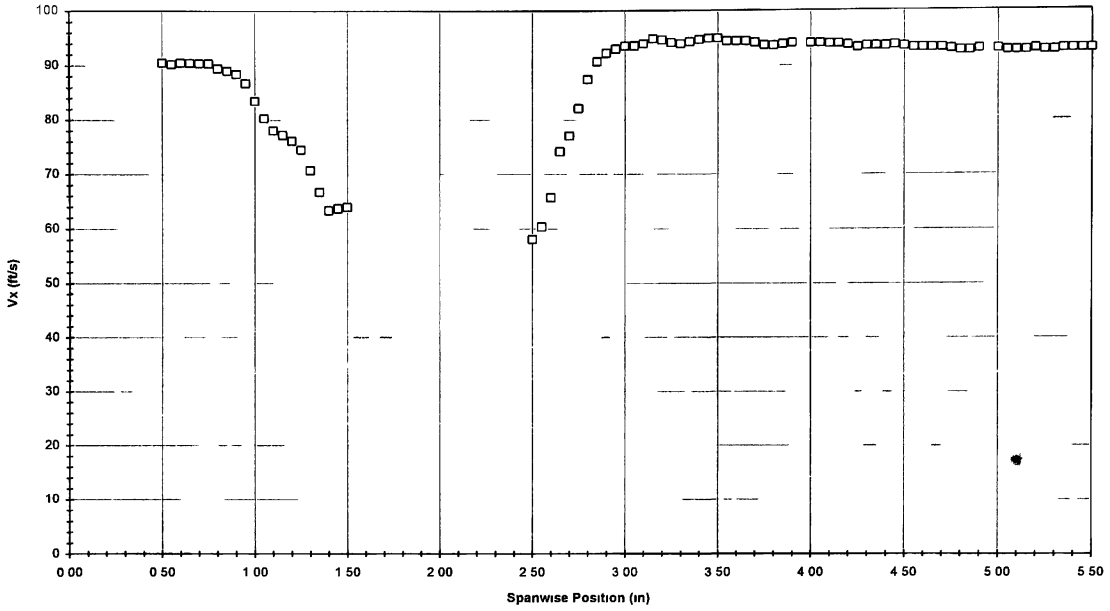

Figure 3.5 Experimental Vortex Axial Flow Measurements Around Nacelle

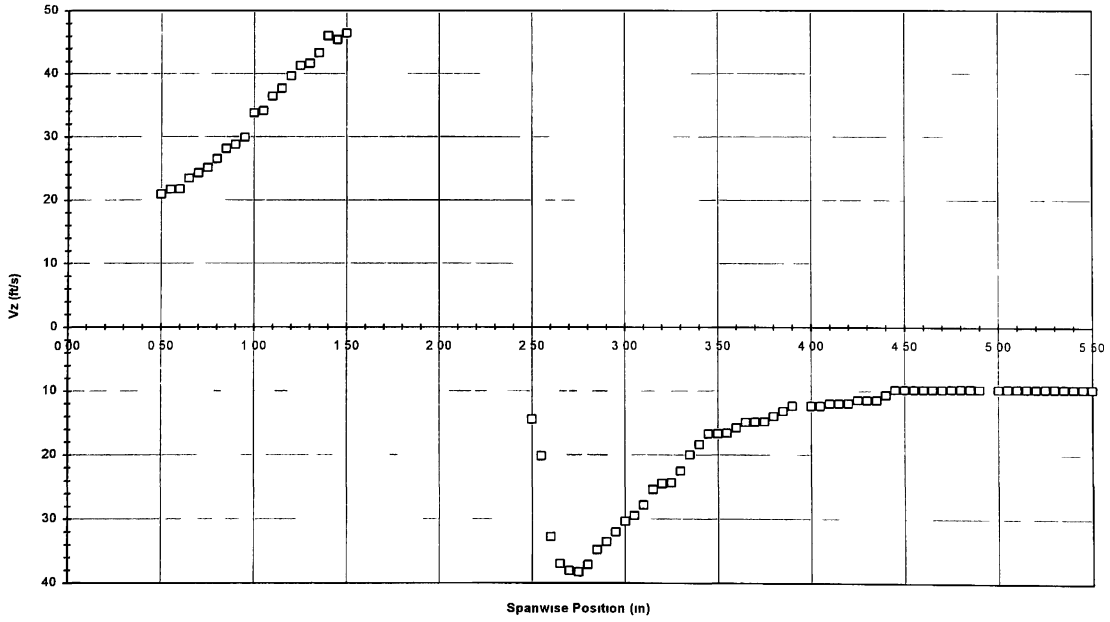

Figure 3.6 Experimental Vortex Tangential Flow Measurements Around Nacelle

Quantitatively, the velocity profiles were very similar to the original measurements, the only differences being the absence of a discrete core, as well as the fluctuating axial velocities. In fact, the axial velocity profile showed some slowing near the nacelle, probably, due to boundary layer effects.

3.2 WVT BLADES

3.2.1 DESIGN PARAMETERS

The blade design process was the primary focus in the WVT's development. It was the author's hypothesis that the turbine could utilize the vortex flow not only to generate power, but also to produce a maximum thrust force to offset the drag of the wing. To achieve this, there were several relevant variables outlined for the design:

- turbine diameter
- blade airfoil
- number of blades
- blade planform
- blade twist
- blade pitch angle

The last four parameters were optimized using a FORTRAN computer program written by the author to predict WVT thrust and torque production. This program, its operation, and a sample output is given in Appendix B.

3.2.1.1 TURBINE DIAMETER

From a practical point of view, the full-scale WVT diameter was a factor in terms of ground clearance on a low-wing aircraft such as the Cherokee. Additionally, the WVT

only needed to be as large as the vortex flowfield, as a larger diameter would result in blade protrusion into the freestream, causing excess drag. As shown in Figures 3.4, 3.5, and 3.6, the majority of the affected vortex flow extended approximately 2" radially from the nacelle boundaries. However, it should be noted that this flowfield was measured for 2^{o} angle of attack -- a relatively low angle. A higher angle of attack in the case of a climbing aircraft would result in a vortex of higher strength and a larger diameter. For these reasons, the overall WVT diameter was set at 7", giving a 3" span to each individual blade.

3.2.1.2 BLADE AIRFOIL

Since the WVT model was designed for maximizing thrust and, of course, minimizing drag while generating power, it was necessary to use a high lift-to-drag airfoil. In addition, both the model and the full-scale WVT were to operate at low Reynolds numbers. Specifically, the model was to operate at Rn=75,000 based on V_{∞}=93.5 ft/sec and a 1.5" average blade chord, and the full-scale turbine at Rn=600,000 based on the cruising flight speed of 190.7 ft/sec and average blade chord of 6" At these low Reynolds numbers, laminar flow tends to dominate and thus the flow over the blades would be subject to laminar separation causing unnecessarily high drag.

Given these factors, the airfoil chosen for use was the ASM-LRN-010 shown in Figure 3.7. This airfoil was designed by Analytical Services and Materials, Inc. of Hampton, Virginia as a 9.5% thick, low Reynolds number (250,000-500,000), high L/D airfoil that intentionally uses turbulator strips for optimum laminar separation and

boundary layer transition control for minimum profile drag. In theory, L/D_{max} was reported to be 115 for Rn=250,000 and 157 for Rn=500,000 as shown in Figure 3.7 [6]. These are theoretical results and are not always possible to reproduce in practice,

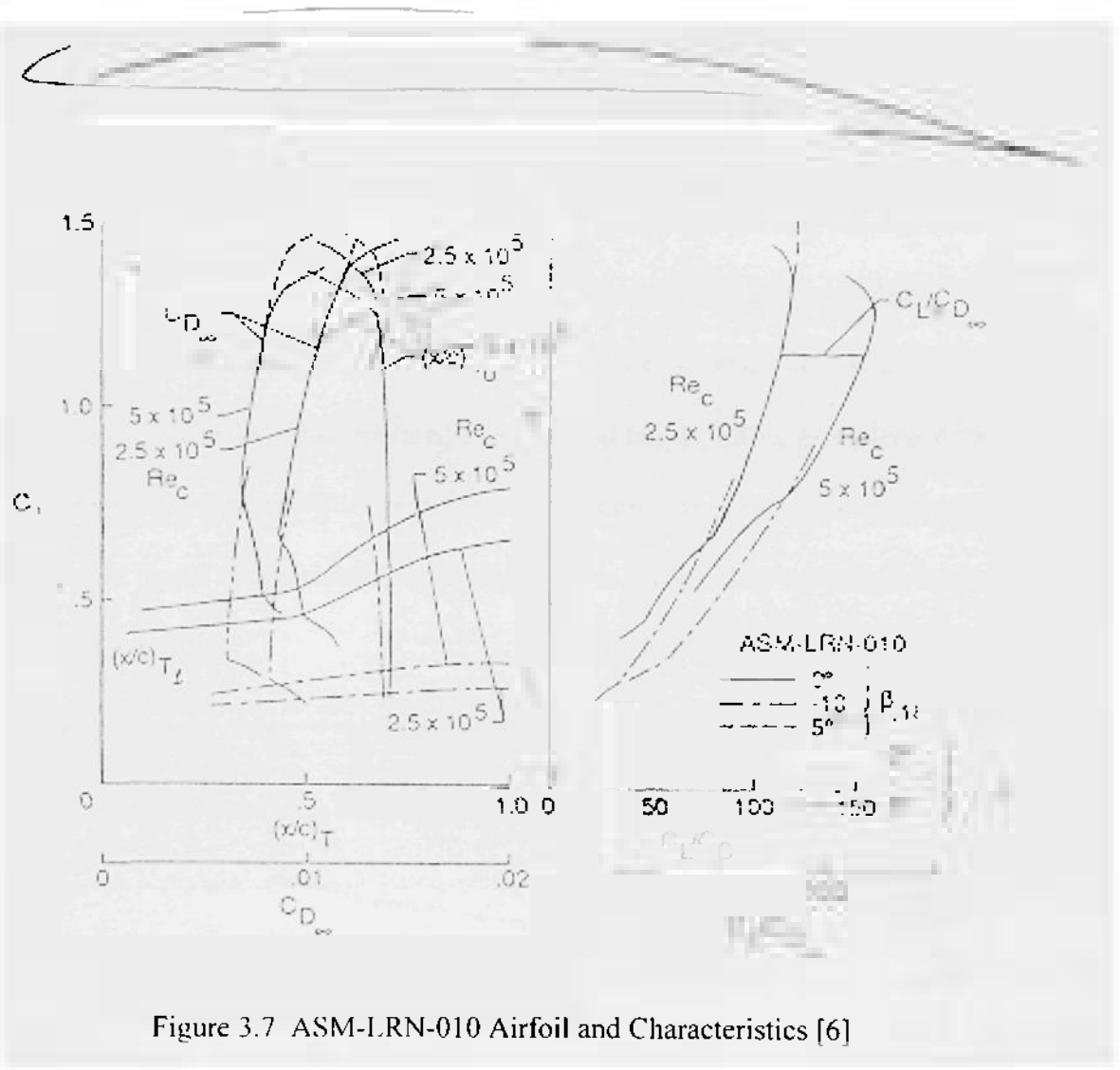

Figure 3.7 ASM-LRN-010 Airfoil and Characteristics [6]

especially since the model Reynolds number was even below this range. Nonetheless, the experimental results obtained by ASM, Inc. were seen to be similarly satisfactory, justifying its use.

3.2.1.3 BLADE NUMBER

From a thrust-to-power-required standpoint, it is known for a given total blade area, that aircraft propellers are more efficient when a greater number of high aspect ratio blades are used [7]. This results in high thrust, while maintaining low induced tip losses. However, in terms of practical structural and blade/nacelle design integration for the WVT, using a large number of blades is not feasible. The blades require mounting provisions and pitch angle variability while still fitting into a rather low-volume nacelle. Thus, for the given nacelle dimensions it was determined that the blade number could only be realistically varied between two and six. This was noted as the first of two optimization variables to be incorporated into the wind tunnel testing procedure of the model. Predictions from the WVT performance program clearly indicated that increasing the number of blades would result in both higher thrust (lower drag) and torque as shown in Figures 3.8 and 3.9.

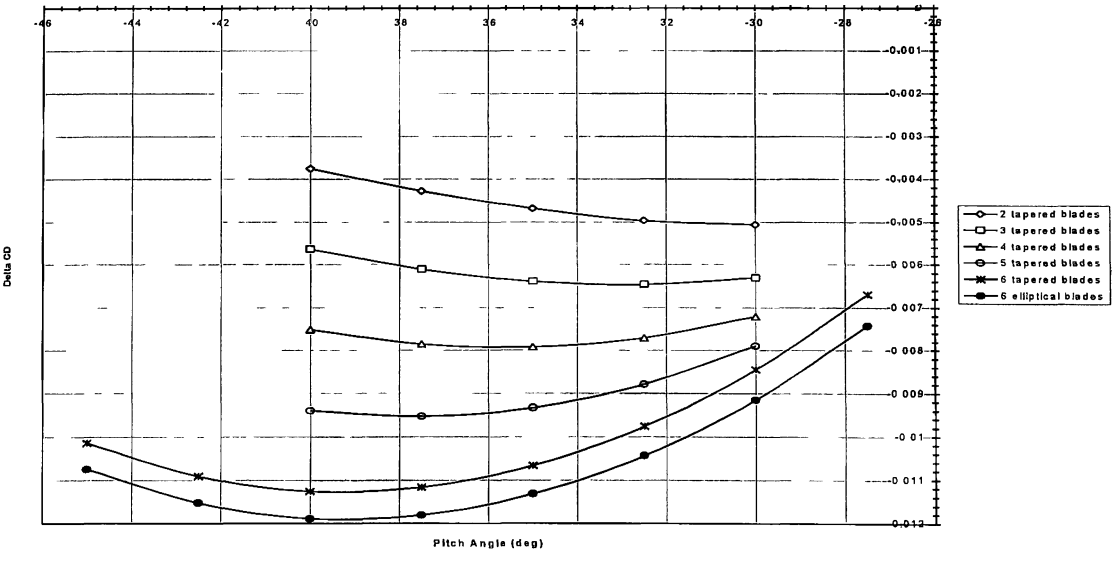

Figure 3.8 Drag Reduction vs. Pitch Angle for Various Blade Number Cases

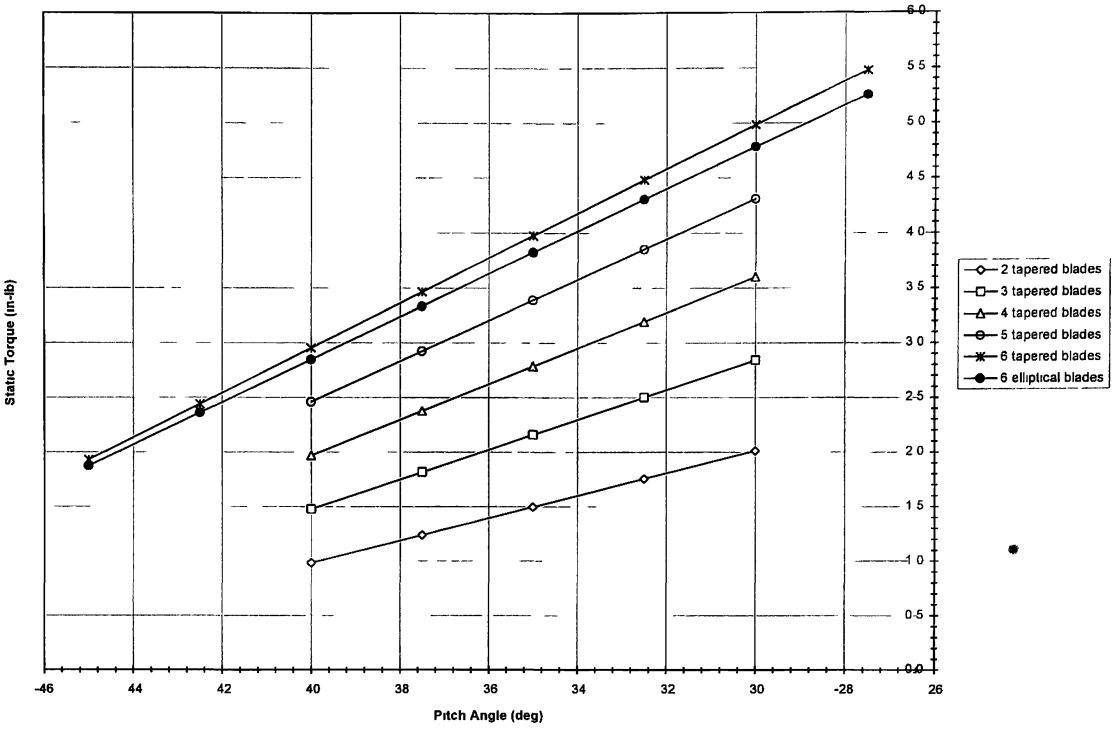

Figure 3.9 Static Torque vs. Pitch Angle for Various Blade Number Cases

3.2.1.4 BLADE PLANFORM

NASA Langley's WVT test results indicated that a tapered planform sacrificed some power output, but reduced drag more significantly than just a straight blade. This also made sense from a thrust production point of view since higher vortex velocities and greater blade area inboard near the hub would combine to give a higher thrust. Conversely, an increased amount of outboard planform area was the driving factor toward increased power from the higher torque output, and hence a balance between the two was necessary when designing the blades for this WVT.

There are probably an infinite number of suitable planform shapes and sizes for a low-speed application such as this. The first planform used in the WVT performance

program analysis was a zero-sweep, 0.45 straight taper ratio blade with a root chord of 2.5" and a tip chord of 1.125". These dimensions were chosen as a starting point due to their similarity to the NASA Langley WVT tapered blades, although the 0.45 taper ratio was chosen since such straight-tapered wings with zero sweep are known to exhibit a more efficient, elliptical lift distribution.

During the program analysis, it was verified from the blade thrust loading output for each case that the majority of the thrust was produced by the inboard sections as illustrated in Figures 3.10 and 3.11. As a second analysis, this planform was modified slightly to increase the inboard area and reduce the outboard area, while keeping the total area the same. The root chord was increased to 3" and the tip was rounded to form an elliptical blade. These modifications resulted in only a 1 count drag reduction (or thrust) per blade with a negligible loss in static torque maintained at about 0.5 in-lb per blade. These results are shown numerically in the sample program output of Appendix B for the two planforms analyzed.

These results indicated that the exact planform was not terribly critical as long as it was tapered in some manner to provide the aforementioned efficiency. However, it was decided to use the elliptical planform for the model since, theoretically, it would provide some additional thrust.

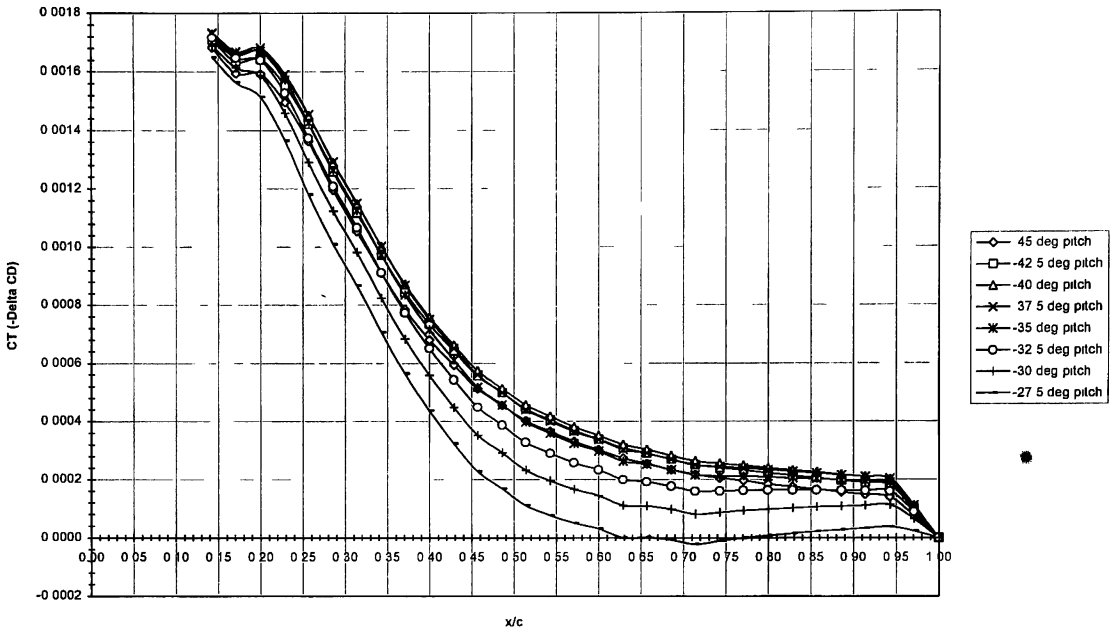

Figure 3.10 Straight-Tapered Blade Thrust Loading Distribution, 6 Blades

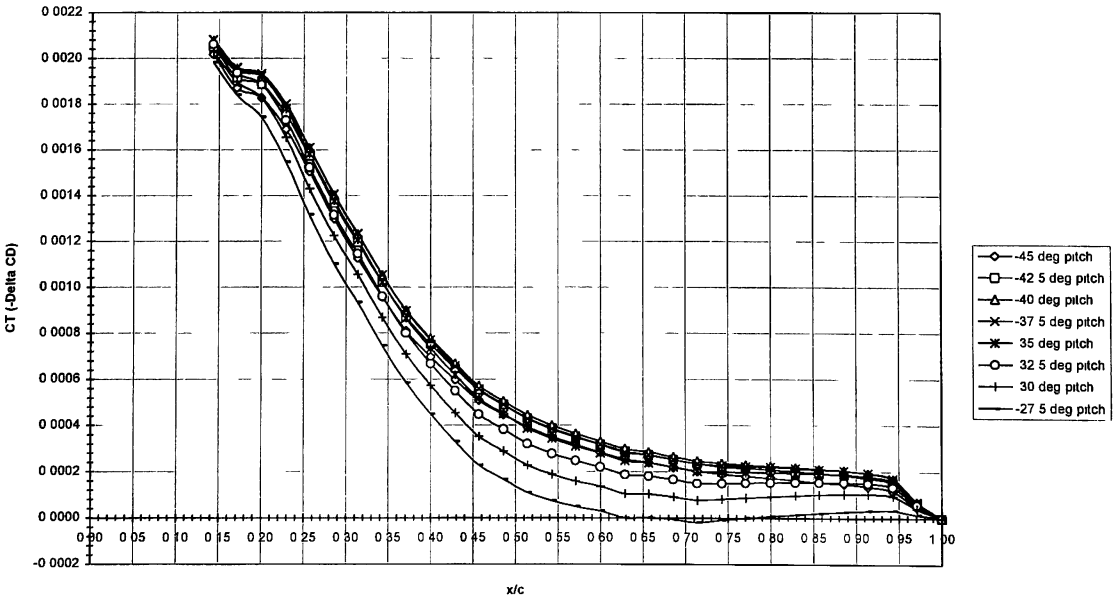

Figure 3.11 Elliptical Blade Thrust Loading Distribution, 6 Blades

3.2.1.5 BLADE TWIST

The twist distribution was seen as a critical parameter which would ensure that the lift and drag of each blade section combine to give the maximum thrust Although any arbitrary twist distribution could be analyzed in the WVT performance program, the hypothesis was that this distribution would likely need to inversely match that of the vortex flow angle measured previously.

37

3.2.1.5 BLADE TWIST

The twist distribution was seen as a critical parameter which would ensure that the lift and drag of each blade section combine to give the maximum thrust Although any arbitrary twist distribution could be analyzed in the WVT performance program, the hypothesis was that this distribution would likely need to inversely match that of the vortex flow angle measured previously.

37

3.2.1.5 BLADE TWIST

The twist distribution was seen as a critical parameter which would ensure that the lift and drag of each blade section combine to give the maximum thrust. Although any arbitrary twist distribution could be analyzed in the WVT performance program, the hypothesis was that this distribution would likely need to inversely match that of the vortex flow angle measured previously.

The twist distribution was seen as a critical parameter which would ensure that the 37

3.2.1.5 BLADE TWIST section combine to give the maximum thrust Although any

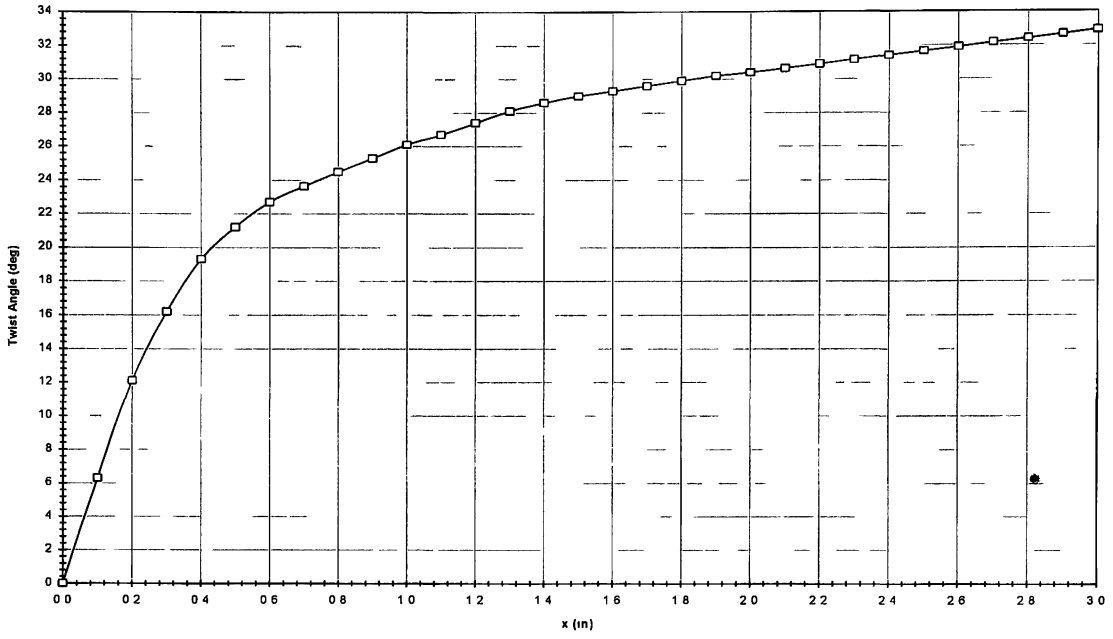

Figure 3.13 Final Blade Twist Distribution (Root. x = 0 in.)

3.2.1.6 BLADE PITCH ANGLE

As described above, the blade pitch angle was used as an input variable to determine the proper setting for maximum thrust at cruise conditions and was found to be approximately -40° at the blade root with respect to the nacelle centerline for the 6-bladed configuration. This was seen only as a starting point though as it would depend on the vortex flowfield properties for any given flight attitude and condition. Therefore, the pitch angle was noted as the second optimization variable during wind tunnel tests, as one setting would be determined for the stationary turbine condition and one setting for the rotating turbine. The singular pitch setting resulted from the fact that this WVT would use fixed-pitch blades for simplicity, size, and cost reasons.

CHAPTER 4

TEST APPARATUS AND PROCEDURE

4.1 WVT MODEL CONSTRUCTION

CHAPTER 4

TEST APPARATUS AND PROCEDURE

4.1 WVT MODEL CONSTRUCTION

CHAPTER 4

TEST APPARATUS AND PROCEDURE

4.1 WVT MODEL CONSTRUCTION

desired setting, and re-tightening the bolt. This assembly was fastened to the clutch by four set screws.

The manually adjustable clutch served as a means of allowing the WVT to be locked in place or rotate while imposing a torsional loading on the 5/16" diameter shaft. The shaft was supported at the internal end of the stationary tube by a locking collar and by an 8x24mm bearing at the external end. A strain gage rosette with two gages oriented at $\pm 45^{o}$ to the nacelle centerline was bonded to the shaft to allow for torsional readings to be made.

4.1.2 BLADE CONSTRUCTION

The WVT blades were first modeled in the 3-D CAD/CAM software, Varimetrix, and were machined from high-density polyethylene using Embry-Riddle's KOMO CNC milling machine. Once finished, each blade was drilled and tapped to accept a 6-32 socket head bolt into the blade root at the 30% chord location. The bolt shank served as the rotatable structure for the blade to be secured into the nacelle, and the bolt head prevented the blade from being pulled out under centrifugal loading while rotating.

A 0.008" thick, 0.0625" wide tape trip strip was applied to the upper surface of each blade at the 50% chord location. Figure 3.7 showed the upper surface natural boundary layer transition point, $(x/c)_{Tu}$, to occur at 70% of the chord at Rn=250,000. Since the model was to be tested at a blade Reynolds number of only 75,000, it was expected that unforced transition would occur at a more aft, yet unknown position. As a

safeguard, the 50% chord location seemed like a reasonable location to prevent any possible laminar separation from occuring.

4.2 SUPPORT EQUIPMENT AND TEST INSTRUMENTATION

4.2.1 LOW-SPEED WIND TUNNEL

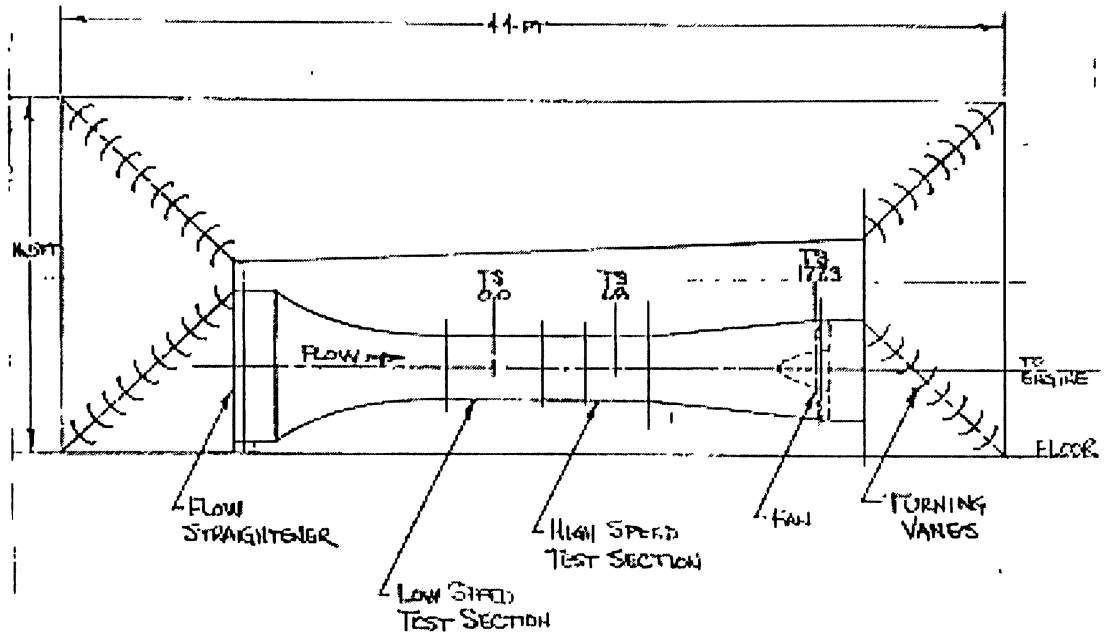

Figure 4.2 Low-Speed Wind Tunnel at ERAU [8]

The low-speed wind tunnel at Embry-Riddle Aeronautical University (Figure 4.2) is a closed-circuit, closed test section, vertical single return tunnel. The low-speed test section is 36" high and 52" wide, with 0.5° of wall divergence to account for boundary layer growth. The tunnel is powered by an 8-cylinder, 160 HP internal combustion engine which drives a 6-bladed, fixed-pitch, 56" diameter, laminated wood propeller. This combination provides a speed range between 0 and 110 ft/sec in the low-speed test

section. The turbulence factor in the test section has been consistently measured to be about 1.38 in lab experiments that, considering a factor of 1.7 or less is acceptable for a small tunnel such as this, indicates a relatively low level of freestream turbulence [8].

4.2.2 FORCE BALANCE AND DATA ACQUISITION SYSTEM

An Aerolab 6-component, pyramidal, load cell force balance is used in the low-speed test section to measure lift, drag, sideforce, pitching moment, rolling moment, yawing moment, and their coefficients. The load limits of the balance for each component and corresponding levels of accuracy are shown in Table 4.1. The test section velocity is monitored by a pitot-static system connected to a pressure transducer and temperature by a thermistor.

Each of the above eight parameters constitute a channel that is sampled 50 times at a rate of 60 samples per second as a voltage signal by a Hewlett Packard 3054C Data Acquisition System. The measurements are averaged, converted to a digital signal, and sent to an IBM PS/2 computer for collection and display using the pre-loaded software entitled "WINDT". The data could then be printed out in hard copy form as shown in Appendix C. Figure 4.3 shows this instrumentation as set up permanently in the wind tunnel lab.

Table 4 1 Force Balance Load Limits and Accuracy [9]

PARAMETER	LOAD LIMIT	ACCURACY
Drag (Fx)	-50 to +50 lb	±0 05 lb
Sideforce (Fy)	-50 to +50 lb	±0 05 lb
Lift (Fz)	-50 to +100 lb	±0 05 lb
Rolling Moment (Mx)	-100 to +100 in-lb	±0 5 in-lb
Pitching Moment (My)	-100 to +100 in-lb	±0 5 in-lb
Yawing Moment (Mz)	-100 to +100 in-lb	±0 5 in-lb

43

Table 4 1 Force Balance Load Limits and Accuracy [9]

PARAMETER	LOAD LIMIT	ACCURACY
Drag (Fx)	-50 to +50 lb	±0 05 lb
Sideforce (Fy)	-50 to +50 lb	±0 05 lb
Lift (Fz)	-50 to +100 lb	±0 05 lb
Rolling Moment (Mx)	-100 to +100 in-lb	±0 5 in-lb
Pitching Moment (My)	-100 to +100 in-lb	±0 5 in-lb
Yawing Moment (Mz)	-100 to +100 in-lb	±0 5 in-lb

43

Table 4 1 Force Balance Load Limits and Accuracy [9]

PARAMETER	LOAD LIMIT	ACCURACY
Drag (Fx)	-50 to +50 lb	±0 05 lb
Sideforce (Fy)	-50 to +50 lb	±0 05 lb
Lift (Fz)	-50 to +100 lb	±0 05 lb
Rolling Moment (Mx)	-100 to +100 in-lb	±0 5 in-lb
Pitching Moment (My)	-100 to +100 in-lb	±0 5 in-lb
Yawing Moment (Mz)	-100 to +100 in-lb	±0 5 in-lb

43

Table 4 1 Force Balance Load Limits and Accuracy [9]

Instruments Switch and Balance Unit that was wired to a Measurements Group P-3500 Digital Strain Indicator Unit to form a half-bridge circuit. The digital strain indicator unit allowed for strain to be read directly in microstrain for any applied torque with an accuracy of ±3 microstrain.

To complete the power measurements, it was also necessary to measure the rotational speed of the WVT. This was done using an Ametek Model 1723 Optical Tachometer attached to the wall inside the test section. The tachometer provided its own light source which was aimed at the nacelle end-cone. A 0.125" wide, 2" long strip of reflective tape was bonded to the end-cone, which provided the necessary light feedback to verify rotation of the WVT. Rotational speed was read directly from the unit in RPM's.

Figures 4.4 and 4.5 show this instrumentation as set up during testing.

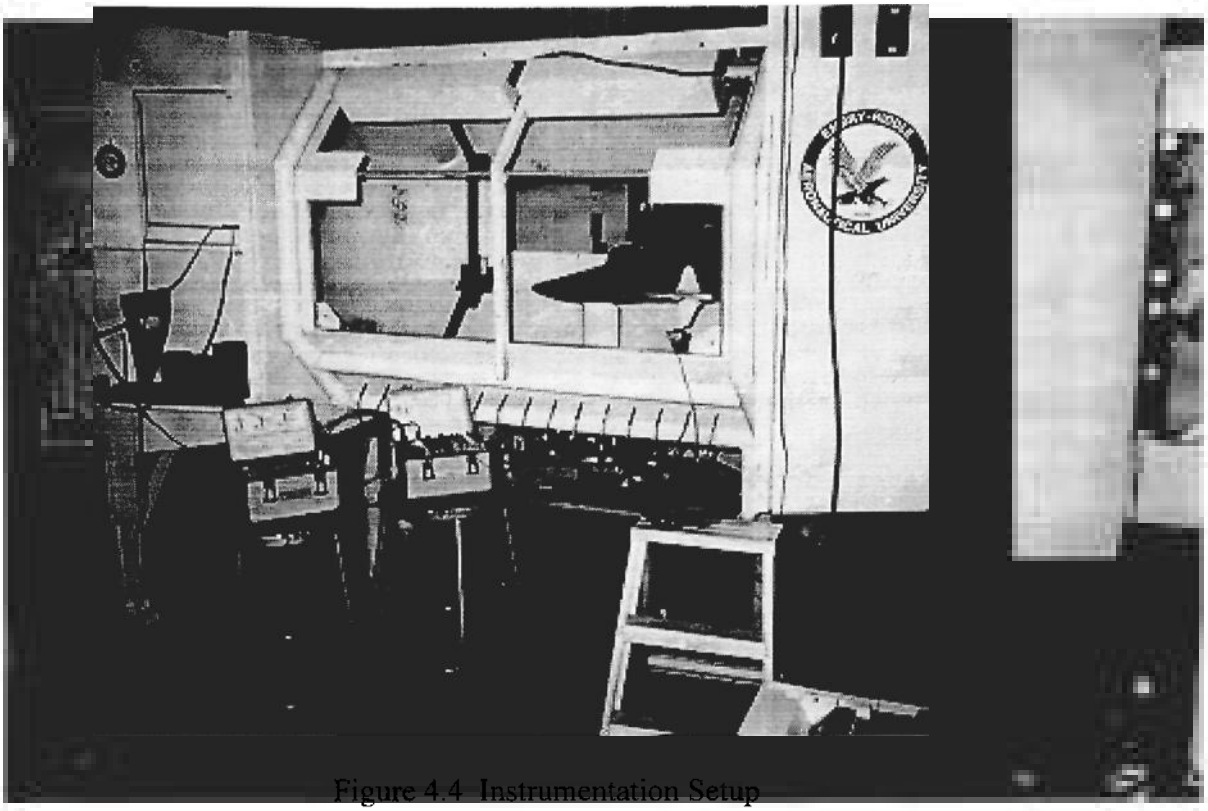

Figure 4.4 Instrumentation Setup

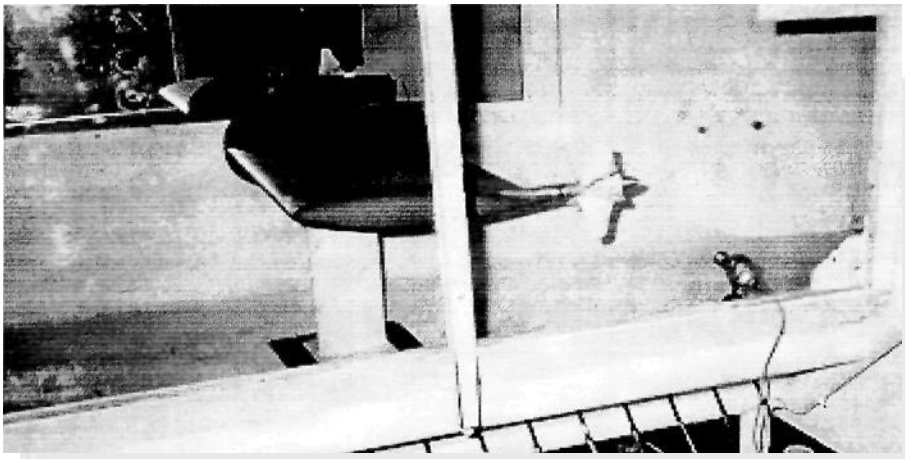

4.3 TEST PROCEDURE

4.3.1 GENERAL

Upon entering the lab, the computer, data acquisition system, and wind tunnel were powered up to record aerodynamic tare measurements that would be used throughout the tests. The semi-span wing model was then bolted to the force balance mounting post, and the angle of attack drive was zeroed using an incidence meter attached to the wing at the mean aerodynamic chord. Zero yaw was maintained throughout the tests.

The strain gage wires were routed down through the force balance fairing and test section floor and were connected to the switch and balance unit and strain indicator unit. With only the nacelle attached, the strain indicator bridge unit was balanced to read zero microstratin. The WVT was then calibrated for static torque measurements by hanging a container with known weights of lead shot on one side of the nacelle as shown in Figure 4.6. The torque calibration curve in Figure 4.7 was then drawn resulting in a linear calibration factor of 0.03472 in-lb/microstrain.

The optical tachometer was magnetically attached to the tunnel wall as shown previously in Figure 4.5.

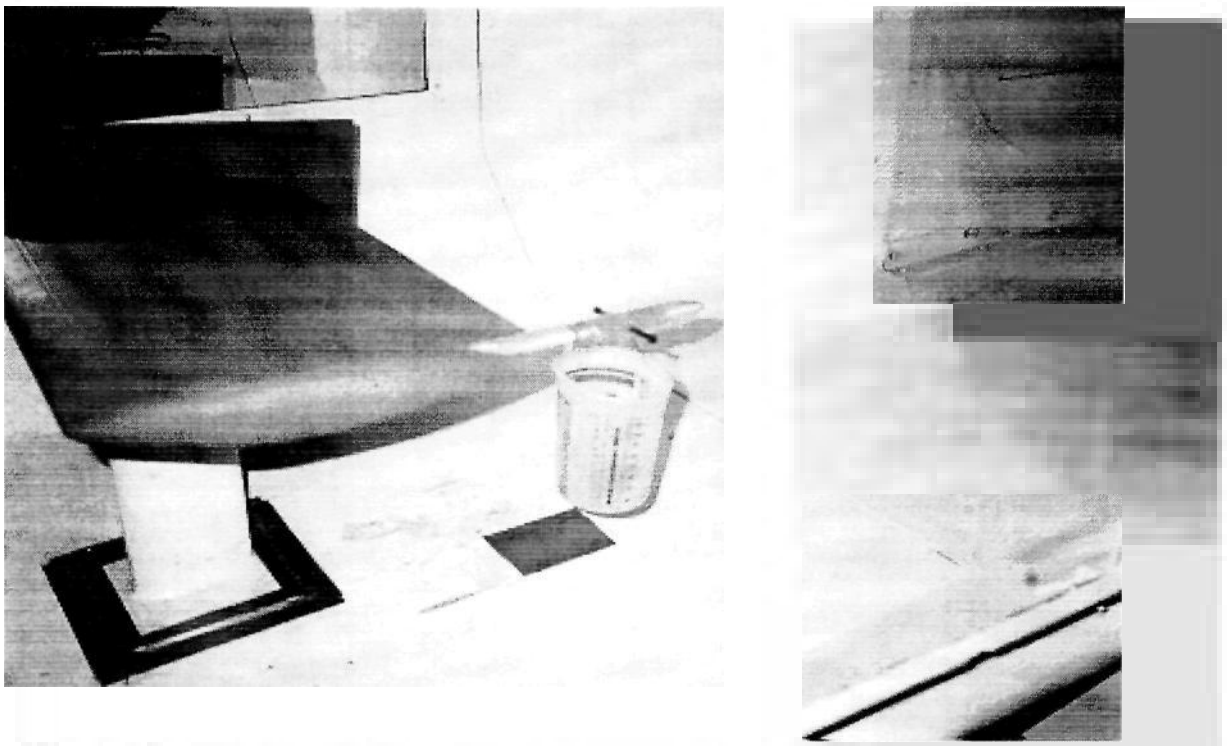

Figure 4 6 Calibration of Strain Gages for Torque Measurement

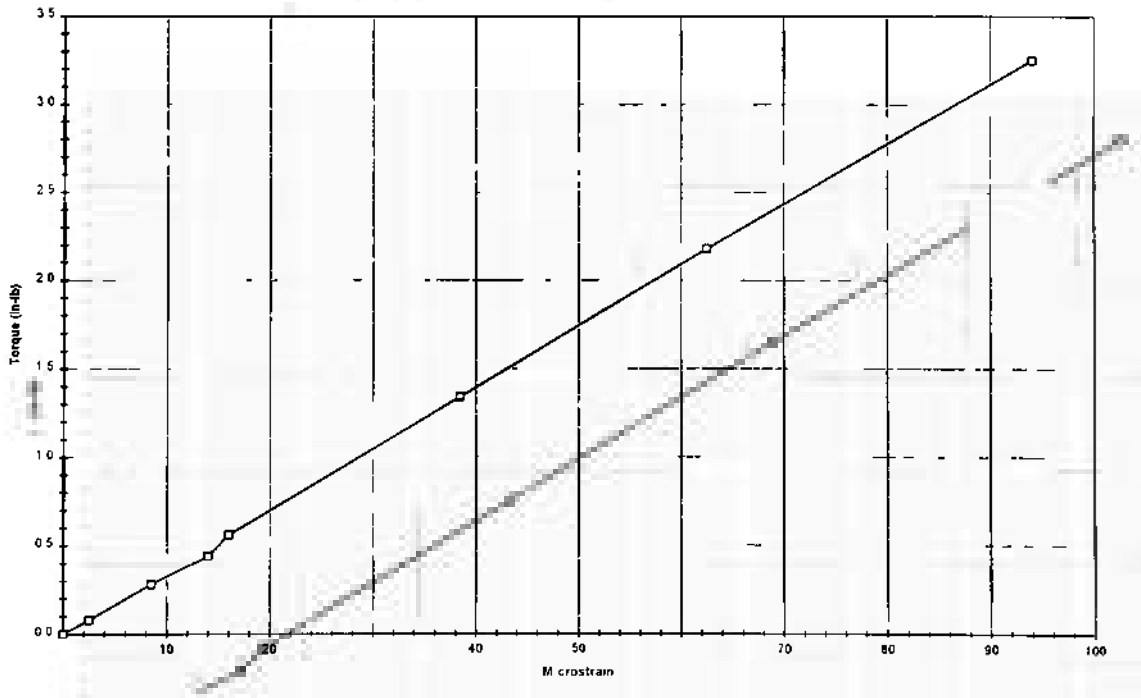

Figure 4 7 Calibration Curve for WVT Torque Output

4.3.2 STATIC WVT TESTS

The first set of tests were run to determine an optimum blade pitch angle that would result in maximum drag reduction for 2, 3, 4, 5, and 6 blades on a non-rotating WVT at the 2^{o} cruise angle of attack. Once the proper number of blades were attached to the nacelle, the clutch was tightened to lock the turbine, and a weight tare measurement was taken by the computer and data acquisition system. The blade pitch angle was varied between 0^{o} and -35^{o} in -5^{o} increments, and a set of three force balance measurements were taken for each configuration to increase the number of samples for added accuracy.

4.3.3 ROTATING WVT TESTS

The same basic procedure applied to the rotating WVT tests except, of course, that the turbine was allowed to rotate. Again, the goal was to determine the optimum blade pitch angle for each configuration that would result in maximum drag reduction. It was hypothesized that the most drag reduction would occur when the turbine was extracting the most energy from the vortex, resulting in the maximum shaft power. NASA Langley's results had indicated that the WVT produced very nearly maximum power when allowed to rotate at one-half the rotational speed under no torsional resistance loading [1]. Although power curves could have been developed for this particular WVT given more time, it was decided that the above criteria would be sufficiently accurate for the purposes of this research. For each configuration, the clutch was first loosened completely to impose no load, the tunnel was brought up to speed, and the free-spinning rotational speed was noted. The clutch was then tightened until the

rotational speed read approximately one-half that of the free-spinning case, and again three sets of force balance measurements were taken. In addition, the loaded rotational speed and torque were recorded to determine a power coefficient for each configuration.

4.3.4 STATIC WVT ALPHA SWEEPS

Once the blade pitch angle was known for the non-rotating WVT case, the blades were set at this angle, and three angle of attack sweeps were done between -5° and 15°. Force balance measurements were taken to determine off-design drag reduction for only the most efficient blade number configuration. The data for the three sweeps was then averaged for subsequent analysis.

4.3.5 ROTATING WVT ALPHA SWEEPS

The same procedure was followed for the rotating WVT case, except that the clutch was adjusted at only one loading to produce maximum rotational power for the cruise angle of attack. This would simulate a constant torque requirement as would be the case for a generator. In addition, the rotational speed and torque were recorded to determine power coefficient values over the entire angle of attack range.

Figures 4.8-4.11 show various blade number configurations being tested.

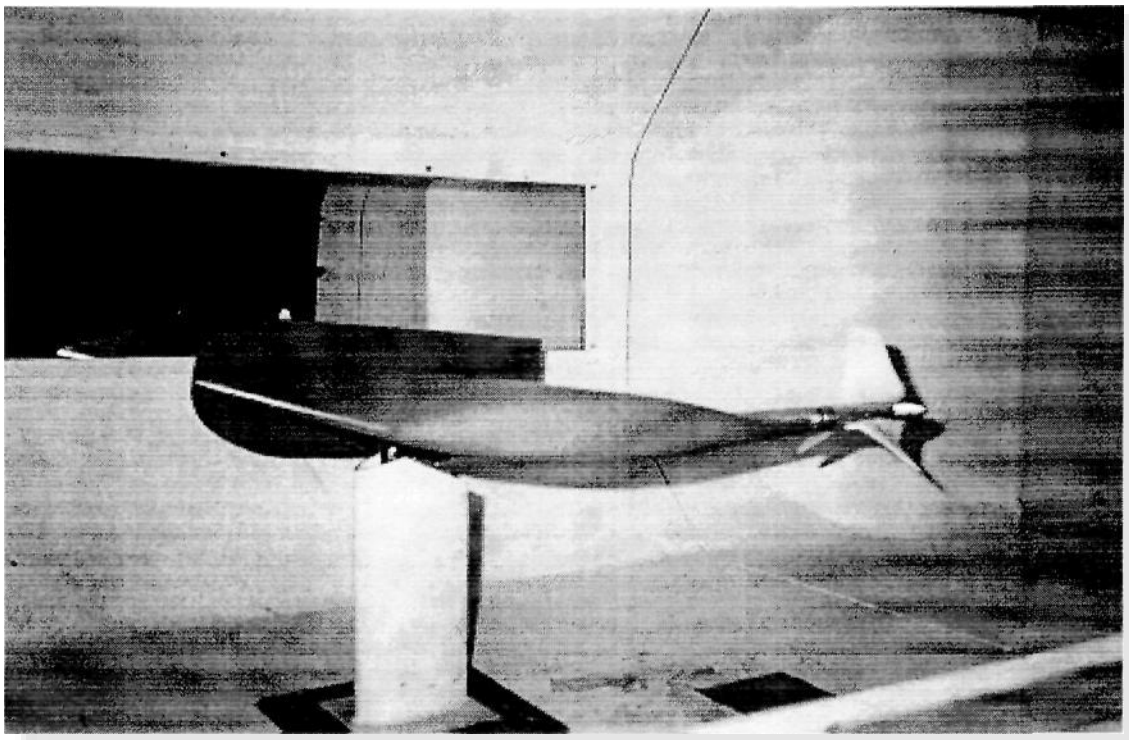

Figure 4.8 3-Bladed WVT During Testing

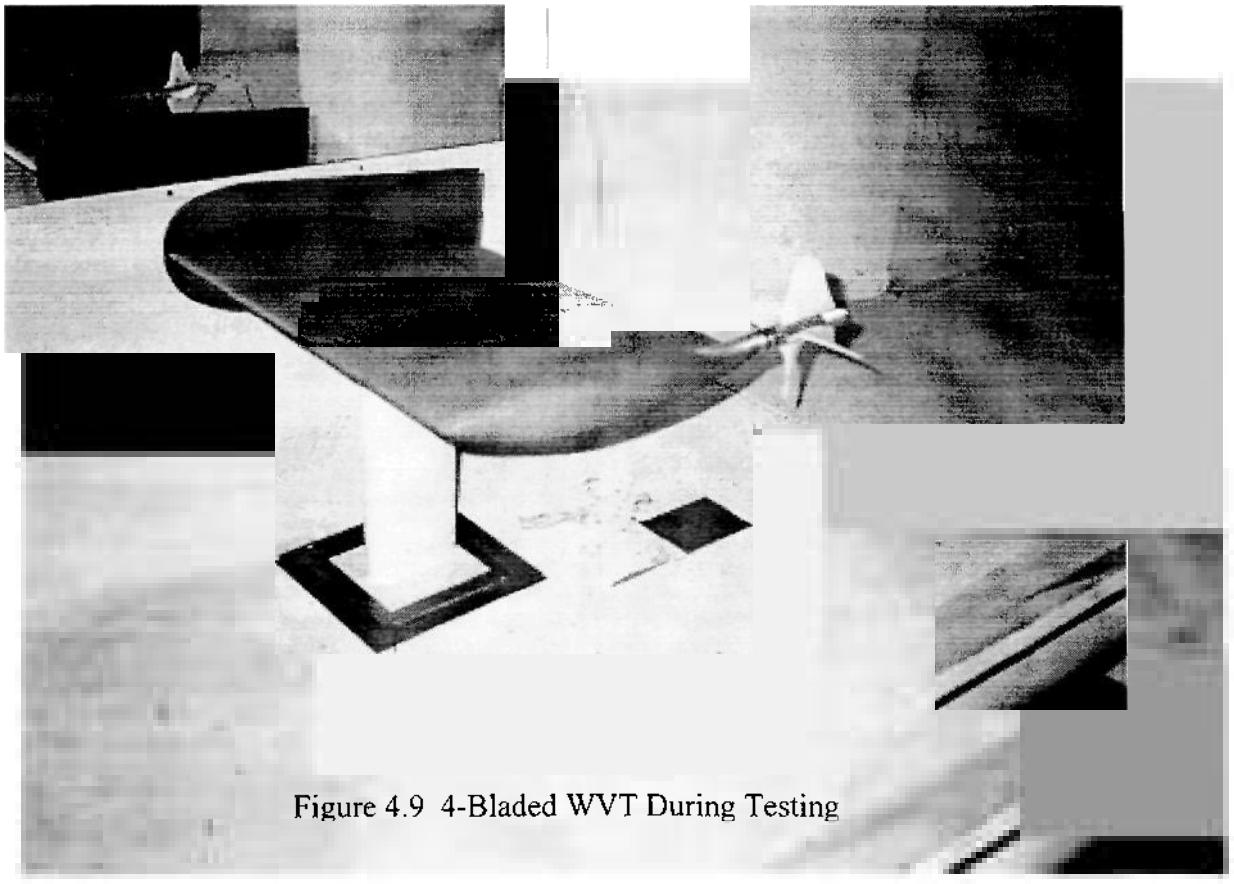

Figure 4.9 4-Bladed WVT During Testing

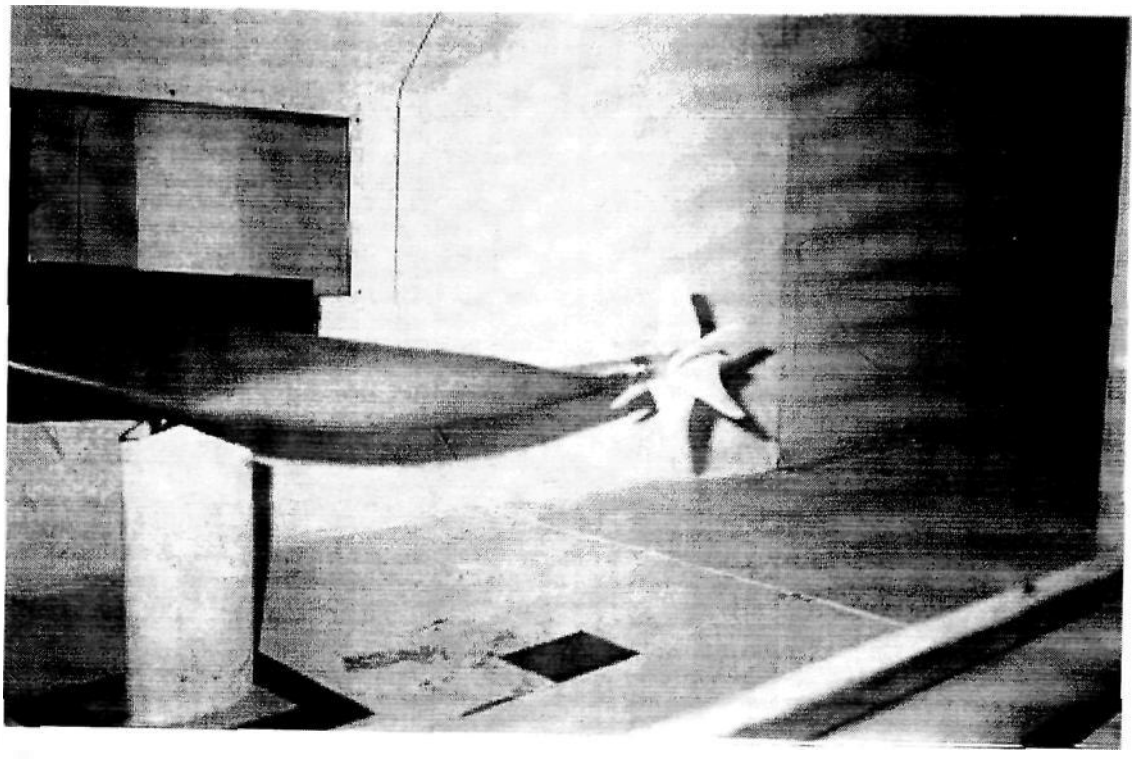

Figure 4.10 6-Bladed WVT During Testing

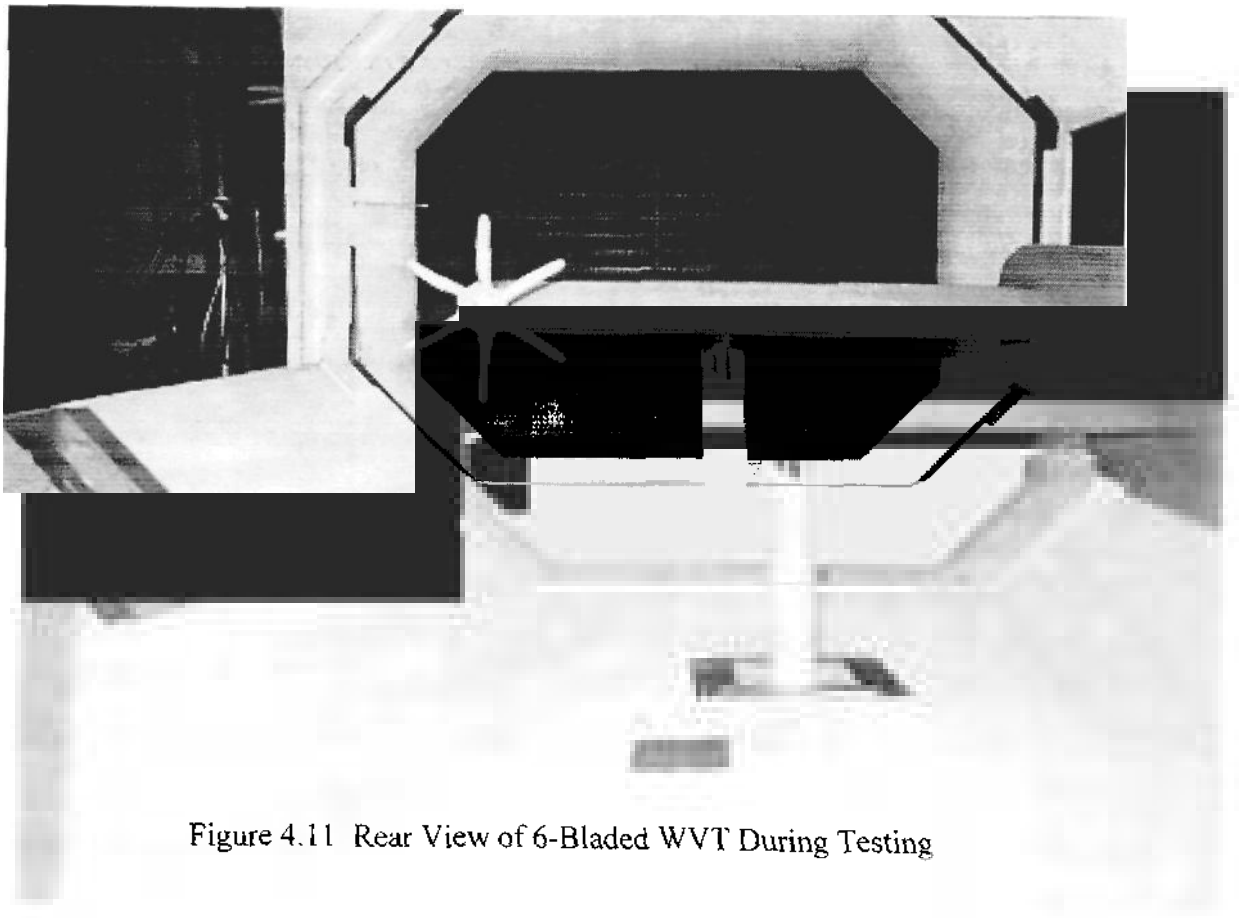

Figure 4.11 Rear View of 6-Bladed WVT During Testing

CHAPTER 5

WIND TUNNEL TEST RESULTS

5.1 CORRECTION OF DRAG COEFFICIENT FOR REYNOLDS NUMBER

Due to the higher skin friction coefficients that naturally occur at low Reynolds numbers, drag coefficient values obtained from the force balance and data acquisition system were higher than would occur under actual full-scale conditions. The following correction factor based on statistical data taken from a 1/12-scale BD-4 wind tunnel model was used to modify the drag coefficients in this research:

$$C_D)_{corrected} = C_D)_{test}\left(\frac{(RN)_{test}}{(RN)_{full-scale}}\right)^{0.20} \qquad [9]$$

The results from this equation gave reasonable drag coefficient values based on an estimated full-scale value of C_{Do}=0.015 for the wing of a Piper Cherokee [10].

5.2 STATIONARY WVT RESULTS

5.2.1 PITCH ANGLE AND BLADE NUMBER OPTIMIZATION

The results in Figure 5.1 show that the stationary WVT minimized the overall drag at a blade pitch angle of -25° for all cases. The advantage was greatest with the 6-bladed configuration resulting in a minimum C_D=0.0244. Within the range of -15° and 35° pitch angles, there was a respective 4 to 10 drag count reduction with the addition of each blade. Normally, this would indicate the favorable increase in thrust expected with a greater number of blades. However, none of the configurations actually reduced the drag coefficient below that of the wing alone as indicated in Figure 5.2, which would imply that any drag reduction that occurred by adding blades was a result of vortex flow straightening and not by an overcompensating thrust. At approximately -12° there was a crossover in the drag curves, which would indicate that the blades began to undergo the effects of flow separation, their own induced drag, or both, where any increase in the blade number or pitch angle became significantly detrimental to the overall drag.

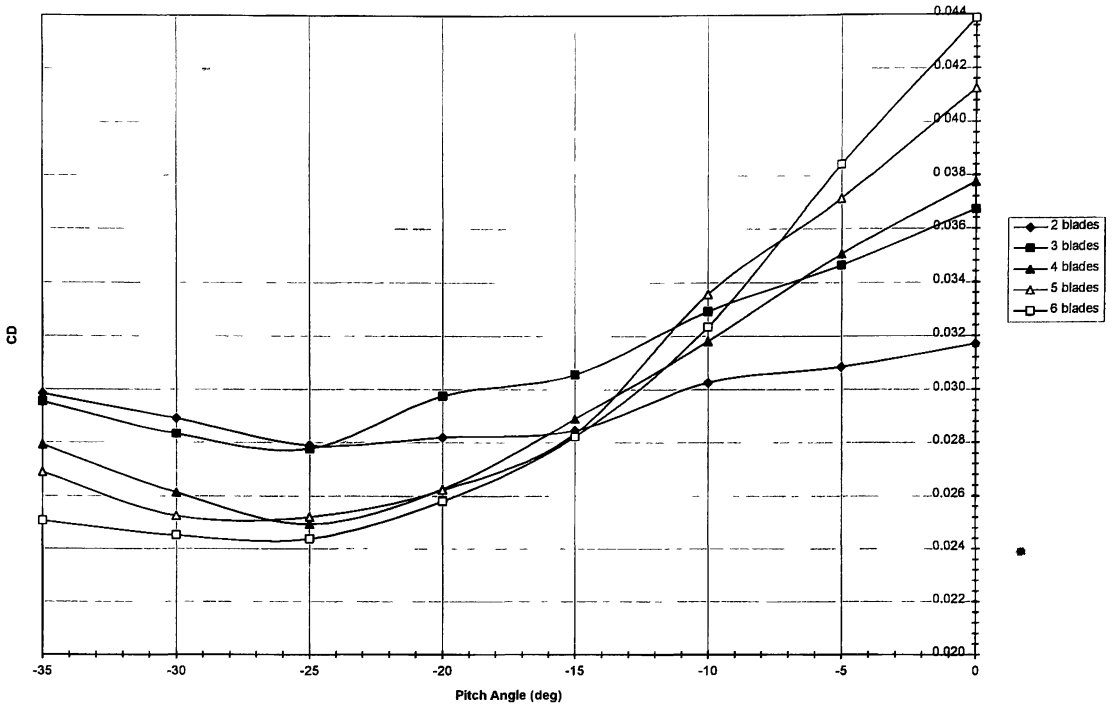

Figure 5.1 Drag Coefficient vs. Pitch Angle, Stationary WVT

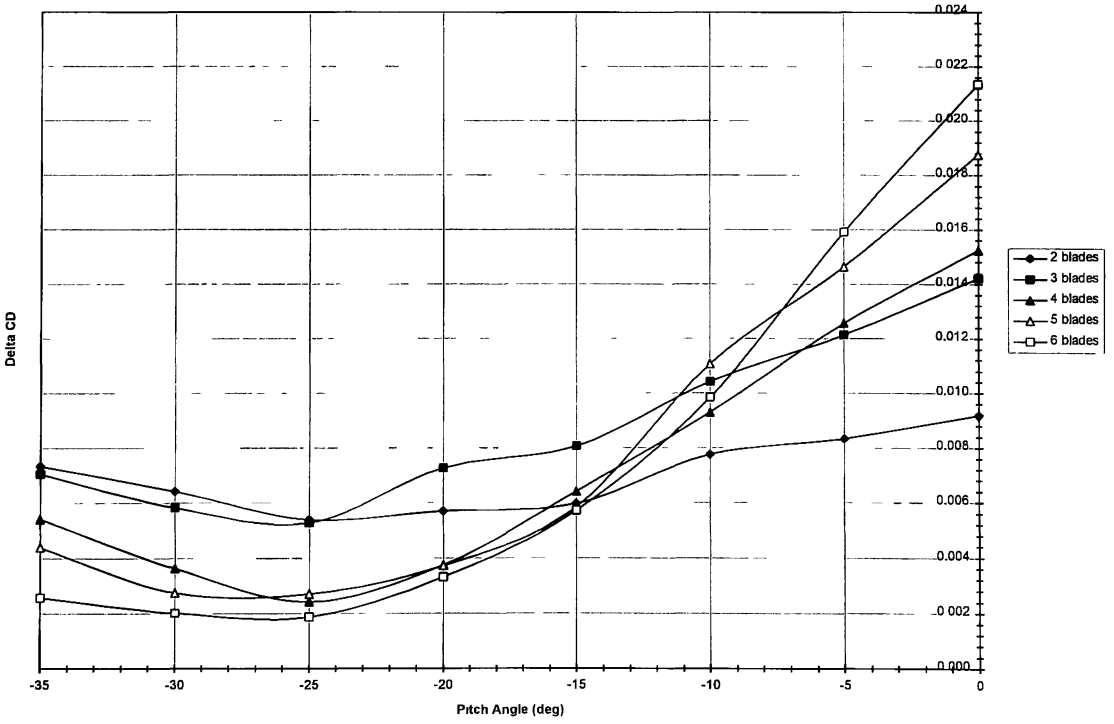

Figure 5.2 Drag Coefficient Increment vs. Pitch Angle, Stationary WVT

5.2.2 ALPHA SWEEP TEST RESULTS

Because the drag reduction between various blade number configurations was not very significant, it was decided to test only the 6-bladed WVT in the alpha sweep test, since it did produce the lowest drag of any configuration. The alpha sweep results are shown in Figure 5.3, for the blade pitch angle set at -25°. These results proved somewhat unfavorable as the overall drag coefficient was actually about 40 counts higher than that of the wing alone at the cruise C_L=0.36. However, at C_L=0.8 and higher, which could correspond to a high-angle climb condition, the WVT did lower the drag coefficient by about 20 counts.

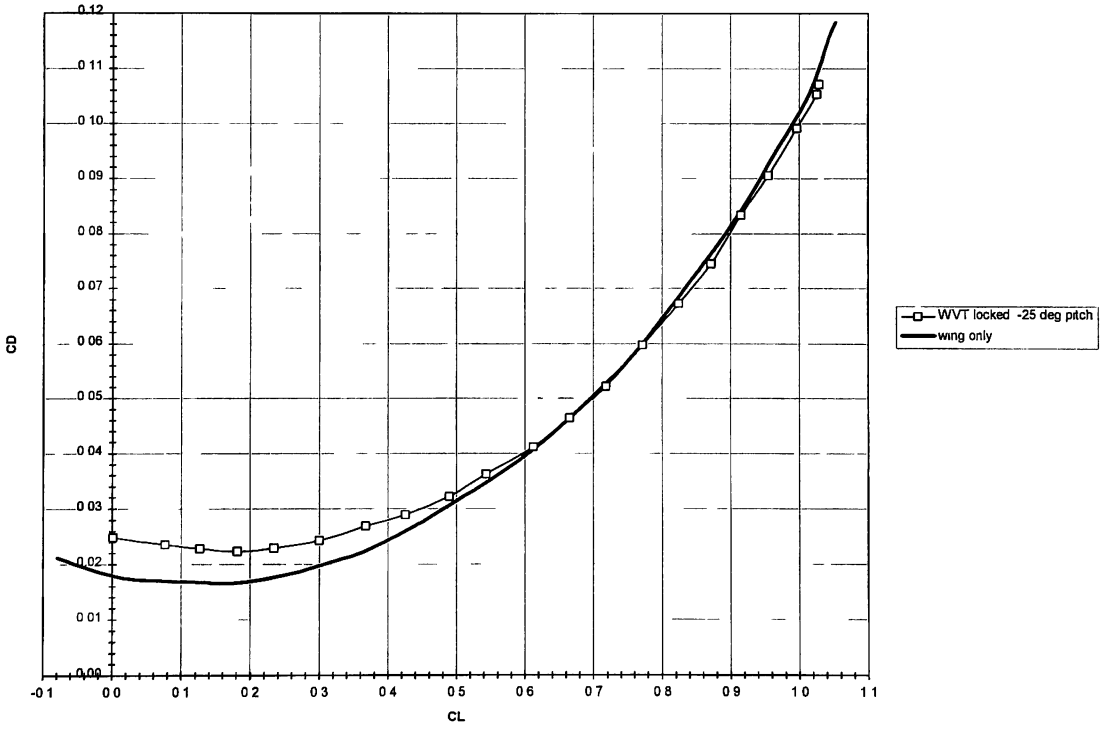

Figure 5.3 Alpha Sweep Results, Stationary WVT

5.3 ROTATING WVT RESULTS

5.3.1 PITCH ANGLE AND BLADE NUMBER OPTIMIZATION

The results of Figures 5.4 and 5.5 in determining an optimum pitch angle for the rotating WVT are not as definitive as those for the stationary case. This is probably due to the fact that although the blades had been balanced, there was still a small amount of vibration, which apparently affected the accuracy of the drag coefficient measurements. This vibration also probably varied the clutch mechanism's ability to impose a consistent torsional load, which resulted in slight variances in power extraction and, consequently, drag reduction. Because of this, the results are somewhat inconclusive in terms of determining an optimum blade number. However, the general trend for each curve is similar to those in Figure 5.1 with the minimum drag coefficients occurring at pitch angles around -20^{o}. On the whole, the measurement uncertainty in drag coefficient readings between -15^{o} and -35^{o} was reasonably small, i.e., between 5 and 10 drag counts.

Figure 5.6 illustrates the effects of blade number and pitch angle on power coefficient, both of which when increased, logically resulted in a higher power coefficient. The pitch angle used for the rotating case would normally be dictated by that which gave minimum drag and occurred at pitch angles between -30^{o} and -20^{o} It was decided again to test only the 6-bladed WVT in the alpha sweep test simply because it did produce the lowest drag in the stationary case test, but more importantly, because of the higher power output over the other configurations. This pitch angle range corresponded to relatively low power coefficients of 0.0006 and 0.0021, respectively. It was seen that higher power output could be obtained by increasing the pitch angle at the expense of

increased overall drag. As a compromise, it was seen from Figure 5.6 that the pitch could be adjusted to -15°, which would increase the power coefficient to 0.0039 for only an 18 drag count increase, a small penalty for achieving twice the power output of that at -20°.

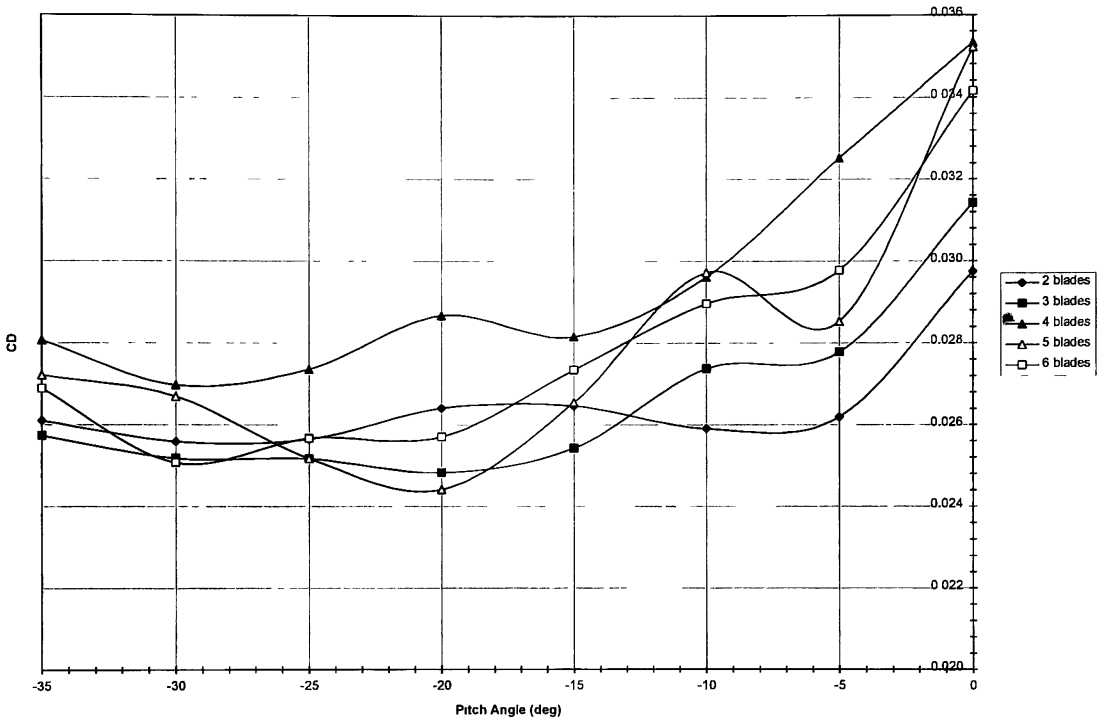

Figure 5.4 Drag Coefficient vs. Pitch Angle, Rotating WVT

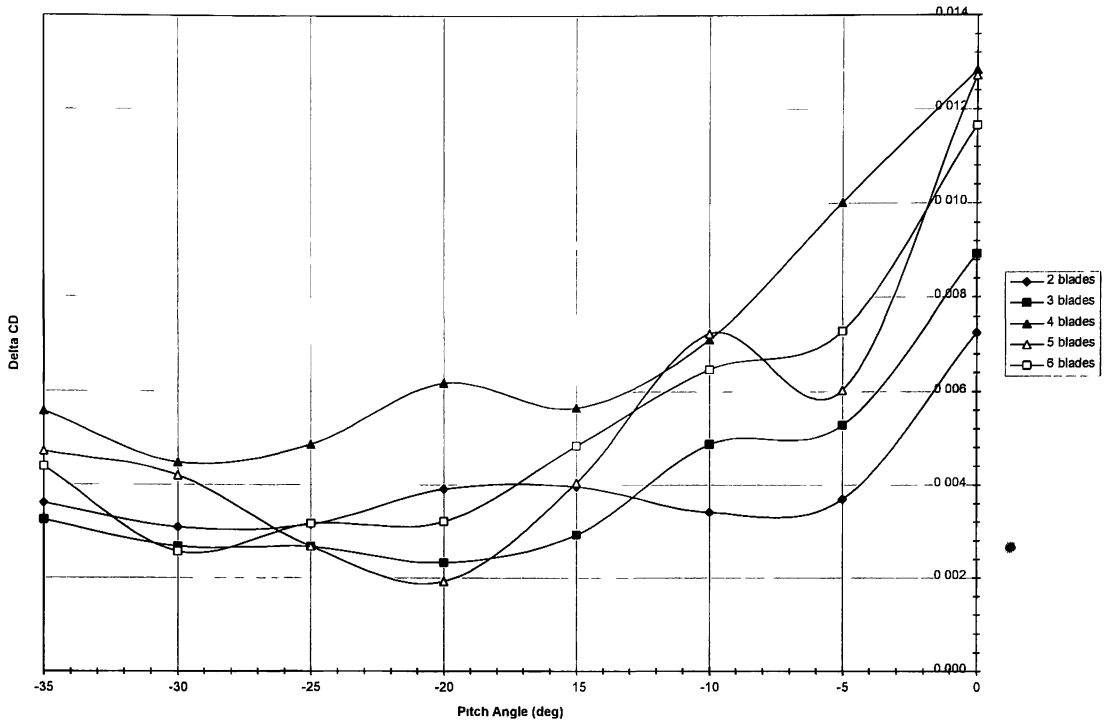

Figure 5.5 Drag Coefficient Increment vs. Pitch Angle, Rotating WVT

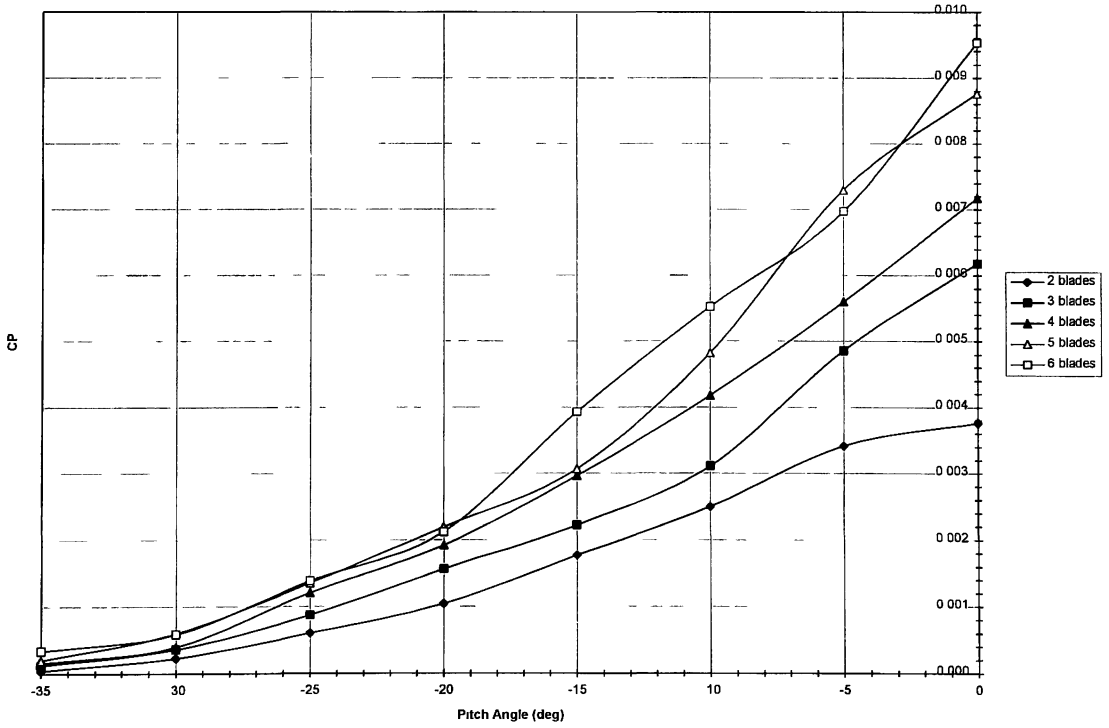

Figure 5.6 Power Coefficient vs. Pitch Angle, Rotating WVT

5.3.2 ALPHA SWEEP TEST RESULTS

The alpha sweep test results in Figure 5.7 are quite similar to those obtained with the stationary WVT in that drag reduction did not occur until C_L=0.8 and higher. Although at these lift coefficients, the rotating WVT reduced the drag from the wing alone case by about 40 counts -- twice that of the stationary case. The downside is that the drag is still higher than that of the wing alone at the cruise C_L=0.36 by about 60 counts.

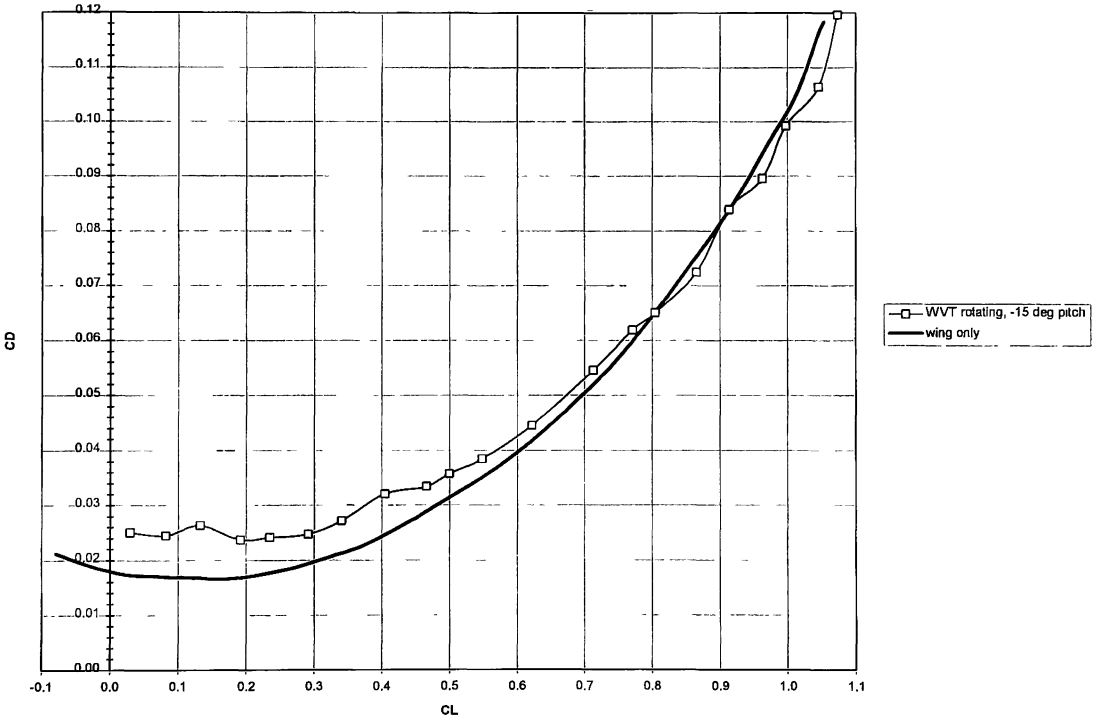

Figure 5.7 Alpha Sweep Results, Rotating WVT

5.3.3 POWER OUTPUT RESULTS

A redeeming quality is that the rotating WVT did produce a significant amount of power as illustrated by Figures 5.8 and 5.9. At cruise, the model produced a power

coefficient of 0.004 and reached a maximum of 0.0059 at a C_L=0.85, corresponding to high-angle climb conditions. The power coefficient for the WVT is given by:

$$C_{P} = \frac{2\pi\eta\tau}{qSV_{\infty}} \qquad [1]$$

where η is the rotational speed in revolutions per second, τ is the torque in ft-lb, q is the freestream dynamic pressure, S is the wing area, and V_∞ is the freestream velocity. When converted to the full-scale aircraft parameters, each turbine could produce 4.5 horsepower (3356 W) at the cruise C_L=0.36 and a maximum of 6.7 horsepower (4996 W) at C_L=0.85.

An important point to note is that the rotational speed is only dependent upon the vortex strength for a given pitch angle and not on the blade number as seen by the data in Table 5.1. However this data also indicates that power output for a given pitch angle varied according to torque output, which was dictated by the blade number.

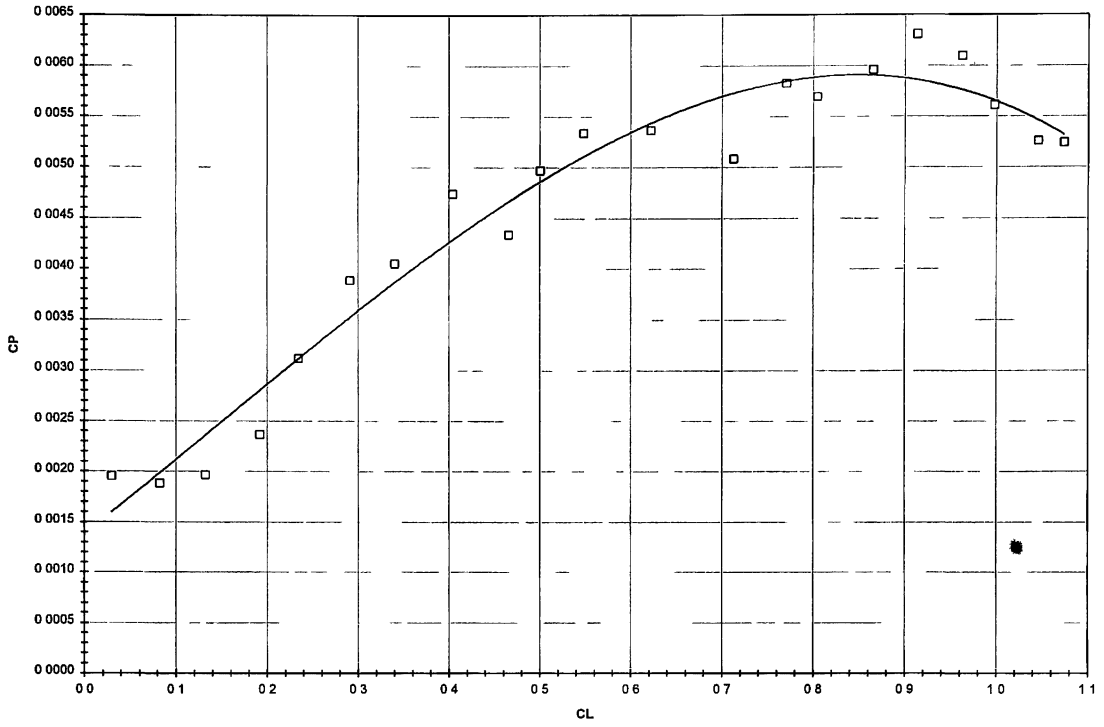

Figure 5.8 Power Coefficient vs. Lift Coefficient, -15° Pitch

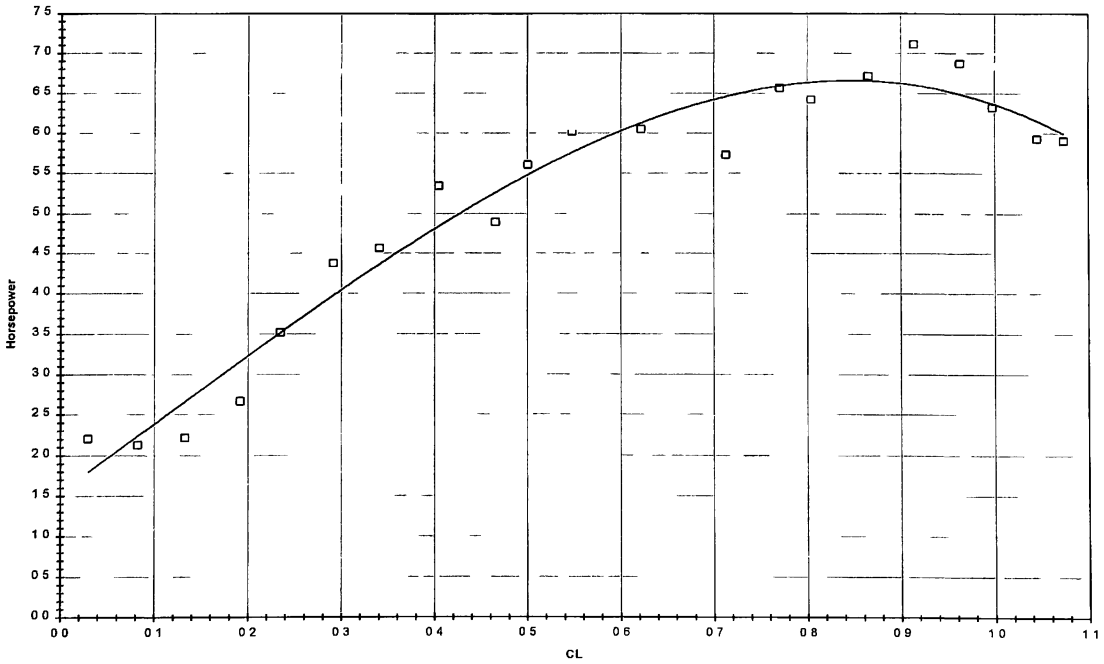

Figure 5.9 Full-Scale Power vs. Lift Coefficient, -15° Pitch

Table 5.1 Torque and Rotational Speed Measurements For All Configurations

	2 BLADES	3 BLADES	4 BLADES	5 BLADES	6 BLADES
PITCH	T (IN-LB)	T (IN-LB)	T (IN-LB)	T (IN-LB)	T (IN-LB)
-35°	0.069	0.156	0.260	0.226	0.486
-30°	0.243	0.330	0.382	0.556	0.486
-25°	0.399	0.556	0.642	0.729	0.799
-20°	0.486	0.660	0.868	0.868	0.799
-15°	0.590	0.781	1.146	1.389	1.215
-10°	0.660	1.059	1.076	1.389	1.389
-5°	0.712	1.007	1.146	1.562	1.493
0°	0.746	1.042	1.250	1.736	1.736
PITCH	RPM	RPM	RPM	RPM	RPM
-35°	200	250	190	280	220
-30°	300	350	330	340	380
-25°	480	500	600	590	550
-20°	680	750	700	800	840
-15°	950	900	820	700	1025
-10°	1200	930	1230	1100	1260
-5°	1520	1530	1550	1480	1480
0°	1600	1880	1820	1600	1740

CHAPTER 6

CONCLUSIONS AND RECOMMENDATIONS

6.1 CONCLUSIONS

6.1.1 DRAG REDUCTION

This research has shown that significant drag reduction on a general aviation aircraft through the use of a thrust-producing, 6-bladed, wingtip vortex turbine is really only possible at higher lift coefficients (C_L>0.8) corresponding to high-angle climb or slow flight conditions. At these conditions, a ΔC_D of -0.001 to -0.002 was achieved for a stationary turbine, and -0.002 to -0.004 for a rotating turbine. At and near cruise conditions, these cases added small, but not insignificant, drag coefficient increments of ΔC_D =0.004 and 0.006, respectively. It was found for this type of turbine that maximizing the number of blades, using a tapered planform, a high lift-to-drag airfoil, a twist distribution that correctly oriented each blade section to the vortex flow, and minimizing all other sources of drag were critical factors in achieving drag reduction.

The ΔC_D vs. pitch angle and C_D vs. angle of attack trends obtained for this WVT were very similar to those previously obtained by NASA Langley's wind tunnel and flight tests. However, the NASA flight-tested WVT was able to reduce the cruise drag coefficient by a maximum ΔC_D of -0.0021 in the stationary mode and -0.0016 in the rotating mode.

6.1.2 COMPARISON OF ACTUAL TO PREDICTED DRAG REDUCTION

In general, the ΔC_D results predicted by the performance program really did not correlate accurately to those obtained in the wind tunnel tests. Although, the program was an accurate means of predicting ΔC_D purely as a thrust coefficient of the blades alone, it did not take into account other sources of drag and inefficiencies that apparently were present in the actual tests.

First of all, the blades used on this WVT had a very small aspect ratio (0.31). Since such lifting surfaces are much more susceptible to vortex-dominant flows, this meant that the blades produced a significant amount of downwash of their own along most or all of the blade span. This would result in a lack of thrust owing to tip losses, a decrease in the effective blade angle of attack, and an increase in induced drag from the blades themselves. The change in angle of attack is evident from the fact that the predicted maximum drag reduction should have occurred at a pitch angle of about -40°, but the actual minimum drag occurred at -25°. Even though tip losses and induced flow angles were accounted for in the prediction program, the trends used in the code were typical of those of a higher aspect ratio blade such as an aircraft propeller.

Secondly, because the blade pitch had to be variable, the blade root was cut as a flat straight edge for clearance near the nacelle. Only the forward 30% of the chord was really accessible as this section was faired into the nacelle with clay. However, at extreme pitch angles, the discontinuity was unavoidable resulting in significant

interference drag as well as thrust losses at the root due to flow leakage similar to tip losses.

Lastly, the program did not account for the drag of the nacelle, which added a ΔC_D of 0.0021 at cruise.

6.1.3 POWER GENERATION

The 6-bladed WVT in this research produced a power coefficient of 0.004 at a cruise C_L=0.36 and a maximum of 0.0059 at a C_L=0.85. Additional power could have been produced by adjusting the pitch angle, but was set at -15° for these tests. As a side note, it is possible that drag could have been reduced further at a pitch angle between -20° and -30°, but this would have also meant a reduction in power. In terms of full-scale power for a Piper Cherokee, these power coefficients correlate to 4.5 horsepower (3356 W) and 6.7 horsepower (4996 W), respectively.

For comparison, NASA Langley's flight-tested WVT produced power within the same relative magnitudes at cruise -- 2 horsepower while achieving a ΔC_D of -0.0021 and 6 horsepower for no net drag reduction.

6.1.4 APPLICATIONS

Although NASA Langley's tests showed that the stationary turbine produced a greater drag reduction than the rotating turbine, the WVT in this research did not exhibit this characteristic. In fact, at higher lift coefficients, this particular turbine was actually more efficient at extracting power from the vortex and reducing drag while rotating than

the stationary turbine was as a thrust-producing or flow-straightening device. Therefore, it would be logical to allow the turbine to always rotate for powering onboard devices. Considering that there would be a turbine on each wingtip, these WVT's would combine to produce a total of 9 horsepower at cruise.

Single-engine aircraft use engine-driven alternators with varying power capacities depending on the system needs of the airplane. As an example, the Mooney M20J uses a 28 volt, 70 amp alternator [11], which corresponds to a power requirement of 1960 W, or 2.63 horsepower. One WVT would easily satisfy this requirement and could possibly even drive two alternators of a slightly lesser power rating, as is often the case with light twin-engine aircraft. Although an engine-driven alternator might still be needed for power during extended running time on the ground, the source could be switched over to the WVT's during flight. This would alleviate the loading on the engine and could result in an additional 2 to 3 knots of airspeed [12].

Another alternative application would be to have a WVT drive an air conditioner compressor for cabin cooling. It is unknown at the time of this writing how much power this would require from an aircraft engine, but most automobile air conditioners require 2 to 3 horsepower to run, which again, would be well within the power capabilities of this turbine.

Lastly, it is quite possible that two WVT's would be sufficient to produce enough power to drive air pumps for boundary layer control (BLC) suction or blowing devices, although no specific power requirements for this could be found at the time of this writing. As BLC methods have been found to be very successful in the past, the drag

reduction from BLC would at least negate and probably exceed the drag addition of the WVT's at cruise.

6.2 RECOMMENDATIONS

Since the changes in drag found in this research were rather small in magnitude relative to the accuracy of the instrumentation available, it would be wise to test a larger WVT on a larger test wing in higher-speed conditions to obtain greater accuracy and consistency in drag measurements. In addition, a wall-mounted force balance would aid in reducing uncertainties produced by interference effects of the wing/force balance mounting interface.

If the WVT is to be researched further as a thrust-producing device, it is recommended that a greater number of tapered, higher aspect ratio blades be used. Although this might require using a larger diameter nacelle, it would hopefully help to alleviate the problem of induced tip and root losses as well as interference drag between the blades and nacelle.

The performance program should be modified to include all present sources of drag as outlined in Section 6.1.2 to predict the drag reduction (or addition) more accurately. Better yet, CFD analysis using the more complex codes (Navier-Stokes, Euler) would probably be more accurate to predict blade loading, pressure contours, and drag reduction.

Further research in WVT's should really be geared more toward vortex flow straightening so as to lessen induced drag more directly. A new design incorporating this

philosophy would entail the above modifications as well as changes to the airfoil and twist distribution so that the blades operate more as stators rather than propellers.

Flight-testing of any WVT design would obviously be desirable.

For the reasons given in section 6.1.2, this WVT design, as a thrust-producing device, although not a complete failure, proved not to be as efficient as anticipated. In addition, since the tip vortices produced by a general aviation aircraft in flight are not especially powerful on a relative scale, based on this research, it is unlikely that thrust effects alone from a WVT would suffice to reduce the overall the drag of such an aircraft significantly. This device should probably be analyzed, configured, and tested for use on heavier transport-type aircraft that produce vortices of more significant strength as the overall benefits would be greater in magnitude.

REFERENCES

1. Patterson, J.C., Jr., Flechner, S.G., "Exploratory Wind Tunnel Investigation of a Wingtip-Mounted Vortex Turbine For Vortex Energy Recovery", NASA TP-2468, 1985.

2. Hallock, J.N., et al., "Aircraft Wake Vortices: A State-of-the-Art Review of the United States R&D Program, Final Report", Report No. DOT-TSC-FAA-77-4, U.S. Department of Transportation, Federal Aviation Administration, Washington, D.C., 1976.

3. Flechner, S.G., Jacobs, P.F., Whitcomb, R.T., "A High Subsonic Speed Wind Tunnel Investigation of Winglets on a Representative Second-Generation Jet Transport Wing", NASA TN D-8264, 1976.

4. Abeyounis, W.K., Patterson, J.C., Jr., Stough, H.P., III, Wunschel, A.J., Curran, P.D., "Wingtip Vortex Turbine Investigation for Vortex Energy Recovery", 1990 SAE Aerospace Technology Conference & Exposition, SAE Paper No. 901936, 1990.

5. Katz, J., Plotkin, A., "Low-Speed Aerodynamics, From Wing Theory to Panel Methods", McGraw-Hill, Inc., 1991.

6. Pfenninger, W., Vemuru, C.S., Mangalam, S., Evangelista, R., "Design of Low Reynolds Number Airfoils - II", AIAA Paper 88-3764-CP, 1988.

7. Lesley, E.P., "Propeller Tests to Determine the Effect of Number of Blades at Two Typical Solidities", NACA TN 698, 1938.

8. Eastlake, C.N., "Embry-Riddle Aeronautical University Experimental Aerodynamics and Wind Tunnel Laboratory Manual, 3rd Ed.", 1986.

9. Almeida, A., "Verification of Wind Tunnel Force Balance Repeatability", 1993.

10. McCormick, B.W., "Aerodynamics Aeronautics and Flight Mechanics", 2nd ed., John Wiley and Sons, Inc., 1995.

11. Moore, T., Collino, B., Ervin, E., "Viper: Wind Tunnel Verification of a Student-Designed Aircraft's Performance Through the Use of a Scale Model", 1994.

12. Mooney Aircraft Corporation, "Mooney M20J Information Manual", 1989.

13. Lombardo, D.A., "Aircraft Systems: Understanding Your Airplane", McGraw-Hill, Inc., 1988.

APPENDIX A

FIVE-HOLE PROBE CALIBRATION DATA

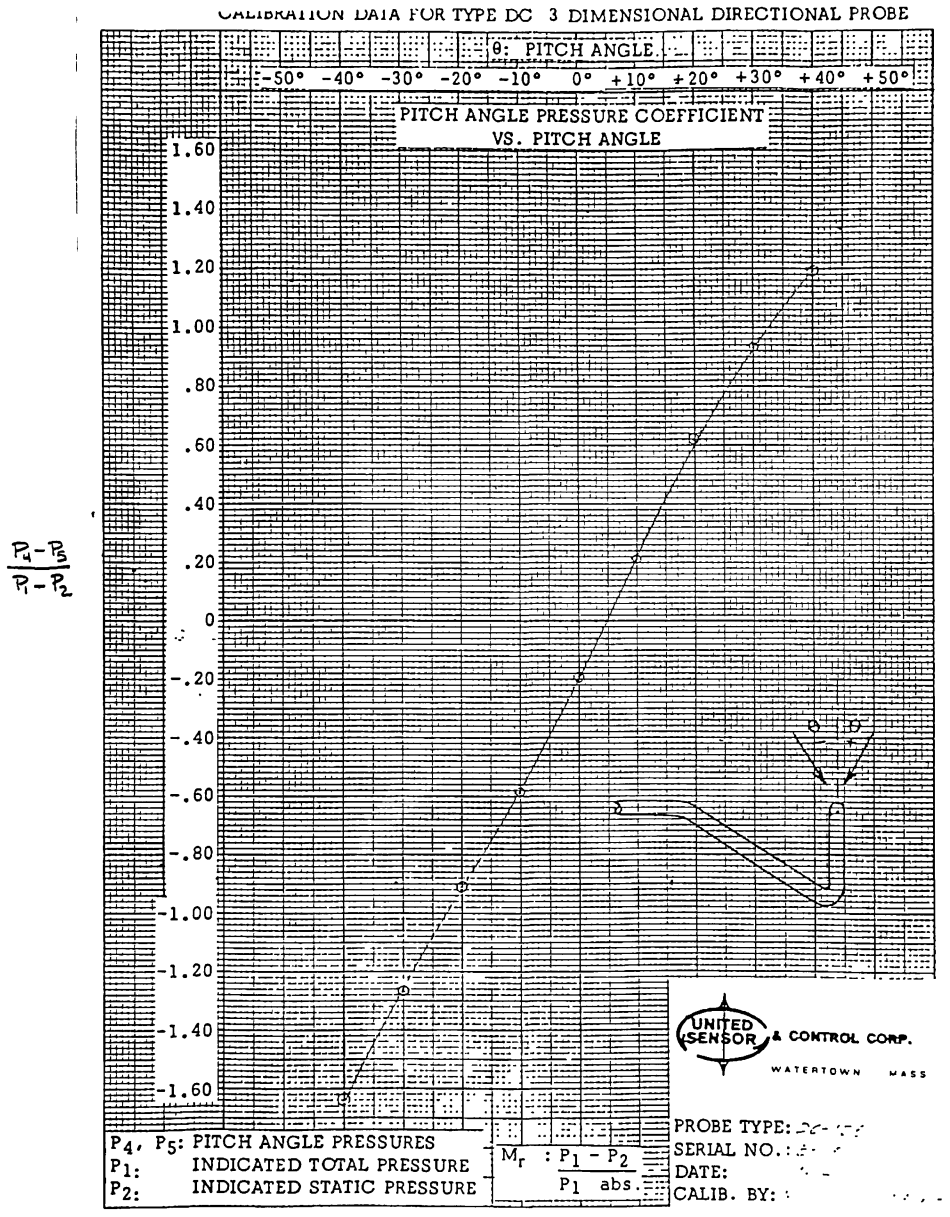

Figure A.1 Pitch Angle Calibration Curve for DC-125-12-CD Probe

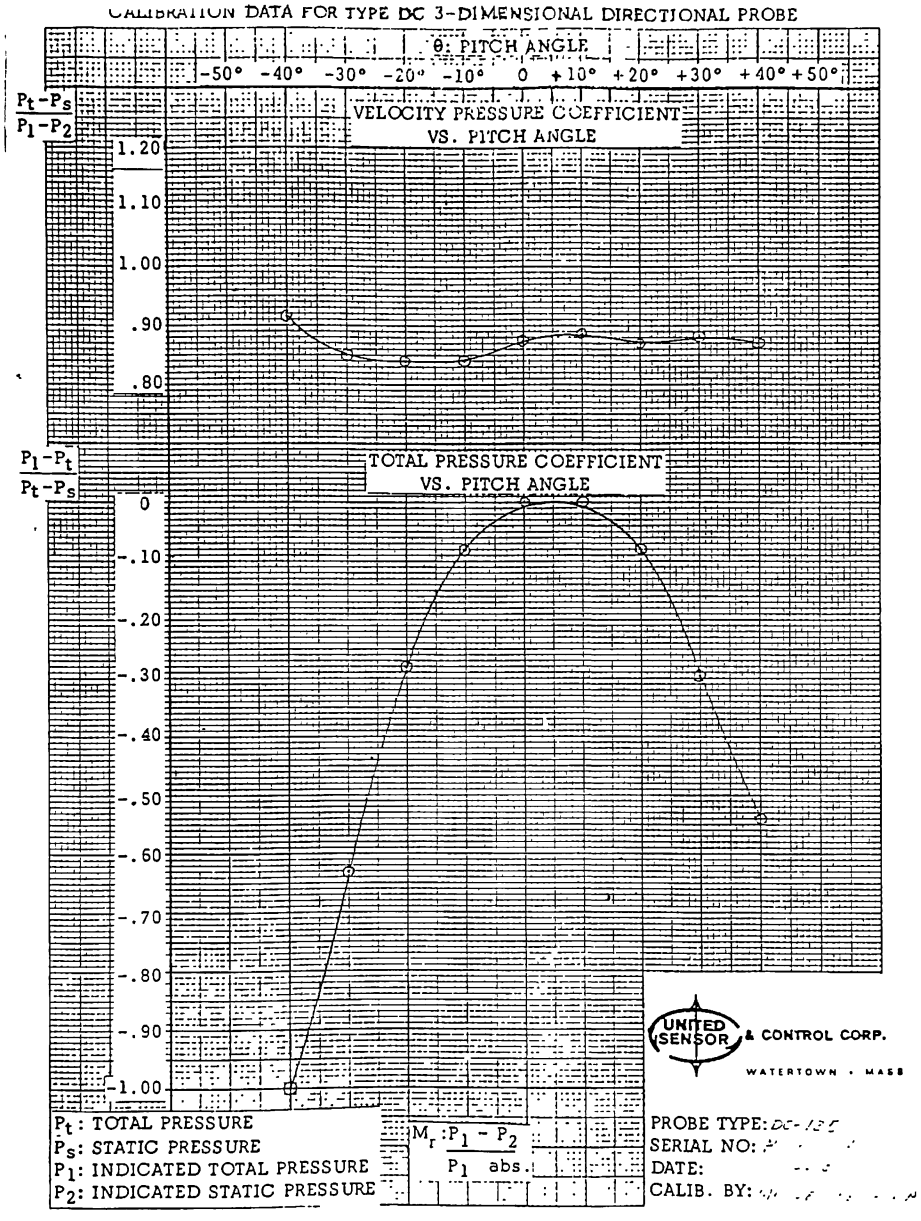

Figure A.2 Velocity and Total Pressure Calibration Curves for DC-125-12-CD Probe

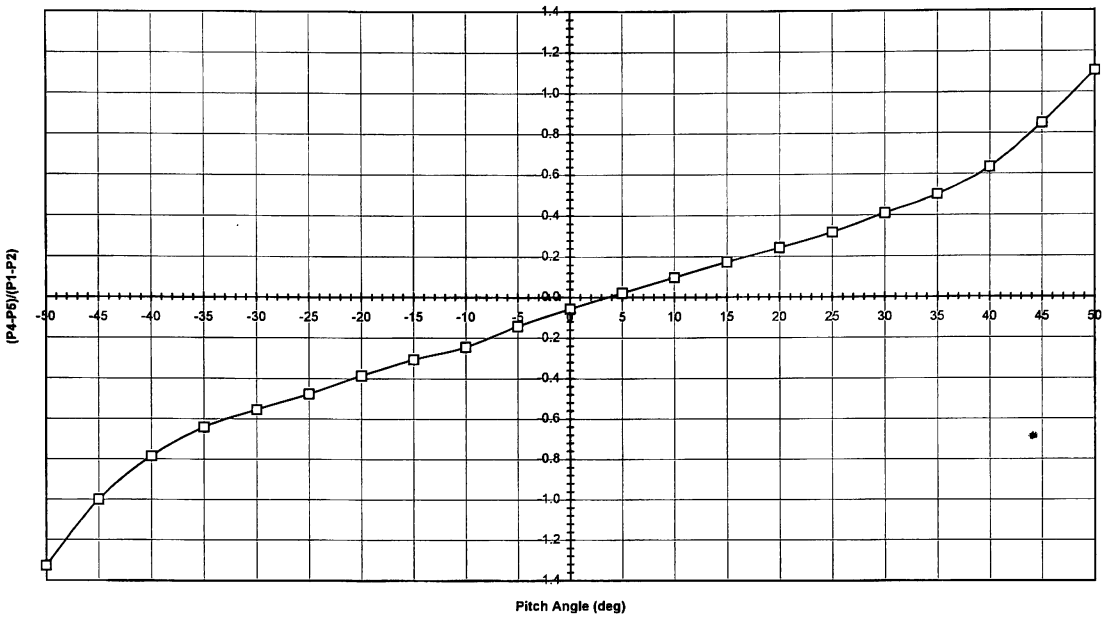

Figure A.3 Pitch Angle Calibration Curve for SDC-12-6-15°-.250 Probe

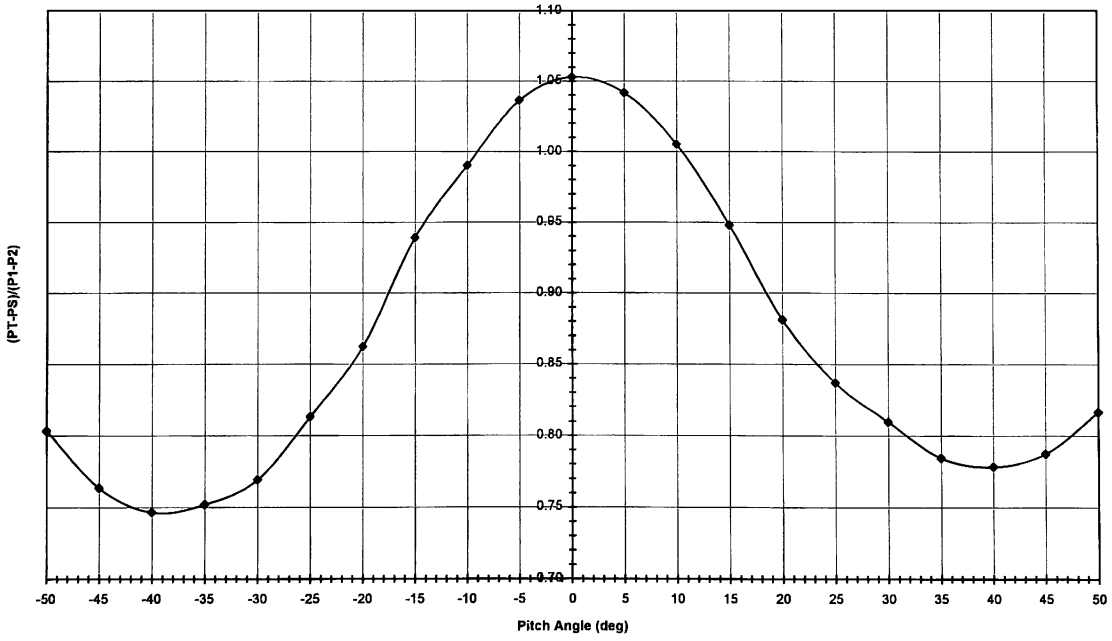

Figure A.4 Velocity Calibration Curve for SDC-12-6-15°-.250 Probe

APPENDIX B

WVT PERFORMANCE PREDICTION PROGRAM AND SAMPLE OUTPUT

WVT PERFORMANCE PREDICTION PROGRAM

PROGRAM DESCRIPTION

The WVT performance program was written by the author as a means to predict the thrust and static torque output of any non-rotating WVT in any flow situation. It was written in FORTRAN 77, and uses a combination of axial momentum and blade element theories, which is a common analytical method used in propeller analysis and design. These theories will not be discussed here for brevity, but can be found in many good aerodynamics references. Propeller and turbine blades are generally dominated by vortex-induced flow owing to their relatively low aspect ratios, which means that an induced flow term must be included in any computations at each spanwise location for proper prediction. The advantage of these combined theories is that an induced flow angle can be computed for each station which influences the effective angle of attack of the blade section. Therefore, only airfoil section data is needed to compute the blade characteristics.

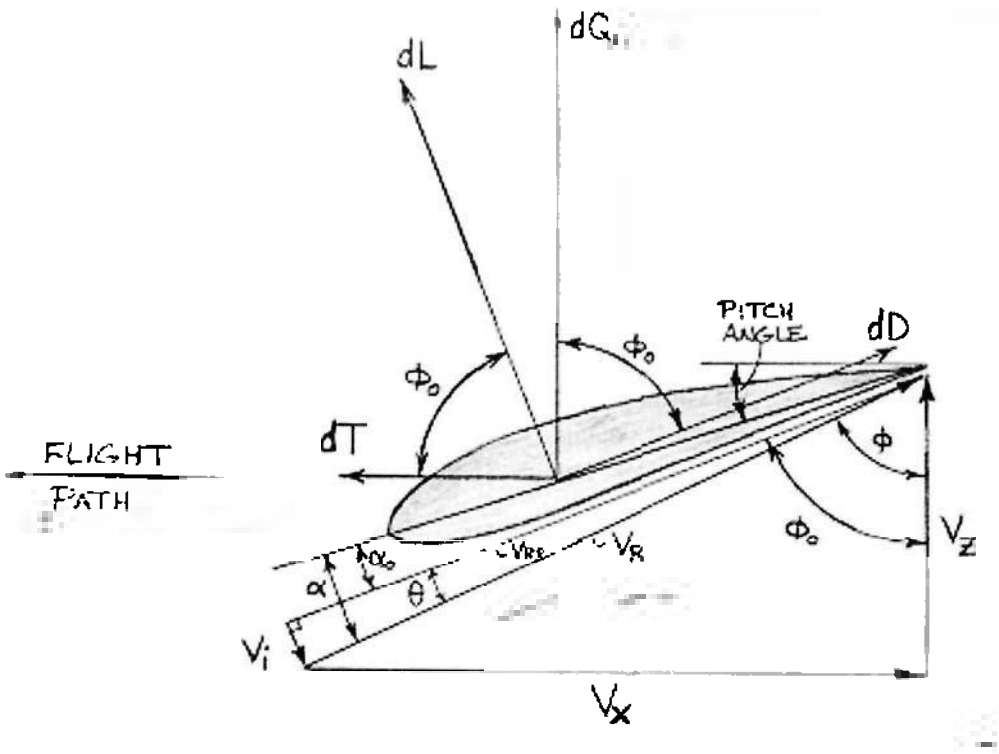

Figure B.1 WVT Blade Section and Variable Nomenclature

Figure B 1 illustrates a typical blade section and the nomenclature that follows that given in the program. Since the blades in this research were optimized for thrust production, it should be noted that only the incremental lift and drag force components perpendicular to the WVT centerline combine to create the torque, while only the incremental lift and drag forces parallel to the WVT centerline create the thrust. Therefore, it is not only imperative that the lift force be greater than the drag force, but the angle at which the two form a resultant thrust must be oriented as far forward as possible, which is a function of the blade pitch angle setting

The program is documented for clarity but the algorithm and equations will be reviewed here:

1) The user is asked to input the radial dimensions of the nacelle (HUBR) and the overall turbine (R);

2) The user enters the tunnel speed (VINF), ambient density (RHO), and wing area (S);

3) The user enters the previously-measured vortex axial (VF) and tangential velocities (VT) at spanwise locations (X) spaced 0.1" apart; From these, the angle (PHI) and the resultant velocity (VR) are calculated:

$$\phi = \arctan\left(\frac{V_F}{V_T}\right)$$

$$V_R = \sqrt{(V_F)^2 + (V_T)^2}$$

4) The user enters the blade chord length (C) at each corresponding spanwise location, and the number of blades (B); The individual blade area (BLAREA) is calculated by a summation of values, and the solidity (SOLID) is calculated by:

$$\sigma = \frac{B * BLAREA}{\pi R^2}$$

5) The user enters the airfoil lift curve slope (AO) and the lift curve CL intercept (Z), and the desired pitch angle (BETA) at each spanwise location (X). The induced flow angle (THETA), the angle (PHIO), and the effective lift coefficient (CL) are then calculated:

$$\theta = \frac{-(\sin\phi + \frac{a_o\sigma}{8x}) + \sqrt{(\sin\phi + \frac{a_o\sigma}{8x})^2 + \frac{\sigma\cos\phi}{2x}(a_o\beta + z - a_o\phi)}}{2\cos\phi}$$

$$\phi_o = \phi + \theta$$

$$c_l = [a_o(\beta - \phi - \theta)] + z$$

For each spanwise location, the user is then asked to enter the airfoil section drag coefficient (CD) that corresponds to the above lift coefficient.

6) The program computes the spanwise thrust increments (DCTDX) and torque increments (DQDX) for each location:

$$\frac{dC_T}{dx} = \left(\frac{V_R^2 C}{V_F^2 S}\right)(\cos^2\theta)(c_l \cos\phi_o - c_d \sin\phi_o)$$

$$\frac{dQ}{dx} = \left(\frac{\rho V_R^2 CXR}{2}\right)(\cos^2\theta)(c_l \sin\phi_o + c_d \cos\phi_o)$$

7) These thrust and torque increments are numerically integrated over the entire blade span, and ΔC_D (CT) and static torque (Q) for the entire WVT are computed and shown along with the individual blade area and WVT solidity;

8) The user is asked if any changes in blade planform, blade number, airfoil characteristics, or blade twist distribution are necessary, at which point the program will loop back to the necessary point for variable changes.

This program is rather tedious and time-consuming to input all of the necessary information, but does give reasonable results nonetheless. It must be noted that the reduction in drag predicted by this program does not include the effects of flow separation due to adverse pressure gradients, interference drag, or viscous drag on the nacelle.

WVT PERFORMANCE PROGRAM CODE

```
C       Wingtip Vortex Turbine (WVT) Performance Prediction Program
C       Written by Andy Roberts in support of thesis research on WVT's.
C       November 1, 1996
C
C       This program predicts the thrust and torque output of a wingtip vortex
C       turbine based on combined axial momentum and simple blade element
C       theories.  This thrust is outputted in the form of a delta drag
C       coefficient, and does NOT include the drag increase due to the nacelle,
C       adverse pressure gradients, or interference effects.
C
C
C
C
C       All variables used in the program are defined.
C
        REAL PI, R, HUBR, XV, VF(500), VT(500), PHI(500), VR(500), SUM, XC
        REAL C(500), CPART(500), BLAREA, SOLID, AO, Z, BETA(500), THETA(500)
        REAL PHIO(500), CL(500), CD(500), FACT, DCTDX(500), DQDX(500)
        REAL FIX, SUMT, SUMQ, CT, Q, NX, NXC, NXV, X(500), VINF, RHO, S
        INTEGER PTS, I, J, K, B
        CHARACTER*1 CHANGE
        PI=3.1415926585
C
C
C
C
C       Basic WVT dimensions are entered.  The variable "PTS" denotes the
C       number of stations to be analyzed along the blade span, spaced 0.1"
C       apart.
C
        PRINT*, 'ENTER THE DESIRED TOTAL WVT (HUB+BLADE) RADIUS IN INCHES: '
        READ*, R
        PRINT*, 'ENTER THE DESIRED HUB RADIUS IN INCHES: '
        READ*, HUBR
        PTS=((R-HUBR)*10)+1
C
C
C
C
C       User enters airspeed, air density, wing model area, and axial and
C       tangential vortex flow speeds, from which a flow angle "PHI" is
C       calculated for each spanwise blade station.
C
        PRINT*,'ENTER THE FREESTREAM TUNNEL VELOCITY (FT/S): '
        READ*, VINF
        PRINT*,'ENTER THE AMBIENT AIR DENSITY (SLUG/FT^3): '
        READ*, RHO
        PRINT*,'ENTER THE TEST WING AREA (IN^2): '
        READ*, S
C
        XV=HUBR/R
```

```
      DO 50 I=1,PTS
      NXV=XV*R
      PRINT 40, NXV
40    FORMAT (1X,'ENTER THE AXIAL AND TANGENTIAL VELOCITY COMPONENTS (FT/S)
     +AT X= ',F4.2,' IN.')
      READ*, VF(I), VT(I)
      PHI(I)=ATAN(VF(I)/VT(I))
      VR(I)=SQRT(((VF(I))**2)+((VT(I))**2))
      XV=XV+(.1/R)
50    CONTINUE
C
C
C
C
C     User enters blade chord at each spanwise location to give the desired
C     planform to be analyzed.  Also, the blade area and solidity are
C     computed.
C
55    SUM=0
      XC=HUBR/R
      DO 70 J=1,PTS
      NXC=XC*R
      PRINT 60, NXC
60    FORMAT (1X,'ENTER THE DESIRED CHORD LENGTH IN INCHES AT X= ',F4.2,' IN.')
      READ*, C(J)
      IF (XC.EQ.(HUBR/R)) THEN
            CPART(J)=C(J)/2
      ELSEIF (XC.EQ.1) THEN
            CPART(J)=C(J)/2
      ELSE
            CPART(J)=C(J)
      ENDIF
      SUM=SUM+CPART(J)
      XC=XC+(.1/R)
70    CONTINUE
      BLAREA=((R-HUBR)/(PTS-1))*SUM
75    PRINT*, 'ENTER THE DESIRED NUMBER OF BLADES: '
      READ*, B
      SOLID=(B*BLAREA)/(PI*((R)**2))
C
C
C
C
C     Airfoil lift curve slope and CL axis intercept data is entered.  The
C     induced flow angle "THETA" is computed for each station.  This angle
C     modifies the local angle of attack for each blade section, the section
C     lift coefficient is calculated, and the section drag coefficient is
C     then entered by the user for each spanwise location.  A typical factor
C     "FACT" is calculated to account for lift losses near the blade tip.
C
80    PRINT*, 'ENTER THE BLADE AIRFOIL LIFT CURVE SLOPE IN UNITS OF /DEG: '
      READ*, AO
      PRINT*, 'ENTER THE BLADE AIRFOIL CL AXIS INTERCEPT: '
      READ*, Z
```

```
85      X(1)=HUBR/R
        DO 100 K=1,PTS
        NX=X(K)*R
        PRINT 90, NX
90      FORMAT (1X,'ENTER THE BLADE PITCH ANGLE IN DEGREES AT X= ',F4.2,' IN.')
        READ*, BETA(K)
C
        THETA(K)=(-(SIN(PHI(K))+(AO*57.3*SOLID)/(8*X(K)))+SQRT(((SIN(PHI(K))
   +    +(AO*57.3*SOLID)/(8*X(K)))**2)+(SOLID*COS(PHI(K)))*((AO*BETA(K))+Z
   +    -(AO*57.3*PHI(K)))/(2*X(K))))/(2*COS(PHI(K)))
C
        PHIO(K)=PHI(K)+THETA(K)
        CL(K)=(AO*57.3*((BETA(K)/57.3)-PHI(K)-THETA(K)))+Z
        PRINT 91, CL(K)
91      FORMAT (1X,'ENTER CD FOR THE BLADE AIRFOIL AT A CL OF ',F4.2)
        READ*, CD(K)
C
        IF (X(K).GE.0.95.AND.X(K).LE.1.0) THEN
                FACT=-19.394+(19.394/X(K))
        ELSE
                FACT=1.0
        ENDIF
C
C
C
C
C       The incremental thrust "DCTDX" is calculated in the form of a
C       coefficient directly from the lift and drag coefficients, and
C       incremental torque "DQDX" is computed for each spanwise station.
C
        DCTDX(K)=FACT*(((VR(K)**2)*C(K))/((VINF**2)*S))*((COS(THETA(K)))**2)*
   +    ((CL(K)*COS(PHIO(K)))-(CD(K)*SIN(PHIO(K))))
C
        DQDX(K)=FACT*0.5*RHO*(VR(K)**2)*(C(K)*X(K)*R/144)*((COS(THETA(K)))**2)*
   +    ((CL(K)*SIN(PHIO(K)))+(CD(K)*COS(PHIO(K))))
C
        X(K+1)=X(K)+(.1/R)
100     CONTINUE
C
C
        PRINT*,'SPANWISE THRUST COEFFICIENT AND TORQUE DISTRIBUTION:'
        PRINT*,'  X/C       DCT/DX       DQ/DX'
        PRINT*
        DO 105 K=1,PTS
        PRINT 103, X(K), DCTDX(K), DQDX(K)
103     FORMAT (1X,F5.3,7X,F9.6,8X,F7.3)
105     CONTINUE
C
C
C
C       The thrust coefficient for the entire WVT is calculated in the form of
C       a delta drag coefficient to be subtracted directly from the drag
C       coefficient of the wing.  The total static torque is also calculated.
C
```

```
      FIX=((1-(HUBR/R))*R)/(PTS-1)
      SUMT=DCTDX(1)/2
      SUMQ=DQDX(1)/2
      DO 110 L=2,PTS
      SUMT=SUMT+DCTDX(L)
      SUMQ=SUMQ+DQDX(L)
110   CONTINUE
      CT=B*FIX*SUMT
      Q=B*FIX*SUMQ
      PRINT*
      PRINT*
      PRINT*
      PRINT 115, CT
115   FORMAT (1X,'THE DELTA DRAG COEFFICIENT IS dCD= - ',F9.6)
      PRINT 120, Q
120   FORMAT (1X,'THE TOTAL TORQUE IS Q= ',F7.3,' IN-LB')
      PRINT 125, BLAREA
125   FORMAT (1X,'THE INDIVIDUAL BLADE AREA IS= ',F6.2,' IN^2')
      PRINT 130, SOLID
130   FORMAT (1X,'THE WVT SOLIDITY IS= ',F5.3)
C
C
C
C
C     The user is asked if any changes are necessary.
C
      PRINT*,'WHAT WOULD YOU LIKE TO CHANGE?'
      PRINT*,'CHORD DISTRIBUTION (C)'
      PRINT*,'NUMBER OF BLADES (B)'
      PRINT*,'AIRFOIL CHARACTERISTICS (A)'
      PRINT*,'BLADE PITCH ANGLE DISTRIBUTION (P)'
      PRINT*,'NOTHING (N)'
      READ*,CHANGE
      IF (CHANGE.EQ.'C') THEN
            GO TO 55
      ELSEIF (CHANGE.EQ.'B') THEN
            GO TO 75
      ELSEIF (CHANGE.EQ.'A') THEN
            GO TO 80
      ELSEIF (CHANGE.EQ.'P') THEN
            GO TO 85
      ELSE
      ENDIF
      END
```

SAMPLE OUTPUT

The following output shows the performance characteristics of the optimized straight-tapered and elliptical blades, respectively, for a turbine using 6 blades.

0.45 STRAIGHT TAPERED
6 BLADES
OPTIMIZED FOR DRAG REDUCTION AT APPROX. -40 DEG PITCH

SPANWISE THRUST COEFFICIENT AND TORQUE DISTRIBUTION:

X/C	DCT/DX	DQ/DX
0.143	0.001735	0.035
0.171	0.001670	0.052
0.200	0.001682	0.078
0.229	0.001591	0.102
0.257	0.001454	0.125
0.286	0.001292	0.139
0.314	0.001151	0.151
0.343	0.001006	0.152
0.371	0.000871	0.151
0.400	0.000758	0.158
0.429	0.000662	0.165
0.457	0.000574	0.171
0.486	0.000514	0.176
0.514	0.000457	0.181
0.543	0.000418	0.186
0.571	0.000381	0.189
0.600	0.000352	0.193
0.629	0.000319	0.198
0.657	0.000304	0.200
0.686	0.000282	0.202
0.714	0.000263	0.206
0.743	0.000255	0.208
0.771	0.000249	0.210
0.800	0.000240	0.211
0.829	0.000232	0.211
0.857	0.000225	0.212
0.886	0.000217	0.211
0.914	0.000211	0.211
0.943	0.000204	0.254
0.971	0.000113	0.143
1.000	0.000000	0.000

THE DELTA DRAG COEFFICIENT IS dCD= - 0.011289
THE TOTAL TORQUE IS Q= 3.038 IN-LB
THE INDIVIDUAL BLADE AREA IS= 5.46 IN^2
THE WVT SOLIDITY IS= 0.851

ELLIPTICAL
6 BLADES
OPTIMIZED FOR DRAG REDUCTION AT APPROX. -40 DEG PITCH

SPANWISE THRUST COEFFICIENT AND TORQUE DISTRIBUTION:

X/C	DCT/DX	DQ/DX
0.143	0.002083	0.042
0.171	0.001961	0.061
0.200	0.001933	0.089
0.229	0.001800	0.116
0.257	0.001610	0.139
0.286	0.001406	0.151
0.314	0.001234	0.162
0.343	0.001056	0.160
0.371	0.000900	0.156
0.400	0.000777	0.162
0.429	0.000668	0.167
0.457	0.000571	0.170
0.486	0.000506	0.173
0.514	0.000445	0.176
0.543	0.000400	0.178
0.571	0.000364	0.181
0.600	0.000331	0.181
0.629	0.000299	0.185
0.657	0.000286	0.189
0.686	0.000265	0.190
0.714	0.000247	0.193
0.743	0.000237	0.193
0.771	0.000230	0.195
0.800	0.000225	0.198
0.829	0.000219	0.199
0.857	0.000212	0.199
0.886	0.000206	0.199
0.914	0.000195	0.236
0.943	0.000171	0.212
0.971	0.000072	0.092
1.000	0.000000	0.000

THE DELTA DRAG COEFFICIENT IS dCD= - 0.011921
THE TOTAL TORQUE IS Q= 2.953 IN-LB
THE INDIVIDUAL BLADE AREA IS= 5.43 IN^2
THE WVT SOLIDITY IS= 0.846

APPENDIX C

HARD COPY WIND TUNNEL TEST DATA

Table C.1 Clean Wing, Run 1

WIND TUNNEL DATA ACQUISITION PROGRAM SUMMARY

TITLE: clean
ZERO TAPE FILE: clean.ATR WEIGHT TAPE FILE: clean.WTR
DATA FILE: clean.DAT DATE: 12-02-1996 TIME: 20:34:00
REF. AREA = 410.00 sq.in. REF. CHORD = 15.75 in. REF. SPAN = 27.00 in.
AR = 1.65 HMT = 0.00 in. VMT = 1.00 in.
FORCE BALANCE = 2 PRESSURE TRANSDUCER = 1 THERMISTOR = 1

RUN	ALFHA	VEL(fps)	TEMP(F)	RN	
FX-DRAG	FY-SIDEFORCE	FZ-Lift	MX-Roll	MY-Pitch	MZ-Yaw
CF	CFY	CFZ	CMX	CMY	CMZ
1	15.0	9.359E+01	7.007E+01	7.522E+05	
5.182E+00	-4.391E-01	3.053E+01	9.407E+01	-3.323E+01	-1.147E+01
1.796E-01	-1.513E-02	1.052E+00	1.201E-01	-7.271E-02	-1.499E-02
2	14.0	9.373E+01	7.081E+01	7.514E+05	
5.163E+00	-4.523E-01	3.030E+01	9.326E+01	-3.289E+01	-1.171E+01
1.776E-01	-1.556E-02	1.042E+00	1.188E-01	-7.154E-02	-1.492E-02
3	13.0	9.371E+01	7.136E+01	7.499E+05	
4.629E-00	-4.327E-01	2.949E+01	9.215E+01	-2.958E+01	-1.131E+01
1.595E-01	-1.494E-02	1.015E+00	1.176E-01	-6.470E-02	-1.443E-02
4	12.0	9.359E+01	7.199E+01	7.473E+05	
4.173E+00	-3.727E-01	2.806E+01	9.015E+01	-2.714E+01	-1.086E+01
1.443E-01	-1.289E-02	9.675E-01	1.155E-01	-5.959E-02	-1.391E-02
5	11.0	9.347E+01	7.235E+01	7.455E+05	
3.715E-00	-3.795E-01	2.661E+01	8.650E+01	-2.480E+01	-1.028E+01
1.289E-01	-1.317E-02	9.234E-01	1.111E-01	-5.462E-02	-1.321E-02
6	10.0	9.344E+01	7.286E+01	7.440E+05	
3.243E+00	-2.836E-01	2.477E+01	8.209E+01	-2.282E+01	-9.525E-00
1.127E-01	-1.155E-02	8.610E-01	1.057E-01	-5.025E-02	-1.226E-02
7	9.0	9.250E+01	7.253E+01	7.347E+05	
2.478E+00	-3.155E-01	2.141E+01	7.207E+01	-2.045E+01	-8.25 E-0
8.800E-02	-1.121E-02	7.603E-01	9.479E-02	4.511E-02	-1.055E-02
8	8.0	9.272E+01	7.391E+01	7.355E+05	
2.467E-00	-3.026E-01	2.132E+01	7.206E+01	-2.038E+01	-8.127E+00
8.733E-02	-1.070E-02	7.539E-01	9.441E-02	-4.575E-02	-1.025E-02
9	7.0	9.235E+01	7.435E+01	7.317E+05	
2.163E+00	-2.549E-01	1.978E+01	6.701E+01	-1.981E+01	-7.746E+00
7.715E-02	-1.023E-02	7.055E-01	8.854E-02	-4.486E-02	-1.023E-02

Table C.1 Clean Wing, Run 1 (cont'd)

10	6.0	9.257E+01	7.462E+01	7.327E+05	
1.647E+00	-2.695E-01	1.794E+01	6.182E+01	-1.897E+01	-7.329E+00
6.560E-02	-9.576E-03	6.382E-01	8.134E-02	-4.279E-02	-9.542E-03
11	5.0	9.259E+01	7.495E+01	7.324E+05	
1.569E+00	-2.585E-01	1.616E+01	5.647E+01	-1.817E+01	-6.688E+00
5.574E-02	-9.182E-03	5.740E-01	7.429E-02	-4.097E-02	-8.799E-03
12	4.0	9.259E+01	7.518E+01	7.314E+05	
1.111E+00	-2.695E-01	1.193E+01	4.331E+01	-1.744E+01	-5.481E+00
3.949E-02	-9.581E-03	4.242E-01	5.704E-02	-3.937E-02	-7.218E-03
13	3.0	9.261E+01	7.538E+01	7.312E+05	
1.109E+00	-2.639E-01	1.192E+01	4.291E+01	-1.737E+01	-5.487E+00
3.944E-02	-9.330E-03	4.235E-01	5.650E-02	-3.920E-02	-7.224E-03
14	2.0	9.27 E+01	7.559E+01	7.314E+05	
9.775E-01	-2.624E-01	1.063E+01	3.935E+01	-1.719E+01	-5.096E+00
3.469E-02	-1.002E-02	3.773E-01	5.172E-02	-3.872E-02	-6.699E-03
15	1.0	9.274E+01	7.582E+01	7.312E+05	
8.719E-01	-2.679E-01	8.960E+00	3.389E+01	-1.764E+01	-4.562E+00
3.093E-02	-9.501E-03	3.178E-01	4.452E-02	-3.974E-02	-6.001E-03
16	0.0	9.284E+01	7.608E+01	7.313E+05	
7.824E-01	-2.651E-01	7.160E+00	2.920E+01	-1.834E+01	-3.958E+00
2.771E-02	-9.389E-03	2.535E-01	3.598E-02	-4.184E-02	-5.247E-03
17	-1.0	9.308E+01	7.638E+01	7.325E+05	
7.139E-01	-2.673E-01	4.769E+00	2.054E+01	-1.951E+01	-3.251E+00
2.517E-02	-9.422E-03	1.691E-01	2.692E-02	-4.369E-02	-4.245E-03
18	-2.0	9.282E+01	7.658E+01	7.307E+05	
7.483E-01	-2.917E-01	2.616E+00	1.343E+01	-2.078E+01	-2.719E+00
2.648E-02	-1.032E-02	9.257E-02	1.760E-02	-4.670E-02	-3.563E-03
19	-3.0	9.203E+01	7.695E+01	7.309E+05	
7.546E-01	-3.241E-01	3.161E-01	5.786E+00	-2.272E+01	-2.407E+00
2.665E-02	-1.145E-02	1.115E-02	7.569E-03	-5.095E-02	-3.149E-03
20	-4.0	9.286E+01	7.704E+01	7.291E+05	
8.437E-01	-3.907E-01	-1.382E+00	-2.400E-01	-2.393E+01	-2.531E+00
2.992E-02	-1.286E-02	-4.902E-02	-3.152E-04	-5.388E-02	-3.324E-03
21	-5.0	9.314E+01	7.729E+01	7.307E+05	
9.187E-01	-4.201E-01	-2.441E+00	-4.581E+00	-2.464E+01	-2.557E+00
3.240E-02	-1.481E-02	-8.609E-02	-5.584E-03	-5.517E-02	-3.340E-03

Table C.2 Clean Wing, Run 2

WIND TUNNEL DATA ACQUISITION PROGRAM SUMMARY

TITLE: clean2
AERO TARE FILE: clean.ATR WEIGHT TARE FILE: clean.WTR
DATA FILE: clean2.DAT DATE: 12-02-1996 TIME: 20:51:23
REF. AREA = 410.00 sq.in. REF. CHORD = 15.75 in. REF. SPAN = 27.00 in.
AR = 1.65 HMT = 0.00 in. VMT = 1.00 in.
FORCE BALANCE = 2 PRESSURE TRANSDUCER = 1 THERMISTOR = 1

RUN	ALPHA	VEL(fps)	TEMP(F)	RN	
FX-DRAG	FY-SIDEFORCE	FZ-Lift	MX-Roll	MY-Pitch	MZ-Yaw
CFX	CFY	CFZ	CMX	CMY	CMZ
1	15.0	9.295E+01	7.546E+01	7.312E+05	
5.052E+00	-4.649E-01	2.972E+01	9.052E+01	-3.281E+01	-1.121E+01
1.786E-01	-1.644E-02	1.051E+00	1.185E-01	-7.365E-02	-1.459E-02
2	14.0	9.290E+01	7.[illegible]E+01	7.309E+05	
4.957E+00	-4.337E-01	2.972E+01	9.998E+01	-3.225E+01	-1.109E+01
1.752E-01	-1.533E-02	1.050E+00	1.178E-01	-7.236E-02	-1.452E-02
3	13.0	9.268E+01	7.720E+01	7.273E+05	
4.[illegible]3E+00	-4.12[illegible]E-01	2.849E+01	8.941E+01	-2.900E+01	-1.095E+01
1.597E-01	-1.471E-02	1.[illegible]15E+00	1.[illegible]79E-01	-6.557E-02	-1.432E-02
4	12.0	9.290E+01	7.739E+01	7.286E+05	
4.065E+00	-4.370E-01	2.731E+01	8.730E+01	-2.672E+01	-1.054E+01
1.441E-01	-1.549E-02	9.682E-01	1.146E-01	-6.[illegible]1E-02	-1.394E-02
5	11.0	9.279E+01	7.760E+01	7.272E+05	
3.642E+00	-3.744E-01	2.591E+01	8.434E+01	-2.449E+01	-9.962E+00
1.295E-01	-1.331E-02	9.213E-01	1.111E-01	-5.529E-02	-1.312E-02
6	10.0	9.290E+01	7.730E+01	7.276E+05	
3.229E+00	-3.634E-01	2.442E+01	8.090E+01	-2.268E+01	-9.417E+00
1.146E-01	-1.290E-02	8.656E-01	1.065E-01	-5.110E-02	-1.238E-02
7	9.0	9.280E+01	7.799E+01	7.264E+05	
2.591E+00	-3.220E-01	2.183E+01	7.340E+01	-2.097E+01	-8.336E+00
9.219E-02	-1.145E-02	7.764E-01	9.673E-02	-4.736E-02	-1.093E-02
8	8.0	9.254E+01	7.823E+01	7.237E+05	
2.305E+00	-3.353E-01	2.054E+01	6.922E+01	-2.024E+01	-7.975E+00
8.250E-02	-1.200E-02	7.350E-01	9.175E-02	-4.600E-02	-1.057E-02
9	7.0	9.265E+01	7.837E+01	7.243E+05	
2.141E+00	-3.197E-01	1.966E+01	6.654E+01	-1.985E+01	-7.754E+00
7.646E-02	-1.139E-02	7.019E-01	8.900E-02	-4.51[illegible]E-02	-1.026E-02

Table C.2 Clean Wing, Run 2 (cont'd)

10	6.0	9.256E+01	7.855E+01	7.231E+05	
1.847E+00	-3.249E-01	1.785E+01	6.127E+01	-1.895E+01	-7.300E+00
6.512E-02	-1.183E-02	6.391E-01	8.124E-02	-4.307E-02	-9.678E-03
11	5.0	9.269E+01	7.867E+01	7.238E+05	
1.525E+00	-2.928E-01	1.572E+01	5.515E+01	-1.838E+01	-6.613E+00
5.445E-02	-1.045E-02	5.613E-01	7.294E-02	-4.166E-02	-8.744E-03
12	4.0	9.275E+01	7.882E+01	7.239E+05	
1.363E+00	-3.000E-01	1.424E+01	5.039E+01	-1.782E+01	-6.204E+00
4.961E-02	-1.070E-02	5.078E-01	6.657E-02	-4.036E-02	-8.195E-03
13	3.0	9.266E+01	7.894E+01	7.229E+05	
1.144E+00	-2.933E-01	1.242E+01	4.487E+01	-1.754E+01	-5.597E+00
4.089E-02	-1.049E-02	4.440E-01	5.941E-02	-3.980E-02	-7.411E-03
14	2.0	9.285E+01	7.915E+01	7.239E+05	
9.040E-01	-2.964E-01	9.839E+00	3.693E+01	-1.771E+01	-4.821E+00
3.219E-02	-1.055E-02	3.504E-01	4.871E-02	-4.005E-02	-6.359E-03
15	1.0	9.293E+01	7.939E+01	7.240E+05	
8.489E-01	-2.840E-01	8.911E+00	3.404E+01	-1.781E+01	-4.563E+00
3.019E-02	-1.010E-02	3.169E-01	4.484E-02	-4.021E-02	-6.011E-03
16	0.0	9.288E+01	7.960E+01	7.231E+05	
7.626E-01	-2.809E-01	7.143E+00	2.828E+01	-1.824E+01	-3.946E+00
2.715E-02	-1.001E-02	2.544E-01	3.731E-02	-4.125E-02	-5.205E-03
17	-1.0	9.327E+01	7.977E+01	7.257E+05	
7.238E-01	-2.759E-01	5.043E+00	2.135E+01	-1.928E+01	-3.323E+00
2.557E-02	-9.748E-03	1.782E-01	2.793E-02	-4.325E-02	-4.348E-03
18	-2.0	9.304E+01	7.993E+01	7.235E+05	
6.944E-01	-2.799E-01	3.669E+00	1.643E+01	-2.017E+01	-2.887E+00
2.465E-02	-9.940E-03	1.303E-01	2.161E-02	-4.549E-02	-3.799E-03
19	-3.0	9.325E+01	8.007E+01	7.248E+05	
7.354E-01	-3.311E-01	8.139E-01	6.907E+00	-2.215E+01	-2.400E+00
2.601E-02	-1.[illegible]	2.879E-02	9.[illegible]	-4.975E-02	-3.144E-03
20	-4.0	9.315E+01	8.022E+01	7.237E+05	
8.045E-01	-3.844E-01	-7.249E-01	1.805E+00	-2.323E+01	-2.402E+00
2.853E-02	-1.343E-02	-2.570E-02	2.371E-03	-5.229E-02	-3.154E-03
21	-5.0	9.311E+01	8.038E+01	7.230E+05	
9.190E-01	-4.497E-01	-2.393E+00	-4.628E+00	-2.428E+01	-2.572E+00
3.262E-02	-1.596E-02	-8.491E-02	-6.092E-03	-5.471E-02	-3.331E-03

Table C.3 Clean Wing, Run 3

WIND TUNNEL DATA ACCUISITION PROGRAM SUMMAR

TITLE: clean3

AERO TARE FILE: clean.ATR WEIGHT TARE FILE: clean.WTR

DATA FILE: clean3.DAT DATE: 12-02-1996 TIME: 21:08:48

REF. AREA = 410.00 sq.in. REF. CHORD = 15.75 in. REF. SPAN = 27.00 in.

AR = 1.65 HMT = 0.00 in. VMT = 1.00 in.

FORCE BALANCE = 2 PRESSURE TRANSDUCER = 1 THERMISTOR = 1

RUN	ALPHA	VEL(fps)	TEMP(F)	RN	
FX-DRAG	FY-SIDEFORCE	FZ-Lift	MX-Roll	MY-Pitch	MZ-Yaw
CFX	CFY	CFZ	CMX	CMY	CMZ
1	15.0	9.347E+01	7.909E+01	7.289E+05	
5.158E+00	-5.012E-01	3.008E+01	9.099E+01	-3.369E+01	-1.122E-01
1.811E-01	-1.759E-02	1.057E+00	1.194E-01	-7.514E-02	-1.460E-02
2	14.0	9.346E+01	7.941E+01	7.290E+05	
5.019E+00	-5.076E-01	2.970E+01	8.115E+01	-3.225E+01	-1.118E+01
1.765E-01	-1.785E-02	1.045E+00	1.187E-01	-7.201E-02	-1.456E-02
3	13.0	9.341E+01	7.969E+01	7.271E+05	
4.883E+00	-4.556E-01	2.875E+01	8.982E-01	-2.986E+01	-1.088E+01
1.699E-01	-1.605E-02	1.013E+00	1.172E-01	-6.676E-02	-1.419E-02
4	12.0	9.252E+01	7.990E+01	7.274E+05	
4.150E+00	-4.615E-01	2.757E+01	8.784E+01	-2.696E+01	-1.065E+01
1.459E-01	-1.622E-02	9.691E-01	1.144E-01	-5.017E-02	-1.386E-02
5	11.0	9.289E+01	8.044E+01	7.211E+05	
3.565E+00	-4.183E-01	2.558E+01	8.311E+01	-2.423E+01	-9.877E+00
1.272E-01	-1.492E-02	9.124E-01	1.093E-01	-5.486E-02	-1.305E-02
6	10.0	9.291E+01	8.054E+01	7.203E+05	
3.185E+00	-4.208E-01	2.417E+01	7.962E+01	-2.248E+01	-9.344E+00
1.138E-01	-1.504E-02	8.639E-01	1.054E-01	-5.100E-02	-1.209E-02
7	9.0	9.279E+01	8.063E+01	7.199E+05	
2.796E+00	-3.975E-01	2.265E+01	7.561E+01	-2.134E+01	-8.805E+00
9.999E-02	-1.421E-02	8.097E-01	1.001E-01	-4.944E-02	-1.140E-02
8	8.0	9.263E+01	8.072E+01	7.185E+05	
2.424E+00	-3.550E-01	2.102E+01	7.049E+01	-2.048E+01	-8.150E+00
8.599E-02	-1.274E-02	7.542E-01	9.369E-02	-4.665E-02	-1.082E-02
9	7.0	9.266E+01	8.081E+01	7.185E+05	
2.147E+00	-3.597E-01	1.951E+01	6.623E+01	-1.974E+01	-7.711E+00
7.701E-02	-1.290E-02	6.996E-01	8.804E-02	-4.495E-02	-1.024E-02

Table C.3 Clean Wing, Run 3 (cont'd)

10	6.0	9.241E+01	8.086E+01	7.165E+05	
1.837E+00	-3.430E-01	1.779E+01	6.109E+01	-1.898E+01	-7.257E+00
6.626E-02	-1.237E-02	5.414E-01	8.160E-02	-4.347E-02	-9.694E-03
11	5.0	9.243E+01	8.094E+01	7.164E+05	
1.586E+00	-3.439E-01	1.591E+01	5.520E+01	-1.833E+01	-6.666E+00
5.717E-02	-1.240E-02	5.737E-01	7.371E-02	-4.195E-02	-8.902E-03
12	4.0	9.254E+01	8.107E+01	7.170E+05	
1.337E+00	-3.190E-01	1.417E+01	4.487E+01	-1.771E+01	-6.199E+00
4.811E-02	-1.148E-02	5.099E-01	6.646E-02	-4.046E-02	-8.260E-03
13	3.0	9.249E+01	8.115E+01	7.163E+05	
1.166E+00	-3.124E-01	1.251E+01	4.464E+01	-1.737E+01	-5.606E+00
4.200E-02	-1.125E-02	4.505E-01	5.956E-02	-3.974E-02	-7.497E-03
14	2.0	9.249E+01	8.127E+01	7.161E+05	
9.780E-01	-3.109E-01	1.048E+01	3.856E+01	-1.713E+01	-5.005E+00
3.524E-02	-1.112E-02	3.777E-01	5.146E-02	-3.918E-02	-6.680E-03
15	1.0	9.252E+01	8.136E+01	7.161E+05	
8.804E-01	-3.176E-01	8.942E+00	3.398E+01	-1.762E+01	-4.489E+00
3.171E-02	-1.144E-02	3.221E-01	4.523E-02	-4.028E-02	-5.922E-03
16	0.0	9.270E+01	8.143E+01	7.174E+05	
7.699E-01	-3.075E-01	7.107E+00	2.930E+01	-1.815E+01	-3.955E+00
2.762E-02	-1.103E-02	2.550E-01	3.760E-02	-4.134E-02	-5.269E-03
17	-1.0	9.250E+01	8.152E+01	7.155E+05	
6.940E-01	-2.806E-01	5.282E+00	2.148E+01	-1.904E+01	-3.339E+00
2.502E-02	-1.011E-02	1.906E-01	2.987E-02	-4.358E-02	-4.456E-03
18	-2.0	9.254E+01	8.167E+01	7.155E+05	
7.044E-01	-3.030E-01	3.549E+00	1.594E+01	-1.995E+01	-2.856E+00
2.537E-02	-1.091E-02	1.278E-01	2.126E-02	-4.562E-02	-3.809E-03
19	-3.0	9.338E+01	8.187E+01	7.216E+05	
7.460E-01	-3.234E-01	9.836E-01	7.240E+00	-2.218E+01	-2.418E+00
2.640E-02	-1.144E-02	3.480E-02	9.498E-03	-4.993E-02	-3.162E-03
20	-4.0	9.338E+01	9.203E+01	7.212E+05	
8.085E-01	-3.864E-01	-6.057E-01	1.289E+00	-2.330E+01	-2.394E+00
2.861E-02	-1.369E-02	-2.144E-02	1.690E-03	-5.235E-02	-3.138E-03
21	-5.0	9.235E+01	8.212E+01	7.207E+05	
3.900E-01	-4.151E-01	-1.899E+00	-2.922E+00	-2.392E+01	-2.447E+00
2.153E-02	-1.470E-02	-6.728E-02	-3.702E-03	-5.381E-02	-3.210E-03

Table C.4 Stationary WVT, 2 Blades

WIND TUNNEL DATA ACQUISITION PROGRAM SUMMARY

TITLE: static2
AERO TARE FILE: official.ATRWEIGHT TARE FILE: static2.WTR
DATA FILE: static2.DAT DATE: 03-12-1997 TIME: 15:25:04
REF. AREA = 410.00 sq.in. REF. CHORD = 15.75 in. REF. SPAN = 27.00 in.
AR = 1.65 HMT = 0.00 in. VMT = 1.00 in.
FORCE BALANCE = 2 PRESSURE TRANSDUCER = 1 THERMISTOR = 1

RUN	ALFHA	VEL(fps)	TEMP(F)	RN	
FX-DRAG	FY-SIDEFORCE	FZ-Lift	MX-Roll	MY-Pitch	MZ-Yaw
CFX	CFY	CFZ	CMX	CMY	CMZ
1	2.0	9.371E+01	8.177E+01	7.243E+05	
1.378E+00	-4.104E-01	1.072E+01	3.708E+01	-1.803E+01	-4.451E-01
4.842E-02	-1.442E-02	3.767E-01	4.864E-02	-4.022E-02	-5.792E-04
2	2.0	9.396E+01	8.221E+01	7.252E+05	
1.377E+00	-3.934E-01	1.068E+01	3.722E+01	-1.795E+01	-4.837E-01
4.817E-02	-1.341E-02	3.736E-01	4.821E-02	-3.986E-02	-6.256E-04
3	2.0	9.414E+01	8.260E+01	7.257E+05	
1.364E+00	-4.006E-01	1.077E+01	3.745E+01	-1.811E+01	-4.225E-01
4.754E-02	-1.387E-02	3.755E-01	4.835E-02	-4.009E-02	-5.456E-04
4	2.0	9.404E+01	8.304E+01	7.239E+05	
1.338E+00	-4.288E-01	1.061E+01	3.737E+01	-1.780E+01	-1.940E+00
4.630E-02	-1.499E-02	3.711E-01	4.839E-02	-3.951E-02	-2.513E-03
5	2.0	9.400E+01	8.355E+01	7.224E+05	
1.335E+00	-4.122E-01	1.067E+01	3.706E+01	-1.763E+01	-1.909E+00
4.642E-02	-1.444E-02	3.738E-01	4.802E-02	-3.922E-02	-2.477E-03
6	2.0	9.383E+01	8.392E+01	7.213E+05	
1.341E+00	-3.984E-01	1.075E+01	3.770E+01	-1.792E+01	-1.922E+00
4.704E-02	-1.397E-02	3.765E-01	4.897E-02	-3.987E-02	-2.504E-03
7	2.0	9.384E+01	8.395E+01	7.202E+05	
1.302E+00	-4.296E-01	1.073E+01	3.727E+01	-1.781E+01	-2.085E+00
4.530E-02	-1.511E-02	3.773E-01	4.856E-02	-3.977E-02	-2.716E-03
8	2.0	9.391E+01	8.439E+01	7.192E+05	
1.300E+00	-4.199E-01	1.074E+01	3.768E+01	-1.786E+01	-2.036E+00
4.548E-02	-1.476E-02	3.776E-01	4.906E-02	-3.997E-02	-2.651E-03
9	2.0	9.358E+01	8.476E+01	7.193E+05	
1.313E+00	-4.177E-01	1.071E+01	3.749E+01	-1.790E+01	-2.027E+00
4.610E-02	-1.467E-02	3.762E-01	4.875E-02	-3.992E-02	-2.637E-03
10	2.0	9.350E+01	8.527E+01	7.145E+05	
1.204E+00	-4.229E-01	1.062E+01	3.690E+01	-1.744E+01	-3.738E+00
4.277E-02	-1.502E-02	3.770E-01	4.854E-02	-3.934E-02	-4.916E-03
11	2.0	9.364E+01	8.567E+01	7.146E+05	
1.223E+00	-4.223E-01	1.060E+01	3.663E+01	-1.755E+01	-3.935E+00
4.335E-02	-1.497E-02	3.757E-01	4.809E-02	-3.950E-02	-5.165E-03
12	2.0	9.362E+01	8.600E+01	7.138E+05	
1.220E+00	-4.112E-01	1.066E+01	3.665E+01	-1.750E+01	-3.762E+00
4.327E-02	-1.452E-02	3.791E-01	4.918E-02	-3.940E-02	-4.942E-03

0°
-5°
-10°
-15°

Table C.4 Stationary WVT, 2 Blades (cont'd)

	13	2.0	9.428E+01	8.625E+01	7.182E+05	
	1.223E+00	-4.096E-01	1.079E+01	3.689E+01	-1.801E+01	-3.158E+00
	4.279E-02	-1.433E-02	3.774E-01	4.780E-02	-4.002E-02	-4.092E-03
-20°	14	2.0	9.422E+01	8.674E+01	7.165E+05	
	1.212E+00	-3.921E-01	1.074E+01	3.704E+01	-1.789E+01	-3.092E+00
	4.252E-02	-1.375E-02	3.765E-01	4.311E-02	-3.994E-02	-4.016E-03
	15	2.0	9.427E+01	8.702E+01	7.162E+05	
	1.224E+00	-4.001E-01	1.076E+01	3.686E+01	-1.793E+01	-3.052E+00
	4.290E-02	-1.403E-02	3.772E-01	4.795E-02	-3.990E-02	-3.963E-03
	1	2.0	9.358E+01	8.697E+01	7.111E+05	
	1.206E+00	-3.972E-01	1.063E+01	3.651E+01	-1.795E+01	-2.758E+00
	4.290E-02	-1.413E-02	3.780E-01	4.809E-02	-4.012E-02	-3.633E-03
-25°	2	2.0	9.401E+01	8.730E+01	7.124E+05	
	1.191E+00	-4.323E-01	1.065E+01	3.590E+01	-1.790E+01	-2.828E+00
	4.200E-02	-1.524E-02	3.756E-01	4.688E-02	-4.008E-02	-3.693E-03
	3	2.0	9.387E+01	8.762E+01	7.119E+05	
	1.184E-00	-3.776E-01	1.067E+01	3.612E+01	-1.805E+01	-2.663E+00
	4.190E-02	-1.336E-02	3.777E-01	4.734E-02	-4.055E-02	-3.517E-03
	4	2.0	9.332E+01	8.742E+01	7.0[illegible]E+05	
	1.225E+00	-4.281E-01	1.060E-01	3.653E+01	-1.773E+01	-2.111E+00
	4.394E-02	-1.522E-02	3.794E-01	4.843E-02	-4.026E-02	-2.799E-03
-30°	5	2.0	9.330E+01	8.779E+01	7.071E+05	
	1.219E+00	-4.288E-01	1.063E+01	3.602E+01	-1.755E+01	-2.129E+00
	4.369E-02	-1.537E-02	3.809E-01	4.780E-02	-3.993E-02	-2.825E-03
	6	2.0	9.325E+01	8.810E+01	7.060E+05	
	1.222E+00	-4.274E-01	1.061E+01	3.628E+01	-1.739E+01	-2.107E+00
	4.387E-02	-1.534E-02	3.806E-01	4.822E-02	-3.963E-02	-2.800E-03
	7	2.0	9.446E+01	8.800E+01	7.154E+05	
	1.294E+00	-4.785E-01	1.083E+01	3.705E+01	-1.769E+01	-1.912E+00
	4.526E-02	-1.573E-02	3.796E-01	4.799E-02	-3.928E-02	-2.547E-03
-35°	8	2.0	9.429E+01	8.837E+01	7.132E+05	
	1.294E+00	-4.652E-01	1.069E+01	3.744E+01	-1.779E+01	-1.851E+00
	4.547E-02	-1.636E-02	3.756E-01	4.871E-02	-3.967E-02	-2.409E-03
	9	2.0	9.434E+01	8.865E+01	7.130E+05	
	1.285E+00	-4.800E-01	1.075E+01	3.689E+01	-1.781E+01	-1.836E-00
	4.499E-02	-1.685E-02	3.773E-01	4.795E-02	-3.969E-02	-2.386E-03

Table C.5 Stationary WVT, 3 Blades

WIND TUNNEL DATA ACQUISITION PROGRAM SUMMARY

TITLE: static3
AERO TARE FILE: official.ATR WEIGHT TARE FILE: static3.WTR
DATA FILE: static3.DAT DATE: 03-13-1997 TIME: 16:20:10
REF. AREA = 410.00 sq.in. REF. CHORD = 15.75 in. REF. SPAN = 27.00 in.
AR = 1.65 HMT = 0.00 in. VMT = 1.00 in.
FORCE BALANCE = 2 PRESSURE TRANSDUCER = 1 THERMISTOR = 1

	RUN	ALPHA	VEL(fps)	TEMP(F)	FN	
	FX-DRAG	FY-SIDEFORCE	FZ-Lift	MX-Roll	MY-Pitch	MZ-Yaw
	CFX	CFY	CFZ	CMX	CMY	CMZ
	1	2.0	9.354E+01	7.785E+01	7.324E+05	
	1.576E+00	-4.950E-01	1.168E+01	4.065E+01	-1.744E+01	-5.903E-02
	5.512E-02	-1.733E-02	4.087E-01	5.270E-02	-3.877E-02	-7.653E-05
0°	2	2.0	9.392E+01	7.815E+01	7.346E+05	
	1.603E+00	-4.840E-01	1.162E+01	4.057E+01	-1.733E+01	-8.140E-02
	5.570E-02	-1.681E-02	4.051E-01	5.221E-02	-3.823E-02	-1.047E-04
	3	2.0	9.371E+01	7.852E+01	7.322E+05	
	1.607E+00	-4.636E-01	1.155E+01	4.047E+01	-1.714E+01	7.261E-02
	5.611E-02	-1.619E-02	4.037E-01	5.234E-02	-3.801E-02	9.591E-05
	4	2.0	9.366E+01	7.878E+01	7.311E+05	
	1.485E+00	-4.532E-01	1.151E+01	4.069E+01	-1.711E+01	-1.002E+00
	5.195E-02	-1.595E-02	4.024E-01	5.271E-02	-3.800E-02	-1.298E-03
-5°	5	2.0	9.337E+01	7.922E+01	7.317E+05	
	1.514E+00	-4.724E-01	1.163E+01	4.070E+01	-1.746E+01	-9.887E-01
	5.275E-02	-1.646E-02	4.053E-01	5.253E-02	-3.964E-02	-1.276E-03
	6	2.0	9.370E+01	7.959E+01	7.295E+05	
	1.507E+00	-4.269E-01	1.155E+01	4.028E+01	-1.709E+01	-1.065E+00
	5.275E-02	-1.494E-02	4.041E-01	5.221E-02	-3.842E-02	-1.390E-03
	7	2.0	9.388E+01	8.288E+01	7.230E+05	
	1.420E+00	-4.669E-01	1.126E+01	3.919E+01	-1.721E+01	-1.742E+00
	4.979E-02	-1.638E-02	3.948E-01	5.512E-02	-3.852E-02	-2.263E-03
	8	2.0	9.371E+01	8.311E+01	7.211E+05	
-10°	1.417E+00	-4.373E-01	1.114E+01	3.839E+01	-1.734E+01	-1.587E+00
	4.989E-02	-1.540E-02	3.923E-01	5.139E-02	-3.878E-02	-2.166E-03
	9	2.0	9.392E+01	8.333E+01	7.215E+05	
	1.424E+00	-4.662E-01	1.128E+01	3.936E+01	-1.716E+01	-1.759E+00
	4.999E-02	-1.637E-02	3.961E-01	5.118E-02	-3.816E-02	-2.567E-03
	10	2.0	9.354E+01	8.253E+01	7.213E+05	
	1.302E+00	-4.036E-01	1.110E+01	3.828E+01	-1.765E+01	-2.727E+00
	4.596E-02	-1.425E-02	3.919E-01	5.005E-02	-3.957E-02	-3.566E-03
-15°	11	2.0	9.377E+01	8.291E+01	7.221E+05	
	1.327E+00	-4.047E-01	1.099E+01	3.835E+01	-1.767E+01	-2.792E+00
	4.665E-02	-1.423E-02	3.864E-01	4.993E-02	-3.945E-02	-3.636E-03
	12	2.0	9.369E+01	8.321E+01	7.209E+05	
	1.315E+00	-4.223E-01	1.100E+01	3.911E+01	-1.740E+01	-2.704E+00
	4.635E-02	-1.488E-02	3.876E-01	4.972E-02	-3.892E-02	-3.529E-03

Table C.5 Stationary WVT, 3 Blades (cont'd)

-20°	13	2.0	9.332E+01	8.281E+01	7.189E+05	
	1.188E+00	-3.344E-01	1.108E+01	3.690E+01	-1.915E+01	-2.591E+00
	4.218E-02	-1.187E-02	3.932E-01	4.851E-02	-4.315E-02	-3.406E-03
	14	2.0	9.361E+01	8.320E+01	7.202E+05	
	1.215E+00	-3.545E-01	1.106E+01	3.639E+01	-1.913E+01	-2.606E+00
	4.290E-02	-1.251E-02	3.[illegible]E-01	4.757E-02	-4.287E-02	-3.407E-03
	15	2.0	9.345E+01	8.349E+01	7.183E+05	
	1.185E+00	-3.654E-01	1.108E+01	3.660E+01	-1.920E+01	-2.552E+00
	4.201E-02	-1.295E-02	3.926E-01	4.805E-02	-4.342E-02	-3.350E-03
-25°	1	2.0	9.392E+01	8.364E+01	7.215E+05	
	1.195E+00	-3.386E-01	1.108E+01	3.715E+01	-1.938E+01	-2.522E+00
	4.[illegible]3E-02	-1.139E-02	3.853E-01	4.823E-02	-4.317E-02	-3.277E-03
	2	2.0	9.404E+01	8.397E+01	7.215E+05	
	1.200E+00	-3.587E-01	1.104E+01	3.714E+01	-1.907E+01	-2.546E+00
	4.205E-02	-1.257E-02	3.867E-01	4.819E-02	-4.241E-02	-3.303E-03
	3	2.0	9.410E+01	8.421E+01	7.215E+05	
	1.210E+00	-3.591E-01	1.115E-01	3.659E+01	-1.933E+01	-2.538E+00
	4.[illegible]3E-02	-1.257E-02	3.[illegible]E-01	4.782E-02	-4.294E-02	-3.259E-03
-30°	4	2.0	9.413E+01	8.263E+01	7.255E+05	
	1.222E+00	-3.205E-01	1.115E+01	3.622E+01	-1.950E+01	-1.[illegible]9E+00
	4.261E-02	-1.119E-02	3.922E-01	4.752E-02	-4.317E-02	-1.549E-03
	5	2.0	9.424E+01	8.323E+01	7.249E+05	
	1.239E+00	-3.131E-01	1.116E+01	3.732E+01	-1.958E+01	-1.152E+00
	4.316E-02	-1.091E-02	3.895E-01	4.915E-02	-4.329E-02	-1.488E-03
	6	2.0	9.413E+01	8.340E+01	7.232E+05	
	1.232E+00	-3.094E-01	1.121E+01	3.672E+01	-1.941E+01	-1.248E+00
	4.304E-02	-1.091E-02	3.916E-01	4.752E-02	-4.306E-02	-1.515E-03
-35°	7	2.0	9.355E+01	8.379E+01	7.183E+05	
	1.264E+00	-3.507E-01	1.101E+01	3.628E+01	-1.943E+01	-8.830E-01
	4.473E-02	-1.241E-02	3.894E-01	4.754E-02	-4.364E-02	-1.157E-03
	8	2.0	9.338E+01	8.409E+01	7.163E+05	
	1.260E+00	-3.279E-01	1.097E+01	3.615E+01	-1.915E+01	-8.651E-01
	4.479E-02	-1.165E-02	3.898E-01	4.757E-02	-4.319E-02	-1.128E-03
	9	2.0	9.324E+01	8.434E+01	7.147E+05	
	1.259E+00	-3.427E-01	1.098E+01	3.623E+01	-1.937E+01	-8.940E-01
	4.485E-02	-1.222E-02	3.915E-01	4.785E-02	-4.396E-02	-1.167E-03

Table C.6 Stationary WVT, 4 Blades

WIND TUNNEL DATA ACQUISITION PROGRAM SUMMARY

TITLE: static4
AERO TARE FILE: official.ATR WEIGHT TARE FILE: static4.WTR
DATA FILE: static4.DAT DATE: 03-11-1997 TIME: 21:36:14
REF. AREA = 410.00 sq.in REF. CHORD = 15.75 in. REF. SPAN = 27.00 in.
AR = 1.65 RMT = 0.00 in. VMT = 1.00 in.
FORCE BALANCE = 2 PRESSURE TRANSDUCER = 1 THERMISTOR = 1

RUN	ALPHA	VEL(fps	TEMP(F)	RN	
FX-DRAG	FY-SIDEFORCE	FZ-Lift	MX-Roll	MY-Pitch	MZ-Yaw
CFX	CFY	CFZ	CMX	CMY	CMZ
1	2.0	9.291E+01	8.041E+01	7.214E+05	
1.622E+00	-5.673E-01	1.065E+01	3.524E+01	-1.711E+01	2.140E+00
5.782E-02	-2.022E-02	3.797E-01	4.653E-02	-3.872E-02	2.925E-03
2	2.0	9.320E+01	8.078E+01	7.227E+05	
1.584E+00	-5.946E-01	1.065E-01	3.593E+01	-1.724E+01	2.214E+00
5.616E-02	-2.109E-02	3.775E-01	4.704E-02	-3.931E-02	2.905E-03
3	2.0	9.338E+01	8.113E+01	7.233E+05	
1.531E+00	-5.815E-01	1.065E-01	3.547E+01	-1.726E+01	2.262E+00
5.742E-02	-2.055E-02	3.764E-01	4.642E-02	-3.871E-02	2.960E-03
4	2.0	9.297E+01	8.123E+01	7.199E+05	
1.491E+00	-4.762E-01	1.044E+01	3.599E+01	-1.726E+01	7.104E-01
5.217E-02	-1.659E-02	3.724E-01	4.753E-02	-3.899E-02	9.376E-04
5	2.0	9.301E+01	8.171E+01	7.190E+05	
1.483E+00	-4.887E-01	1.043E+01	3.569E+01	-1.743E+01	6.964E-01
5.290E-02	-1.743E-02	3.719E-01	4.713E-02	-3.946E-02	9.197E-04
6	2.0	9.297E+01	8.209E+01	7.170E+05	
1.491E+00	-4.873E-01	1.046E+01	3.573E+01	-1.702E+01	6.024E-01
5.337E-02	-1.744E-02	3.743E-01	4.737E-02	-3.869E-02	7.995E-04
7	2.0	9.389E+01	8.175E+01	7.258E+05	
1.374E+00	-4.482E-01	1.072E+01	3.660E+01	-1.726E+01	-5.695E-01
4.809E-02	-1.568E-02	3.752E-01	4.744E-02	-3.967E-02	-7.291E-04
8	2.0	9.377E+01	8.242E+01	7.233E+05	
1.323E+00	-4.466E-01	1.078E-01	3.638E+01	-1.765E+01	-4.647E-01
4.654E-02	-1.569E-02	3.764E-01	4.733E-02	-3.936E-02	-6.045E-04
9	2.0	9.380E+01	8.283E+01	7.225E+05	
1.366E+00	-4.581E-01	1.075E+01	3.640E+01	-1.790E+01	-4.173E-01
4.798E-02	-1.609E-02	3.776E-01	4.736E-02	-3.993E-02	-5.430E-04
10	2.0	9.373E+01	8.214E+01	7.236E+05	
1.273E+00	-3.930E-01	1.073E+01	3.624E+01	-1.791E+01	-2.390E+00
4.473E-02	-1.381E-02	3.771E-01	4.717E-02	-3.996E-02	-2.111E-03
11	2.0	9.375E+01	8.271E+01	7.224E+05	
1.237E+00	-4.104E-01	1.069E+01	3.584E+01	-1.799E+01	-2.367E+00
4.349E-02	-1.443E-02	3.759E-01	4.667E-02	-4.016E-02	-3.082E-03
12	2.0	9.372E+01	8.325E+01	7.209E+05	
1.227E+00	-3.959E-01	1.067E+01	3.612E+01	-1.769E+01	-2.333E+00
4.321E-02	-1.394E-02	3.757E-01	4.712E-02	-3.957E-02	-3.109E-03

0°
-5°
-10°
-15°

Table C.6 Stationary WVT, 4 Blades (cont'd)

-20°	13	2.0	9.417E+01	8.216E+01	7.270E+05	
	1.142E+00	-3.479E-01	1.083E+01	3.680E+01	-1.830E+01	-2.392E+00
	3.974E-02	-1.211E-02	3.772E-01	4.745E-02	-4.045E-02	-3.093E-03
	14	2.0	9.429E+01	8.288E+01	7.261E+05	
	1.140E+00	-3.075E-01	1.085E+01	3.643E+01	-1.839E+01	-2.426E+00
	3.966E-02	-1.069E-02	3.772E-01	4.692E-02	-4.061E-02	-3.125E-03
	15	2.0	9.410E+01	8.337E+01	7.235E+05	
	1.142E+00	-3.043E-01	1.081E+01	3.643E+01	-1.843E+01	-2.465E+00
	3.990E-02	-1.064E-02	3.777E-01	4.715E-02	-4.089E-02	-3.190E-03
-25°	1	2.0	9.356E+01	8.231E+01	7.219E+05	
	1.081E+00	-3.381E-01	1.074E+01	3.550E+01	-1.907E+01	-2.692E+00
	3.814E-02	-1.193E-02	3.786E-01	4.636E-02	-4.271E-02	-3.518E-03
	2	2.0	9.344E+01	8.276E+01	7.199E+05	
	1.083E+00	-3.398E-01	1.074E+01	3.558E+01	-1.892E+01	-2.681E+00
	3.822E-02	-1.203E-02	3.801E-01	4.665E-02	-4.254E-02	-3.516E-03
	3	2.0	9.315E+01	8.313E+01	7.168E+05	
	1.085E+00	-3.406E-01	1.064E+01	3.565E+01	-1.910E+01	-2.744E+00
	3.870E-02	-1.214E-02	3.794E-01	4.706E-02	-4.382E-02	-3.628E-03
	4	2.0	9.316E+01	8.325E+01	7.1[illegible]E+05	
	1.124E+00	-3.065E-01	1.069E+01	3.579E+01	-1.[illegible]9E+01	-1.594E+00
	4.007E-02	-1.083E-02	3.810E-01	4.713E-02	-4.321E-02	-2.[illegible]4E-03
-30°	5	2.0	9.308E+01	8.266E+01	7.15[illegible]E+05	
	1.106E+00	-3.408E-01	1.059E+01	3.554E+01	-1.903E+01	-1.594E+00
	3.950E-02	-1.219E-02	3.779E-01	4.702E-02	-4.317E-02	-2.110E-03
	6	2.0	9.341E+01	8.402E+01	7.167E+05	
	1.105E+00	-3.326E-01	1.[illegible]65E+01	3.537E+01	-1.899E+01	-1.571E+00
	3.925E-02	-1.181E-02	3.782E-01	4.551E-02	-4.230E-02	-2.044E-03
-35°	7	2.0	9.297E+01	8.349E+01	7.147E+05	
	1.173E+00	-3.774E-01	1.062E+01	3.515E+01	-1.886E+01	-2.153E+00
	4.195E-02	-1.351E-02	3.822E-01	4.792E-02	-4.295E-02	-2.854E-03
	8	2.0	9.286E+01	8.297E+01	7.129E+05	
	1.190E+00	-3.855E-01	1.061E+01	3.589E+01	-1.894E+01	-2.192E+00
	4.273E-02	-1.389E-02	3.809E-01	4.774E-02	-4.295E-02	-2.916E-03
	9	2.0	9.289E+01	8.420E+01	7.122E+05	
	1.175E+00	-3.736E-01	1.062E+01	3.599E+01	-1.864E+01	-2.158E+00
	4.222E-02	-1.331E-02	3.814E-01	4.788E-02	-4.252E-02	-2.872E-03

Table C.7 Stationary WVT, 5 Blades

WIND TUNNEL DATA ACQUISITION PROGRAM SUMMARY

TITLE: static5
AERO TARE FILE: official.ATRWEIGHT TARE FILE: static5.WTR
DATA FILE: static5.DAT DATE: 03-14-1997 TIME: 00:10:33
REF. AREA = 410.00 sq.in. REF. CHORD = 15.75 in. REF. SPAN = 27.00 in.
AR = 1.65 HMT = 0.00 in. VMT = 1.00 in.
FORCE BALANCE = 2 PRESSURE TRANSDUCER = 1 THERMISTOR = 1

RUN	ALPHA	VEL(fps)	TEMP(F)	RN	
FX-DRAG	FY-SIDEFORCE	FZ-Lift	MX-Roll	MY-Pitch	MZ-Yaw
CFX	CFY	CFZ	CMX	CMY	CMZ
1	2.0	9.416E+01	7.945E+01	7.335E+05	
1.790E+00	-5.842E-01	1.009E+01	3.409E+01	-1.788E+01	4.681E+00
6.202E-02	-2.024E-02	3.4[illegible]E-01	4.374E-02	-3.933E-02	6.006E-03
2	2.0	9.434E+01	7.979E+01	7.333E+05	
1.816E+00	-5.902E-01	1.001E+01	3.407E+01	-1.813E+01	4.616E+00
6.283E-02	-2.042E-02	3.462E-01	4.267E-02	-3.983E-02	5.917E-03
3	2.0	9.402E+01	8.006E+01	7.309E+05	
1.803E+00	-5.423E-01	1.[illegible]03E+01	3.413E+01	-1.792E+01	4.662E+00
6.273E-02	-1.[illegible]26E-02	3.[illegible]3E-01	4.397E-02	-3.957E-02	6.006E-03
4	2.0	9.326E+01	7.969E+01	7.252E+05	
1.619E+00	-5.052E-01	9.875E+00	3.366E+01	-1.809E+01	2.826E+00
5.722E-02	-1.735E-02	3.467E-01	4.404E-02	-4.[illegible]3E-02	3.693E-03
5	2.0	9.315E+01	8.011E+01	7.240E+05	
1.569E+00	-5.293E-01	9.[illegible]9E+00	3.356E+01	-1.797E+01	2.964E+00
5.559E-02	-1.972E-02	3.5[illegible]E-01	4.406E-02	-4.043E-02	3.891E-03
6	2.0	9.342E+01	8.042E+01	7.254E+05	
1.590E+00	-5.141E-01	9.898E+00	3.361E+01	-1.791E+01	2.952E+00
5.606E-02	-1.812E-02	3.490E-01	4.289E-02	-4.008E-02	3.855E-03
7	2.0	9.429E+01	7.978E+01	7.336E+05	
1.477E+00	-4.526E-01	1.009E+01	3.418E+01	-1.873E+01	1.359E+00
5.106E-02	-1.565E-02	3.499E-01	4.377E-02	-4.112E-02	1.740E-03
8	2.0	9.323E+01	8.132E+01	7.217E+05	
1.419E+00	-4.406E-01	9.[illegible]52E+00	3.391E+01	-1.792E+01	1.245E+00
5.022E-02	-1.562E-02	3.494E-01	4.449E-02	-4.035E-02	1.625E-03
9	2.0	9.305E+01	8.157E+01	7.197E+05	
1.439E+00	-4.681E-01	9.820E+00	3.332E+01	-1.814E+01	1.214E+00
5.124E-02	-1.667E-02	3.499E-01	4.396E-02	-4.102E-02	1.602E-03
10	2.0	9.405E+01	8.068E+01	7.296E+05	
1.256E+00	-3.143E-01	1.014E+01	3.393E+01	-1.998E+01	-1.165E+00
4.371E-02	-1.094E-02	3.529E-01	4.374E-02	-4.194E-02	-1.502E-03
11	2.0	9.420E+01	8.116E+01	7.296E+05	
1.221E+00	-3.394E-01	1.010E+01	3.356E+01	-1.877E+01	-1.157E+00
4.241E-02	-1.179E-02	3.506E-01	4.317E-02	-4.138E-02	-1.488E-03
12	2.0	9.427E+01	8.152E+01	7.272E+05	
1.233E+00	-3.202E-01	1.011E+01	3.377E+01	-1.891E+01	-1.134E+00
4.272E-02	-1.111E-02	3.504E-01	4.239E-02	-4.1[illegible]E-02	-1.[illegible]1E-03

0°
-5°
-10°
-15°

Table C.7 Stationary WVT, 5 Blades (cont'd)

	13	2.0	9.390E+01	8.073E+01	7.283E+05	
	1.140E+00	-2.638E-01	9.992E+00	3.419E+01	-1.821E+01	-5.341E-01
	3.983E-02	-9.213E-03	3.490E-01	4.423E-02	-4.037E-02	-6.902E-04
-20°	14	2.0	9.413E+01	8.124E+01	7.288E+05	
	1.141E+00	-2.747E-01	1.001E+01	3.385E+01	-1.831E+01	-5.430E-01
	3.971E-02	-9.556E-03	3.481E-01	4.362E-02	-4.045E-02	-6.996E-04
	15	2.0	9.446E+01	8.163E+01	7.304E+05	
	1.146E+00	-2.705E-01	1.003E+01	3.416E+01	-1.842E+01	-5.174E-01
	3.963E-02	-9.352E-03	3.466E-01	4.374E-02	-4.044E-02	-6.625E-04
	1	2.0	9.407E+01	8.077E+01	7.295E+05	
	1.110E+00	-2.564E-01	1.010E+01	3.452E+01	-1.827E+01	-8.257E-01
	3.864E-02	-8.923E-03	3.516E-01	4.449E-02	-4.036E-02	-1.064E-03
-25°	2	2.0	9.400E+01	8.129E+01	7.277E+05	
	1.087E+00	-2.444E-01	1.002E+01	3.463E+01	-1.842E+01	-8.002E-01
	3.791E-02	-8.527E-03	3.494E-01	4.474E-02	-4.081E-02	-1.034E-03
	3	2.0	9.401E+01	8.169E+01	7.259E+05	
	1.090E+00	-2.509E-01	1.006E+01	3.424E+01	-1.833E+01	-7.492E-01
	3.804E-02	-9.755E-03	3.512E-01	4.426E-02	-4.062E-02	-9.684E-04
	4	2.0	9.320E+01	8.172E+01	7.205E+05	
	1.073E+00	-2.410E-01	9.864E+00	3.403E+01	-1.852E+01	3.994E-01
	3.810E-02	-8.559E-03	3.503E-01	4.476E-02	-4.176E-02	5.254E-04
-30°	5	2.0	9.378E+01	8.249E+01	7.231E+05	
	1.083E+00	-2.357E-01	9.958E+00	3.449E+01	-1.864E+01	3.906E-01
	3.800E-02	-8.279E-03	3.499E-01	4.488E-02	-4.157E-02	5.082E-04
	6	2.0	9.346E+01	8.274E+01	7.201E+05	
	1.094E+00	-2.435E-01	9.931E+00	3.460E+01	-1.866E+01	3.203E-01
	3.871E-02	-8.514E-03	3.514E-01	4.481E-02	-4.172E-02	4.197E-04
	7	2.0	9.416E+01	8.183E+01	7.277E+05	
	1.175E+00	-2.980E-01	1.012E+01	3.478E+01	-1.931E+01	6.575E-01
	4.090E-02	-1.037E-02	3.522E-01	4.493E-02	-4.266E-02	8.475E-04
-35°	8	2.0	9.425E+01	8.228E+01	7.273E+05	
	1.169E+00	-2.887E-01	1.010E+01	3.505E+01	-1.935E+01	6.324E-01
	4.065E-02	-1.004E-02	3.511E-01	4.512E-02	-4.272E-02	8.142E-04
	9	2.0	9.424E+01	8.262E+01	7.264E+05	
	1.171E+00	-2.973E-01	1.009E+01	3.471E+01	-1.927E+01	6.135E-01
	4.073E-02	-1.034E-02	3.510E-01	4.472E-02	-4.256E-02	7.906E-04

Table C.8 Stationary WVT, 6 Blades

WIND TUNNEL DATA ACQUISITION PROGRAM SUMMARY

TITLE: static6
AERO TARE FILE: official.ATR WEIGHT TARE FILE: static6.WTR
DATA FILE: static6.DAT DATE: 03-14-1997 TIME: 21:28:25
REF. AREA = 410.00 sq.in. REF. CHORD = 15.75 in. REF. SPAN = 27.00 in.
AR = 1.65 HMT = 0.00 in. VMT = 1.00 in.
FORCE BALANCE = 2 PRESSURE TRANSDUCER = 1 THERMISTOR = 1

RUN	ALFHA	VEL(fps)	TEMP(F)	RN	
FX-DRAG	FY-SIDEFORCE	FZ-Lift	MX-Roll	MY-Pitch	MZ-Yaw
CFX	CFY	CFZ	CMX	CMY	CMZ
1	2.0	9.327E+01	7.893E+01	7.277E+05	
1.874E+00	-6.615E-01	9.993E+00	3.358E+01	-1.717E+01	6.496E+00
6.511E-02	-2.334E-02	3.525E-01	4.389E-02	-3.845E-02	8.475E-03
2	2.0	9.333E+01	7.926E+01	7.274E+05	
1.886E+00	-6.441E-01	9.925E+00	3.294E+01	-1.697E+01	6.522E+00
6.647E-02	-2.271E-02	3.499E-01	4.419E-02	-3.798E-02	8.529E-03
3	2.0	9.346E+01	7.957E+01	7.277E+05	
1.900E+00	-6.452E-01	9.991E+00	3.379E+01	-1.717E+01	6.402E+00
6.695E-02	-2.270E-02	3.480E-01	4.403E-02	-3.825E-02	8.242E-03
4	2.0	9.345E+01	7.984E+01	7.270E+05	
1.681E+00	-5.709E-01	1.001E+01	3.384E+01	-1.735E+01	3.654E+00
5.919E-02	-2.010E-02	3.522E-01	4.413E-02	-3.977E-02	4.764E-03
5	2.0	9.394E+01	2.024E+01	7.291E+05	
1.671E+00	-5.378E-01	1.004E+01	3.417E+01	-1.752E+01	3.649E+00
5.937E-02	-1.886E-02	3.507E-01	4.421E-02	-3.896E-02	4.980E-03
6	2.0	9.371E+01	8.053E+01	7.273E+05	
1.629E+00	-5.458E-01	9.976E+00	3.413E+01	-1.726E+01	3.845E+00
5.711E-02	-1.913E-02	3.497E-01	4.431E-02	-3.840E-02	5.017E-03
7	2.0	9.370E+01	8.006E+01	7.293E+05	
1.404E+00	-4.274E-01	1.015E+01	3.290E+01	-1.812E+01	9.247E-01
4.918E-02	-1.497E-02	3.556E-01	4.269E-02	-4.030E-02	1.280E-03
8	2.0	9.350E+01	8.059E+01	7.255E+05	
1.395E+00	-4.260E-01	1.001E+01	3.316E+01	-1.849E+01	9.612E-01
4.913E-02	-1.500E-02	3.525E-01	4.324E-02	-4.134E-02	1.254E-03
9	2.0	9.349E+01	8.090E+01	7.246E+05	
1.382E+00	-4.165E-01	9.990E+00	3.312E+01	-1.847E+01	9.207E-01
4.873E-02	-1.469E-02	3.521E-01	4.323E-02	-4.133E-02	1.202E-03
10	2.0	9.351E+01	8.078E+01	7.252E+05	
1.228E+00	-3.304E-01	1.012E+01	3.218E+01	-1.941E+01	-1.429E-01
4.324E-02	-1.154E-02	3.563E-01	4.197E-02	-4.340E-02	-1.864E-04
11	2.0	9.321E+01	8.115E+01	7.220E+05	
1.205E+00	-3.224E-01	1.002E+01	3.223E+01	-1.934E+01	-1.578E-01
4.274E-02	-1.144E-02	3.554E-01	4.235E-02	-4.354E-02	-2.074E-04
12	2.0	9.299E+01	8.153E+01	7.194E+05	
1.188E+00	-3.054E-01	9.914E+00	3.230E+01	-1.925E+01	-1.169E-01
4.225E-02	-1.089E-02	3.535E-01	4.266E-02	-4.380E-02	-1.544E-04

0°

-5°

-10°

-15°

Table C.8 Stationary WVT, 6 Blades (cont'd)

	13	2.0	9.356E+01	8.086E+01	7.254E+05	
	1.102E+00	-2.260E-01	1.012E+01	3.315E+01	-1.826E+01	2.877E-01
	3.877E-02	-7.952E-03	3.562E-01	4.320E-02	-4.079E-02	3.749E-04
-20°	14	2.0	9.342E+01	8.124E+01	7.233E+05	
	1.106E+00	-2.178E-01	9.976E+00	3.352E+01	-1.855E+01	3.224E-01
	3.905E-02	-7.692E-03	3.523E-01	4.384E-02	-4.160E-02	4.217E-04
	15	2.0	9.345E+01	8.159E+01	7.229E+05	
	1.119E+00	-2.088E-01	9.991E+00	3.331E+01	-1.821E+01	3.061E-01
	3.949E-02	-7.373E-03	3.527E-01	4.356E-02	-4.082E-02	4.008E-04
	1	2.0	9.344E+01	8.101E+01	7.241E+05	
	1.054E+00	-2.176E-01	1.005E+01	3.389E+01	-1.856E+01	-3.447E-01
	3.718E-02	-7.678E-03	3.549E-01	4.428E-02	-4.181E-02	-4.505E-04
-25°	2	2.0	9.35?E-01	8.139E+01	7.244E+05	
	1.044E+00	-1.929E-01	1.0?2E+01	3.409E+01	-1.872E+01	-3.226E-01
	3.672E-02	-?.?97E-03	3.535E- 1	4.442E-02	-4.184E-02	-4.2?5E-04
	3	2.0	9.331E+01	8.171E+01	7.214E+05	
	1.042E+00	-1.897E-01	9.954E+00	3.384E+01	-1,862E+01	-3.757E-01
	3.690E-02	-6.720E-03	3.527E-01	4.440E-02	-4.190E-02	-4.930E-04
	4	2.0	9.344E+01	8.116E+01	7.237E+05	
	1.068E+00	-2.018E-01	1.008E+01	3.291E+01	-1.868E+01	-2.473E-01
	3.758E-02	-7.122E-03	3.557E-01	4.432E-02	-4.196E-02	-3.233E-04
-30°	5	2.0	9.334E+01	8.147E+01	7.222E+05	
	1.024E+00	-1.918E-01	1.008E+01	3.432E+01	-1.892E+01	-2.535E-01
	3.623E-02	-6.433E-03	3.567E-01	4.499E-02	-4.251E-02	-3.323E-04
	6	2.0	9.311E+01	8.175E+01	7.199E+05	
	1.055E+00	-1.773E-01	9.964E+00	3.422E+01	-1.875E+01	-2.191E-01
	3.755E-02	-6.310E-03	3.546E-01	4.510E-02	-4.236E-02	-2.875E-04
	7	2.0	9.365E+01	8.099E+01	7.260E+05	
	1.090E+00	-1.600E-01	1.021E+01	3.396E+01	-2.004E+01	1.968E+00
	3.828E-02	-5.619E-03	3.585E-01	4.404E-02	-4.468E-02	2.552E-03
-35°	8	2.0	9.345E+01	8.134E+01	7.233E+05	
	1.066E+00	-1.516E-01	1.017E+01	3.346E+01	-2.022E+01	2.006E+00
	3.763E-02	-5.352E-03	3.592E-01	4.375E-02	-4.522E-02	2.623E-03
	9	2.0	9.309E+01	8.164E+01	7.192E+05	
	1.070E+00	-1.512E-01	1.007E+01	3.351E+01	-1.981E+01	1.885E+00
	3.809E-02	-5.738E-03	3.584E-01	4.418E-02	-4.479E-02	2.485E-03

Table C.9 Rotating WVT, 2 Blades

WIND TUNNEL DATA ACQUISITION PROGRAM SUMMARY

TITLE: spin2

AERO TARE FILE: official.ATR WEIGHT TARE FILE: spin2.WTR

DATA FILE: spin2.DAT DATE: 03-12-1997 TIME: 18:29:08

REF. AREA = 410.00 sq.in. REF. CHORD = 15.75 in. REF. SPAN = 27.00 in.

AR = 1.65 HMT = 0.00 in. VMT = 1.00 in.

FORCE BALANCE = 2 PRESSURE TRANSDUCER = 1 THERMISTOR = 1

RUN	ALPHA	VEL(fps)	TEMP(F)	RN	
FX-DRAG	FY-SIDEFORCE	FZ-Lift	MX-Roll	MY-Pitch	MZ-Yaw
CFX	CFY	CFZ	CMX	CMY	CMZ
1	2.0	9.364E+01	8.580E+01	7.143E+05	
1.115E+00	-2.551E-01	1.071E+01	3.743E+01	-1.872E+01	-2.619E+00
3.953E-02	-1.011E-02	3.795E-01	4.915E-02	-4.213E-02	-3.438E-03
2	2.0	9.355E+01	8.625E+01	7.125E+05	
-35° 1.101E+00	-2.650E-01	1.066E+01	3.718E+01	-1.883E+01	-2.727E+00
3.912E-02	-9.420E-03	3.798E-01	4.895E-02	-4.249E-02	-3.590E-03
3	2.0	9.356E+01	8.655E+01	7.120E+05	
1.127E+00	-2.546E-01	1.062E+01	3.701E+01	-1.891E+01	-2.735E+00
4.005E-02	-9.052E-03	3.795E-01	4.874E-02	-4.245E-02	-3.491E-03
4	2.0	9.327E+01	8.757E+01	7.073E+05	
1.135E+00	-3.485E-01	1.060E+01	3.677E+01	-1.883E+01	-2.908E+00
4.037E-02	-1.249E-02	3.792E-01	4.892E-02	-4.296E-02	-3.861E-03
5	2.0	9.299E+01	8.781E+01	7.047E+05	
-30° 1.055E+00	-1.788E-01	1.063E+01	3.692E+01	-1.825E+01	-2.790E+00
3.805E-02	-6.485E-03	3.836E-01	4.920E-02	-4.180E-02	-3.727E-03
6	2.0	9.292E+01	8.805E+01	7.037E+05	
1.040E+00	-2.108E-01	1.060E+01	3.660E+01	-1.780E+01	-2.760E+00
3.759E-02	-7.419E-03	3.822E-01	4.899E-02	-4.093E-02	-3.694E-03
7	2.0	9.314E+01	8.797E+01	7.054E+05	
1.060E+00	-2.599E-01	1.047E+01	3.638E+01	-1.835E+01	-2.605E+00
3.912E-02	-9.350E-03	3.766E-01	4.847E-02	-4.191E-02	-3.470E-03
8	2.0	9.305E+01	8.823E+01	7.042E+05	
-25° 1.080E+00	-2.655E-01	1.055E+01	3.635E+01	-1.841E+01	-2.670E+00
3.894E-02	-9.572E-03	3.813E-01	4.954E-02	-4.215E-02	-3.566E-03
9	2.0	9.302E+01	8.847E+01	7.034E+05	
1.096E+00	-2.216E-01	1.063E+01	3.653E+01	-1.820E+01	-2.719E+00
3.956E-02	-7.997E-03	3.838E-01	4.883E-02	-4.171E-02	-3.625E-03
10	2.0	9.297E+01	8.868E+01	7.025E+05	
1.097E+00	-2.788E-01	1.058E+01	3.637E+01	-1.825E+01	-3.014E+00
3.966E-02	-1.008E-02	3.824E-01	4.869E-02	-4.190E-02	-4.035E-03
11	2.0	9.302E+01	8.893E+01	7.024E+05	
-20° 1.108E+00	-2.809E-01	1.032E+01	3.598E+01	-1.789E+01	-2.824E+00
4.003E-02	-1.015E-02	3.728E-01	4.813E-02	-4.102E-02	-3.779E-03
12	2.0	9.289E+01	8.916E+01	7.009E+05	
1.115E+00	-3.199E-01	1.054E+01	3.591E+01	-1.819E+01	-2.926E+00
4.041E-02	-1.159E-02	3.818E-01	4.920E-02	-4.185E-02	-3.923E-03

Table C.9 Rotating WVT, 2 Blades (cont'd)

-15°	13	2.0	9.324E+01	8.925E+01	7.033E+05	
	1.124E+00	-2.693E-01	1.074E+01	3.681E+01	-1.816E+01	-2.655E+00
	4.044E-02	-9.686E-03	3.864E-01	4.904E-02	-4.148E-02	-3.551E-03
	14	2.0	9.335E+01	8.948E+01	7.036E+05	
	1.084E+00	-2.624E-01	1.061E+01	3.624E+01	-1.827E+01	-2.755E+00
	3.892E-02	-9.422E-03	3.809E-01	4.818E-02	-4.164E-02	-3.664E-03
	15	2.0	9.333E+01	8.969E+01	7.029E+05	
	1.140E+00	-3.037E-01	1.084E+01	3.581E+01	-1.825E+01	-2.684E+00
	4.097E-02	-1.091E-02	3.824E-01	4.767E-02	-4.164E-02	-3.578E-03
-10°	1	2.0	9.331E+01	8.913E+01	7.041E+05	
	1.113E+00	-3.803E-01	1.058E+01	3.572E+01	-1.840E+01	-2.184E+00
	3.996E-02	-1.366E-02	3.802E-01	4.751E-02	-4.196E-02	-2.905E-03
	2	2.0	9.209E+01	8.939E+01	7.018E+05	
	1.089E+00	-3.441E-01	1.071E+01	3.617E+01	-1.822E+01	-2.1[illegible]E
	3.931E-02	-1.242E-02	3.868E-01	4.936E-02	-4.200E-02	-2.928E-03
	3	2.0	9.309E+01	8.958E+01	7.014E+05	
	1.067E+00	-3.394E-01	1.079E+01	3.544E+01	-1.801E+01	-2.347E+00
	3.855E-02	-1.226E-02	3.897E-01	4.740E-02	-4.129E-02	-3.139E-03
-5°	9	2.0	9.300E+01	8.975E+01	6.999E+05	
	1.115E+00	-4.696E-01	1.050E+01	3.553E+01	-1.375E+01	-1.961E+00
	4.025E-02	-1.700E-02	3.902E-01	4.764E-02	-4.309E-02	-2.630E-03
	[illegible]	2.0	9.270E+01	9.017E+01	6.971E+05	
	1.[illegible]31E+00	-2.636E-01	1.[illegible]3E+01	3.610E+01	-1.[illegible]7E+01	-1.[illegible]3E+00
	3.722E-02	-9.611E-03	3.712E-01	4.874E-02	-4.066E-02	-2.159E-03
	10	2.0	9.293E+01	9.034E+01	6.984E+05	
	1.145E+00	-2.252E-01	1.049E+01	3.638E+01	-1.829E+01	-1.416E+00
	4.154E-02	-8.173E-03	3.808E-01	4.890E-02	-4.215E-02	-1.903E-03
0°	1	2.0	9.334E+01	8.885E+01	7.049E+05	
	1.215E+00	-4.644E-01	1.062E+01	3.482E+01	-2.224E+01	9.774E-01
	4.357E-02	-1.666E-02	3.810E-01	4.626E-02	-5.067E-02	1.299E-03
	2	2.0	9.327E+01	9.011E+01	7.015E+05	
	1.294E+00	-4.832E-01	1.163E+01	3.664E+01	-1.121E+01	-2.018E+00
	4.561E-02	-1.740E-02	4.187E-01	4.997E-02	-2.554E-02	-2.692E-03

Table C.10 Rotating WVT, 3 Blades

WIND TUNNEL DATA ACQUISITION PROGRAM SUMMARY

TITLE: spin3
AERO TARE FILE: official.ATR WEIGHT TARE FILE: spin3.WTR
DATA FILE: spin3.DAT DATE: 03-13-1997 TIME: 18:35:34
REF. AREA = 410.00 sq.in. REF. CHORD = 15.75 in. REF. SPAN = 27.00 in.
AR = 1.65 HMT = 0.00 in. VMT = 1.00 in.
FORCE BALANCE = 2 PRESSURE TRANSDUCER = 1 THERMISTOR = 1

	RUN	ALFHA	VEL(fps)	TEMP(F)	RN	
	FX-DRAG	FY-SIDEFORCE	FZ-Lift	MX-Roll	MY-Pitch	MZ-Yaw
	CFX	CFY	CFZ	CMX	CMY	CMZ
	4	2.0	9.304E+01	8.372E+01	7.146E+05	
	1.087E+00	-1.756E-01	1.006E+01	3.465E+01	-1.998E+01	-8.611E-01
	3.887E-02	-6.287E-03	3.600E-01	4.590E-02	-4.311E-02	-1.141E-03
-35°	5	2.0	9.295E+01	8.295E+01	7.128E+05	
	1.086E+00	-1.602E-01	9.961E+00	3.481E+01	-1.851E+01	-7.897E-01
	3.900E-02	-5.752E-03	3.577E-01	4.529E-02	-4.220E-02	-1.050E-03
	6	2.0	9.306E+01	8.421E+01	7.136E+05	
	1.094E+00	-1.742E-01	1.011E+01	3.509E+01	-1.898E+01	-7.354E-01
	3.916E-02	-6.282E-03	3.616E-01	4.651E-02	-4.311E-02	-9.749E-04
	7	2.0	9.347E+01	8.325E+01	7.189E+05	
	1.050E+00	-1.421E-01	1.013E+01	3.513E+01	-1.922E+01	-1.129E+00
	3.717E-02	-5.225E-03	3.588E-01	4.607E-02	-4.321E-02	-1.491E-03
-30°	8	2.0	9.331E+01	8.361E+01	7.169E+05	
	1.075E+00	-1.664E-01	1.011E+01	3.507E+01	-1.901E+01	-1.169E+00
	3.822E-02	-5.915E-03	3.596E-01	4.618E-02	-4.290E-02	-1.539E-03
	9	2.0	9.356E+01	8.390E+01	7.181E+05	
	1.105E+00	-1.280E-01	1.017E+01	3.470E+01	-1.912E+01	-1.102E+00
	3.910E-02	-4.527E-03	3.600E-01	4.547E-02	-4.294E-02	-1.444E-03
	1	2.0	9.305E+01	8.314E+01	7.160E+05	
	1.051E+00	-1.399E-01	1.010E+01	3.444E+01	-1.905E+01	-1.162E+00
	3.754E-02	-4.997E-03	3.607E-01	4.557E-02	-4.326E-02	-1.538E-03
-25°	2	2.0	9.307E+01	8.342E+01	7.155E+05	
	1.075E+00	-9.643E-02	1.012E+01	3.386E+01	-1.956E+01	-1.205E+00
	3.239E-02	-3.098E-03	3.614E-01	4.481E-02	-4.436E-02	-1.594E-03
	3	2.0	9.314E+01	8.368E+01	7.154E+05	
	1.079E+00	-1.341E-01	1.022E+01	3.399E+01	-1.843E+01	-1.068E+00
	3.850E-02	-4.797E-03	3.647E-01	4.493E-02	-4.176E-02	-1.438E-03
	10	2.0	9.344E+01	8.342E+01	7.182E+05	
	1.075E+00	-1.355E-01	1.013E+01	3.451E+01	-1.878E+01	-1.004E+00
	3.811E-02	-4.802E-03	3.589E-01	4.530E-02	-4.226E-02	-1.319E-03
-20°	11	2.0	9.347E+01	8.370E+01	7.179E+05	
	1.008E+00	-1.457E-01	1.002E+01	3.422E+01	-1.877E+01	-9.930E-01
	3.573E-02	-5.164E-03	3.551E-01	4.491E-02	-4.222E-02	-1.303E-03
	12	2.0	9.326E+01	8.394E+01	7.157E+05	
	1.096E+00	-1.477E-01	9.948E+00	3.434E+01	-1.857E+01	-9.189E-01
	3.905E-02	-5.332E-03	3.550E-01	4.532E-02	-4.198E-02	-1.212E-03

Table C.10 Rotating WVT, 3 Blades (cont'd)

	13	2.0	9.335E+01	8.395E+01	7.164E+05	
	1.091E+00	-1.675E-01	1.001E+01	3.406E+01	-1.899E+01	-8.906E-01
	3.877E-02	-5.952E-03	3.558E-01	4.483E-02	-4.285E-02	-1.172E-03
-15°	14	2.0	9.346E+01	8.417E+01	7.167E+05	
	1.088E+00	-1.531E-01	1.002E+01	3.430E+01	-1.916E+01	-9.749E-01
	3.860E-02	-5.432E-03	3.554E-01	4.507E-02	-4.317E-02	-1.281E-03
	15	2.0	9.341E+01	8.436E+01	7.155E+05	
	1.077E+00	-1.511E-01	9.977E+00	3.398E+01	-1.867E+01	-9.506E-01
	3.825E-02	-5.369E-03	3.545E-01	4.471E-02	-4.210E-02	-1.251E-03
	1	2.0	9.317E+01	8.448E+01	7.138E+05	
	1.166E+00	-2.317E-01	1.001E+01	3.367E+01	-1.901E+01	-2.829E-01
	4.165E-02	-8.275E-03	3.574E-01	4.454E-02	-4.310E-02	-3.742E-04
-10°	2	2.0	9.31EE+01	8.469E+01	7.131E+05	
	1.157E+00	-2.477E-01	1.00EE+01	3.323E+01	-1.25EE+01	-3.237E-01
	4.135E-02	-8.854E-03	3.5E3E-01	4.400E-02	-4.255E-02	-4.235E-04
	3	2.0	9.326E+01	8.486E+01	7.136E+05	
	1.162E+00	-1.870E-01	9.934E+00	3.267E+01	-1.905E+01	-3.442E-01
	4.145E-02	-6.704E-03	3.544E-01	4.448E-02	-4.314E-02	-4.547E-04
	4	2.0	9.328E+01	8.291E+01	7.183E+05	
	1.335E+00	-2.744E-01	1.032E+01	3.320E+01	-1.772E+01	3.154E-01
	4.743E-02	-9.747E-03	3.657E-01	4.369E-02	-4.000E-02	4.150E-04
-5°	5	2.0	9.334E+01	8.340E+01	7.176E+05	
	1.115E+00	-3.133E-01	1.030E+01	3.309E+01	-1.816E+01	4.165E-02
	3.961E-02	-1.113E-02	3.659E-01	4.353E-02	-4.096E-02	5.480E-05
	6	2.0	9.304E+01	8.281E+01	7.143E+05	
	1.098E+00	-2.303E-01	1.010E+01	3.307E+01	-1.822E+01	2.892E-01
	3.929E-02	-8.239E-03	3.613E-01	4.381E-02	-4.137E-02	3.832E-04
	7	2.0	9.328E+01	8.382E+01	7.162E+05	
	1.302E+00	-3.269E-01	1.010E+01	3.319E+01	-1.879E+01	1.352E+00
	4.635E-02	-1.163E-02	3.595E-01	4.375E-02	-4.247E-02	1.782E-03
0°	8	2.0	9.321E+01	8.410E+01	7.150E+05	
	1.376E+00	-3.798E-01	9.706E+00	3.324E+01	-1.952E+01	1.277E+00
	4.907E-02	-1.355E-02	3.461E-01	4.404E-02	-4.423E-02	1.697E-03
	9	2.0	9.294E+01	8.433E+01	7.123E+05	
	1.322E+00	-2.707E-01	1.027E+01	3.312E+01	-1.760E+01	1.465E+00
	4.745E-02	-9.713E-03	3.685E-01	4.403E-02	-4.010E-02	1.947E-03

Table C.11 Rotating WVT, 4 Blades

WIND TUNNEL DATA ACQUISITION PROGRAM SUMMARY

TITLE: spin4
AERO TARE FILE: official.ATRWEIGHT TARE FILE: spin4.WTR
DATA FILE: spin4.DAT DATE: 03-12-1997 TIME: 00:35:15
REF. AREA = 410.00 sq.in. REF. CHORD = 15.75 in. REF. SPAN = 27.00 in.
AR = 1.65 RMT = 0.00 in. VMT = 1.00 in.
FORCE BALANCE = 2 PRESSURE TRANSDUCER = 1 THERMISTOR = 1

RUN	ALFHA	VEL(fps)	TEMP(F)	RN	
FX-DRAG	FY-SIDEFORCE	FZ-Lift	MX-Roll	MY-Pitch	MZ-Yaw
CFX	CFY	CFZ	CMX	CMY	CMZ
1	2.0	9.272E+01	8.311E+01	7.135E+05	
1.140E+00	-2.915E-01	1.056E+01	3.600E+01	-1.866E+01	-7.956E-01
4.102E-02	-1.049E-02	3.798E-01	4.797E-02	-4.863E-02	-1.060E-03
2	2.0	9.252E+01	8.348E+01	7.119E+05	
1.187E+00	-2.714E-01	1.057E+01	3.686E+01	-1.909E-01	-9.133E-01
4.280E-02	-9.791E-03	3.813E-01	4.925E-02	-4.372E-02	-1.220E-03
3	2.0	9.284E+01	8.372E+01	7.130E+05	
1.219E+00	-2.624E-01	1.062E+01	3.635E+01	-1.903E+01	-9.415E-01
4.391E-02	-9.427E-03	3.814E-01	4.836E-02	-4.339E-02	-1.253E-03
4	2.0	9.299E+01	8.443E+01	7.125E+05	
1.127E+00	-2.375E-01	1.060E+01	3.652E+01	-1.981E+01	-1.204E+00
4.042E-02	-8.525E-03	3.802E-01	4.857E-02	-4.231E-02	-1.579E-03
5	2.0	9.314E+01	8.471E+01	7.130E+05	
1.149E+00	-2.143E-01	1.051E+01	3.693E+01	-1.896E+01	-1.041E+00
4.104E-02	-7.663E-03	3.757E-01	4.891E-02	-4.292E-02	-1.378E-03
6	2.0	9.288E+01	8.497E+01	7.104E+05	
1.146E+00	-2.102E-01	1.064E+01	3.652E+01	-1.905E+01	-1.079E+00
4.123E-02	-7.563E-03	3.829E-01	4.866E-02	-4.351E-02	-1.437E-03
7	2.0	9.317E+01	8.571E+01	7.109E+05	
1.151E+00	-2.489E-01	1.061E+01	3.639E+01	-1.864E+01	-1.291E+00
4.121E-02	-8.911E-03	3.796E-01	4.523E-02	-4.225E-02	-1.711E-03
8	2.0	9.351E+01	8.599E+01	7.129E+05	
1.141E+00	-2.650E-01	1.057E+01	3.626E+01	-1.884E+01	-1.484E+00
4.056E-02	-9.423E-03	3.788E-01	4.775E-02	-4.254E-02	-1.954E-03
9	2.0	9.327E+01	8.623E+01	7.105E+05	
1.193E+00	-1.914E-01	1.047E+01	3.670E+01	-1.886E+01	-1.336E+00
4.264E-02	-6.842E-03	3.743E-01	4.960E-02	-4.281E-02	-1.770E-03
10	2.0	9.372E+01	8.691E+01	7.123E+05	
1.276E+00	-2.415E-01	1.059E+01	3.634E+01	-1.825E+01	-1.159E+00
4.526E-02	-8.564E-03	3.754E-01	4.772E-02	-4.109E-02	-1.523E-03
11	2.0	9.373E+01	8.716E+01	7.118E+05	
1.248E+00	-2.792E-01	1.080E+01	3.664E+01	-1.854E+01	-1.442E+00
4.427E-02	-9.902E-03	3.829E-01	4.814E-02	-4.174E-02	-1.894E-03
12	2.0	9.361E+01	8.740E+01	7.104E+05	
1.149E+00	-2.432E-01	1.082E+01	3.654E+01	-1.779E+01	-1.227E+00
4.089E-02	-8.649E-03	3.849E-01	4.926E-02	-4.019E-02	-1.516E-03

-35°

-30°

-25°

-20°

Table C.11 Rotating WVT, 4 Blades (cont'd)

15°	13	2.0	9.380E+01	8.585E+01	7.154E+05	
	1.188E+00	-2.969E-01	1.055E+01	3.608E+01	-1.844E+01	-1.753E+00
	4.198E-02	-1.049E-02	3.727E-01	4.721E-02	-4.136E-02	-2.294E-03
	14	2.0	9.368E+01	8.619E+01	7.137E+05	
	1.181E+00	-3.276E-01	1.049E+01	3.674E+01	-1.862E+01	-1.541E+00
	4.184E-02	-1.161E-02	3.718E-01	4.822E-02	-4.190E-02	-2.022E-03
	15	2.0	9.372E+01	8.647E+01	7.133E+05	
	1.246E+00	-3.513E-01	1.051E+01	3.598E+01	-1.858E+01	-1.356E+00
	4.416E-02	-1.245E-02	3.725E-01	4.722E-02	-4.180E-02	-1.780E-03
-10°	1	2.0	9.4[illegible]E+01	8.645E+01	7.155E+05	
	1.184E+00	-4.409E-01	1.052E+01	3.892E+01	-1.810E+01	-7.925E-01
	4.169E-02	-1.553E-02	3.706E-01	5.076E-02	-4.047E-02	-1.024E-03
	2	2.0	9.3[illegible]E+01	8.648E+01	7.144E+05	
	1.297E+00	-3.450E-01	1.[illegible]E+01	3.636E+01	-1.883E+01	-3.144E-01
	4.575E-02	-1.217E-02	3.810E-01	4.751E-02	-4.218E-02	-1.064E-03
	3	2.0	9.391E+01	8.691E+01	7.137E+05	
	1.337E+00	-4.357E-01	1.038E+01	3.280E+01	-1.931E+01	-6.640E-01
	4.721E-02	-1.539E-02	3.665E-01	4.290E-02	-4.231E-02	-8.685E-04
-5°	4	2.0	9.307E+01	8.674E+01	7.078E+05	
	1.409E+00	-3.006E-01	1.057E+01	3.376E+01	-2.217E+01	-1.835E+00
	5.063E-02	-1.090E-02	3.799E-01	4.494E-02	-5.059E-02	-2.509E-03
	5	2.0	9.293E+01	8.697E+01	7.[illegible]EE+05	
	1.358E+00	-3.[illegible]E-01	1.076E+01	3.536E+01	-1.848E+01	9.753E-03
	4.998E-02	-2.174E-02	3.991E-01	4.724E-02	-4.233E-02	1.303E-05
	6	2.0	9.318E+01	8.715E+01	7.077E+05	
	1.345E+00	-5.004E-01	1.073E+01	3.520E+01	-1.858E+01	7.326E-02
	4.826E-02	-1.796E-02	3.850E-01	4.678E-02	-4.234E-02	9.736E-05
0°	7	2.0	9.350E+01	8.491E+01	7.153E+05	
	1.399E+00	-5.249E-01	1.106E+01	3.496E+01	-1.799E+01	1.938E+00
	4.964E-02	-1.863E-02	3.925E-01	4.596E-02	-4.032E-02	2.543E-03
	8	2.0	9.317E+01	9.525E+01	7.120E+05	
	1.503E+00	-5.[illegible]5E-01	1.059E+01	3.487E+01	-1.601E+01	2.253E+00
	5.375E-02	-2.132E-02	3.787E-01	4.619E-02	-3.637E-02	2.985E-03
	9	2.0	9.324E+01	8.559E+01	7.117E+05	
	1.602E+00	-7.509E-01	1.100E+01	3.497E+01	-2.244E+01	9.850E-01
	5.724E-02	-2.694E-02	3.932E-01	4.629E-02	-5.092E-02	1.304E-03

Table C.12 Rotating WVT, 5 Blades

WIND TUNNEL DATA ACQUISITION PROGRAM SUMMARY

TITLE: spin5

AERO TARE FILE: official.ATRWEIGHT TARE FILE: spin5.WTR

DATA FILE: spin5.DAT DATE: 03-14-1997 TIME: 15:22:42

REF. AREA = 410.00 sq.in. REF. CHORD = 15.75 in. REF. SPAN = 27.00 in.

AR = 1.65 HMT = 0.00 in. VMT = 1.00 in.

FORCE BALANCE = 2 PRESSURE TRANSDUCER = 1 THERMISTOR = 1

	RUN	ALFHA	VEL(fps)	TEMP(F)	RN	
	FX-DRAG	FY-SIDEFORCE	FZ-Lift	MX-Roll	MY-Pitch	MZ-Yaw
	CFX	CFY	CFZ	CMX	CMY	CMZ
	1	2.0	9.249E+01	7.707E+01	7.261E+05	
	1.167E+00	-2.439E-01	1.002E+01	3.425E+01	-1.922E+01	8.187E-01
	4.171E-02	-8.721E-03	3.582E-01	4.535E-02	-4.362E-02	1.024E-02
-35°	2	2.0	9.271E+01	7.747E+01	7.269E+05	
	1.157E+00	-2.484E-01	1.005E+01	3.446E+01	-1.922E+01	9.544E-01
	4.119E-02	-8.843E-03	3.578E-01	4.544E-02	-4.345E-02	1.127E-03
	3	2.0	9.303E+01	7.780E+01	7.286E+05	
	1.155E+00	-2.395E-01	1.009E+01	3.468E+01	-1.925E+01	8.776E-01
	4.085E-02	-8.476E-03	3.572E-01	4.545E-02	-4.347E-02	1.150E-03
	4	2.0	9.250E+01	7.970E+01	7.199E+05	
	1.120E+00	-2.275E-01	9.974E+00	3.359E+01	-1.887E+01	3.035E-01
	4.022E-02	-8.170E-03	3.583E-01	4.469E-02	-4.303E-02	4.036E-04
-30°	5	2.0	9.256E+01	7.999E+01	7.197E+05	
	1.124E+00	-2.233E-01	9.915E+00	3.389E+01	-1.909E+01	2.718E-01
	4.042E-02	-8.015E-03	3.558E-01	4.505E-02	-4.349E-02	3.614E-04
	6	2.0	9.245E+01	8.023E+01	7.182E+05	
	1.132E+00	-2.592E-01	9.874E+00	3.376E+01	-1.879E+01	2.906E-01
	4.076E-02	-9.351E-03	3.554E-01	4.501E-02	-4.339E-02	3.874E-04
	7	2.0	9.266E+01	8.127E+01	7.189E+05	
	1.082E+00	-2.819E-01	9.952E+00	3.320E+01	-1.894E+01	8.234E-02
	3.867E-02	-1.008E-02	3.557E-01	4.409E-02	-4.275E-02	1.099E-04
-25°	8	2.0	9.297E+01	8.151E+01	7.192E+05	
	1.061E+00	-3.352E-01	1.024E+01	3.246E+01	-1.850E+01	-1.580E-01
	3.786E-02	-1.196E-02	3.654E-01	4.239E-02	-4.191E-02	-2.092E-04
	9	2.0	9.254E+01	8.203E+01	7.154E+05	
	1.056E+00	-2.850E-01	9.879E+00	3.424E+01	-1.844E+01	3.716E-01
	3.798E-02	-1.025E-02	3.553E-01	4.561E-02	-4.210E-02	4.950E-04
	10	2.0	9.306E+01	8.265E+01	7.173E+05	
	1.029E+00	-2.939E-01	1.016E+01	3.348E+01	-1.827E+01	6.405E-01
	3.672E-02	-1.049E-02	3.626E-01	4.424E-02	-4.139E-02	8.463E-04
-20°	11	2.0	9.275E+01	8.317E+01	7.134E+05	
	1.024E+00	-3.272E-01	1.016E+01	3.319E+01	-1.829E+01	7.508E-02
	3.683E-02	-1.176E-02	3.655E-01	4.419E-02	-4.175E-02	1.000E-04
	12	2.0	9.290E+01	8.420E+01	7.123E+05	
	1.044E+00	-3.123E-01	1.017E+01	3.343E+01	-1.847E+01	2.032E-01
	3.750E-02	-1.121E-02	3.652E-01	4.442E-02	-4.210E-02	2.702E-04

Table C.12 Rotating WVT, 5 Blades (cont'd)

-15°	13	2.0	9.339E+01	9.394E+01	7.167E+05	
	1.143E+00	-3.570E-01	1.002E+01	3.435E+01	-1.819E+01	3.915E-01
	4.061E-02	-1.268E-02	3.559E-01	4.520E-02	-4.101E-02	5.149E-04
	14	2.0	9.328E+01	9.423E+01	7.152E+05	
	1.157E+00	-4.320E-01	9.791E+00	3.260E+01	-1.770E+01	7.091E-01
	4.122E-02	-1.539E-02	3.487E-01	4.301E-02	-4.003E-02	9.354E-04
	15	2.0	9.353E+01	8.447E+01	7.165E+05	
	1.097E+00	-4.341E-01	1.032E+01	3.392E+01	-1.958E+01	5.850E-01
	3.889E-02	-1.539E-02	3.659E-01	4.453E-02	-4.406E-02	7.679E-04
-10°	2	2.0	9.271E+01	8.456E+01	7.101E+05	
	1.265E+00	-4.913E-01	1.008E+01	3.244E+01	-1.904E+01	1.132E+00
	4.562E-02	-1.773E-02	3.639E-01	4.334E-02	-4.362E-02	1.513E-03
	3	2.0	9.274E+01	8.480E+01	7.098E+05	
	1.224E+00	-3.526E-01	9.831E+00	3.194E+01	-1.776E+01	1.305E+00
	4.415E-02	-1.330E-02	3.565E-01	4.267E-02	-4.067E-02	1.743E-03
	4	2.0	9.259E+01	8.503E+01	7.088E+05	
	1.257E+00	-7.995E-01	9.762E+00	3.190E+01	-1.834E+01	1.135E+00
	4.541E-02	-2.288E-02	3.527E-01	4.269E-02	-4.207E-02	1.518E-03
-5°	7	2.0	9.361E+01	7.970E+01	7.285E+05	
	1.116E+00	-5.992E-01	1.051E+01	3.072E+01	-1.406E+01	3.233E+00
	3.913E-02	-2.102E-02	3.687E-01	3.990E-02	-3.132E-02	4.195E-03
	8	2.0	9.323E+01	8.050E+01	7.[illegible]E+05	
	1.333E+00	-7.946E-01	1.084E+01	3.452E+01	-1.417E+01	1.227E+00
	4.711E-02	-2.808E-02	3.829E-01	4.518E-02	-3.180E-02	2.390E-03
	9	2.0	9.352E+01	9.108E+01	7.246E+05	
	1.235E+00	-6.949E-01	9.573E+00	3.148E+01	-1.339E+01	-1.537E-02
	4.351E-02	-2.448E-02	3.372E-01	4.107E-02	-4.112E-02	-2.[illegible]5E-05
0°	10	2.0	9.245E+01	8.333E+01	7.187E+05	
	1.523E+00	-8.959E-01	1.051E+01	3.497E+01	-2.479E+01	1.404E+00
	5.395E-02	-3.139E-02	3.723E-01	4.589E-02	-5.576E-02	1.843E-03
	11	2.0	9.340E+01	8.424E+01	7.161E+05	
	1.330E+00	-6.472E-01	9.931E+00	3.104E+01	-2.173E+01	2.995E+00
	4.725E-02	-2.299E-02	3.528E-01	4.084E-02	-4.902E-02	3.941E-03
	12	2.0	9.354E+01	8.449E+01	7.174E+05	
	1.667E+00	-7.220E-01	1.040E+01	3.237E+01	-2.417E+01	1.381E+00
	5.896E-02	-2.552E-02	3.677E-01	4.239E-02	-5.427E-02	1.808E-03

Table C.13 Rotating WVT, 6 Blades

WIND TUNNEL DATA ACQUISITION PROGRAM SUMMARY

TITLE: spin6
AERO TARE FILE: official.ATRWEIGHT TARE FILE: spin6.WTR
DATA FILE: spin6.DAT DATE: 03-14-1997 TIME: 23:14:45
REF. AREA = 410.00 sq.in. REF. CHORD = 15.75 in. REF. SPAN = 27.00 in.
AR = 1.65 HMT = 0.00 in. VMT = 1.00 in.
FORCE BALANCE = 2 PRESSURE TRANSDUCER = 1 THERMISTOR = 1

RUN	ALPHA	VEL(fps)	TEMP(F)	RN	
FX-DRAG	FY-SIDEFORCE	FZ-Lift	MX-Roll	MY-Pitch	MZ-Yaw
CFX	CFY	CFZ	CMX	CMY	CMZ
1	2.0	9.314E+01	8.151E+01	7.206E+05	
1.144E+00	-1.969E-01	1.019E+01	3.469E+01	-1.923E+01	5.042E-01
4.067E-02	-6.997E-03	3.620E-01	4.556E-02	-4.339E-02	6.638E-04
2	2.0	9.309E+01	8.175E+01	7.195E+05	
-35° 1.138E+00	-2.164E-01	1.014E+01	3.468E+01	-1.900E+01	5.990E-01
4.051E-02	-7.706E-03	3.612E-01	4.573E-02	-4.294E-02	7.898E-04
3	2.0	9.320E+01	8.204E+01	7.197E+05	
1.156E+00	-2.250E-01	1.009E+01	3.487E+01	-1.904E+01	6.785E-01
4.109E-02	-7.997E-03	3.595E-01	4.589E-02	-4.295E-02	8.931E-04
4	2.0	9.346E+01	8.217E+01	7.214E+05	
1.083E+00	-2.200E-01	1.029E+01	3.433E+01	-1.919E+01	6.225E-01
3.837E-02	-7.775E-03	3.637E-01	4.495E-02	-4.307E-02	8.149E-04
-30° 6	2.0	9.336E+01	8.274E+01	7.192E+05	
1.070E+00	-2.358E-01	1.022E+01	3.444E+01	-1.834E+01	8.279E-01
3.794E-02	-8.360E-03	3.622E-01	4.523E-02	-4.241E-02	1.087E-03
7	2.0	9.339E+01	8.314E+01	7.186E+05	
1.066E+00	-2.148E-01	1.024E+01	3.423E+01	-1.905E+01	8.242E-01
3.780E-02	-7.617E-03	3.631E-01	4.496E-02	-4.290E-02	1.092E-03
8	2.0	9.365E+01	8.201E+01	7.223E+05	
1.106E+00	-2.140E-01	1.025E+01	3.475E+01	-1.879E+01	2.377E-01
3.892E-02	-7.531E-03	3.608E-01	4.522E-02	-4.199E-02	4.201E-04
-25° 9	2.0	9.355E+01	8.230E+01	7.213E+05	
1.099E+00	-2.357E-01	1.016E+01	3.442E+01	-1.881E+01	5.582E-01
3.879E-02	-8.318E-03	3.594E-01	4.499E-02	-4.215E-02	7.876E-04
10	2.0	9.359E+01	8.257E+01	7.215E+05	
1.106E+00	-2.079E-01	1.016E+01	3.417E+01	-1.904E+01	3.252E-01
3.902E-02	-7.335E-03	3.582E-01	4.464E-02	-4.265E-02	4.250E-04
11	2.0	9.354E+01	8.204E+01	7.224E+05	
1.137E+00	-2.291E-01	1.013E+01	3.455E+01	-1.866E+01	6.963E-01
4.010E-02	-8.081E-03	3.573E-01	4.514E-02	-4.180E-02	8.967E-04
12	2.0	9.319E+01	8.235E+01	7.190E+05	
-20° 1.083E+00	-1.990E-01	1.010E+01	3.398E+01	-1.847E+01	7.869E-01
3.850E-02	-7.079E-03	3.592E-01	4.475E-02	-4.170E-02	1.036E-03
13	2.0	9.327E+01	8.261E+01	7.190E+05	
1.078E+00	-1.698E-01	1.002E+01	3.425E+01	-1.844E+01	7.783E-01
3.830E-02	-6.030E-03	3.557E-01	4.505E-02	-4.157E-02	1.024E-03

Table C.13 Rotating WVT, 6 Blades (cont'd)

	14	2.0	9.331E+01	8.214E+01	7.204E+05	
	1.188E+00	-2.511E-01	1.029E+01	3.353E+01	-1.882E+01	9.594E-01
	4.214E-02	-9.256E-03	3.649E-01	4.404E-02	-4.237E-02	1.259E-03
-15°	15	2.0	9.322E+01	8.242E+01	7.190E+05	
	1.127E+00	-2.180E-01	1.015E+01	3.252E+01	-1.893E+01	1.127E+00
	4.007E-02	-7.750E-03	3.608E-01	4.296E-02	-4.272E-02	1.484E-03
	16	2.0	9.328E+01	8.267E+01	7.189E+05	
	1.186E+00	-3.139E-01	1.005E+01	3.353E+01	-1.838E+01	9.218E-01
	4.213E-02	-1.114E-02	3.568E-01	4.410E-02	-4.145E-02	1.212E-03
	1	2.0	9.351E+01	9.201E+01	7.222E+05	
	1.217E+00	-2.619E-01	1.031E+01	3.399E+01	-1.852E+01	1.681E+00
	4.296E-02	-9.245E-03	3.640E-01	4.421E-02	-4.150E-02	2.197E-03
-10°	2	2.0	9.356E+01	8.228E+01	7.220E+05	
	1.272E+00	-2.881E-01	1.020E+01	3.319E+01	-1.898E+01	1.614E+00
	4.490E-02	-1.016E-02	3.598E-01	4.337E-02	-4.251E-02	2.108E-03
	3	2.0	9.359E+01	9.254E+01	7.215E+05	
	1.244E+00	-2.592E-01	1.010E+01	3.472E+01	-1.846E+01	1.677E+00
	4.389E-02	-9.146E-03	3.562E-01	4.538E-02	-4.135E-02	2.192E-03
	4	2.0	9.312E+01	7.890E+01	7.267E+05	
	1.287E+00	-5.548E-01	1.039E+01	3.376E+01	-1.912E+01	1.556E+00
	4.553E-02	-1.963E-02	3.679E-01	4.424E-02	-4.256E-02	2.038E-03
-5°	5	2.0	9.288E+01	9.064E+01	7.206E+05	
	1.144E+00	-2.929E-01	1.036E+01	3.324E+01	-1.799E+01	1.285E+00
	4.084E-02	-1.045E-02	3.695E-01	4.410E-02	-4.077E-02	4.341E-03
	6	2.0	9.282E+01	9.091E+01	7.195E+05	
	1.371E+00	-4.423E-01	1.001E+01	3.357E+01	-1.830E+01	1.819E+00
	4.902E-02	-1.581E-02	3.580E-01	4.445E-02	-4.154E-02	2.409E-03
	7	2.0	9.313E+01	9.200E+01	7.193E+05	
	1.420E+00	-3.576E-01	1.023E+01	3.363E+01	-1.891E+01	3.219E+00
	5.053E-02	-1.272E-02	3.642E-01	4.439E-02	-4.272E-02	5.033E-03
0°	8	2.0	9.323E+01	8.224E+01	7.195E+05	
	1.494E+00	-2.392E-01	1.017E+01	3.328E+01	-1.842E+01	3.152E+00
	5.309E-02	-8.498E-03	3.612E-01	4.378E-02	-4.156E-02	4.149E-03
	9	2.0	9.329E+01	9.244E+01	7.194E+05	
	1.455E+00	-1.606E-01	1.003E+01	3.207E+01	-2.003E+01	3.148E+00
	5.166E-02	-5.702E-03	3.561E-01	4.347E-02	-4.515E-02	4.139E-03

Table C.14 Stationary WVT Alpha Sweep, 6 Blades (One Run Only)

WIND TUNNEL DATA ACQUISITION PROGRAM SUMMARY

TITLE: final6
AERO TARE FILE: official.AIRWEIGHT TARE FILE: final6.WTR
DATA FILE: final6.DAT DATE: 03-17-1997 TIME: 13:51:19
REF. AREA = 410.00 sq.in. REF. CHORD = 15.75 in. REF. SPAN = 27.00 in.
AR = 1.65 HMT = 0.00 in. VMT = 1.00 in.
FORCE BALANCE = 2 PRESSURE TRANSDUCER = 1 THERMISTOR = 1

RUN	ALPHA	VEL(fps)	TEMP(F)	RN	
FX-DRAG	FY-SIDEFORCE	FZ-Lift	MX-Roll	MY-Pitch	MZ-Yaw
CFX	CFY	CFZ	CMX	CMY	CMZ
1	15.0	9.435E+01	7.694E+01	7.411E+05	
4.726E+00	-6.511E-01	2.995E+01	8.103E+01	-3.676E+01	-1.269E+01
1.623E-01	-2.236E-02	1.029E+00	1.031E-01	-8.017E-02	-1.614E-02
2	14.0	9.500E+01	7.757E+01	7.446E+05	
4.706E+00	-6.345E-01	3.024E+01	8.174E+01	-3.687E+01	-1.279E+01
1.596E-01	-2.152E-02	1.026E+00	1.027E-01	-7.940E-02	-1.621E-02
3	13.0	9.539E+01	7.818E+01	7.461E+05	
4.688E+00	-6.197E-01	2.985E+01	8.133E+01	-3.689E+01	-1.280E+01
1.503E-01	-2.023E-02	9.966E-01	1.014E-01	-7.462E-02	-1.534E-02
4	12.0	9.402E+01	7.904E+01	7.333E+05	
3.952E+00	-5.357E-01	2.752E+01	7.769E+01	-3.141E+01	-1.120E+01
1.372E-01	-1.814E-02	9.554E-01	9.991E-02	-6.925E-02	-1.441E-02
5	11.0	9.383E+01	7.952E+01	7.305E+05	
3.820E+00	-5.131E-01	2.622E+01	7.492E+01	-2.964E+01	-1.055E+01
1.263E-01	-1.791E-02	9.152E-01	9.694E-02	-6.569E-02	-1.363E-02
6	10.0	9.405E+01	8.010E+01	7.307E+05	
3.242E+00	-4.944E-01	2.507E+01	7.247E+01	-2.910E+01	-9.871E+00
1.129E-01	-1.719E-02	8.717E-01	9.333E-02	-6.205E-02	-1.271E-02
7	9.0	9.405E+01	8.059E+01	7.298E+05	
2.837E+00	-4.675E-01	2.369E+01	6.939E+01	-2.659E+01	-9.193E+00
1.019E-01	-1.627E-02	8.246E-01	8.945E-02	-5.977E-02	-1.185E-02
8	8.0	9.391E+01	8.171E+01	7.261E+05	
2.526E+00	-4.502E-01	2.206E+01	6.516E+01	-2.540E+01	-8.372E+00
9.045E-02	-1.574E-02	7.715E-01	8.440E-02	-5.540E-02	-1.085E-02
9	7.0	9.390E+01	8.219E+01	7.249E+05	
2.260E+00	-4.161E-01	2.051E+01	6.151E+01	-2.464E+01	-7.192E+00
7.912E-02	-1.457E-02	7.183E-01	7.976E-02	-5.477E-02	-9.326E-03

Table C.14 Stationary WVT Alpha Sweep, 6 Blades (One Run Only, cont'd)

10	6.0	9.413E+01	8.262E+01	7.255E+05	
2.018E+00	-3.866E-01	1.908E+01	5.748E+01	-2.382E+01	-6.170E+00
7.036E-02	-1.348E-02	6.654E-01	7.425E-02	-5.274E-02	-7.970E-03
11	5.0	9.428E+01	8.295E+01	7.259E+05	
1.795E+00	-3.567E-01	1.759E+01	5.353E+01	-2.312E+01	-5.260E+00
6.243E-02	-1.241E-02	6.120E-01	6.897E-02	-5.105E-02	-6.776E-03
12	4.0	9.463E+01	9.341E+01	7.275E+05	
1.590E+00	-3.125E-01	1.572E+01	4.806E+01	-2.218E+01	-3.682E+00
5.495E-02	-1.090E-02	5.432E-01	6.151E-02	-4.867E-02	-4.713E-03
13	3.0	9.431E+01	8.370E+01	7.243E+05	
1.402E+00	-3.179E-01	1.406E+01	4.331E+01	-2.146E+01	-2.675E+00
4.882E-02	-1.107E-02	4.894E-01	5.595E-02	-4.744E-02	-3.449E-03
14	2.0	9.433E+01	8.399E+01	7.235E+05	
1.259E+00	-3.205E-01	1.322E+01	3.890E+01	-2.029E+01	-1.378E+00
4.378E-02	-1.116E-02	4.654E-01	5.002E-02	-4.484E-02	-1.776E-03
15	1.0	9.405E+01	8.432E+01	7.209E+05	
1.162E+00	-3.105E-01	1.048E+01	3.460E+01	-1.896E+01	-3.224E-01
4.072E-02	-1.089E-02	3.671E-01	4.492E-02	-4.219E-02	-4.184E-04
16	0.0	9.424E+01	8.463E+01	7.216E+05	
1.054E+00	-3.172E-01	8.594E+00	3.002E+01	-1.762E+01	5.997E-01
3.688E-02	-1.105E-02	3.001E-01	3.823E-02	-3.905E-02	7.755E-04
17	-1.0	9.414E+01	8.500E+01	7.230E+05	
9.912E-01	-2.886E-01	6.691E+00	2.655E+01	-1.652E+01	1.147E+00
3.471E-02	-1.010E-02	2.343E-01	2.315E-02	-3.672E-02	1.487E-03
18	-2.0	9.414E+01	8.525E+01	7.194E+05	
8.643E-01	-3.243E-01	5.163E+00	2.143E+01	-1.554E+01	1.605E+00
3.378E-02	-1.136E-02	1.810E-01	2.731E-02	-3.479E-02	2.083E-03
19	-3.0	9.401E+01	8.551E+01	7.178E+05	
9.832E-01	-3.517E-01	3.599E+00	1.748E+01	-1.523E+01	1.851E+00
3.455E-02	-1.236E-02	1.265E-01	2.276E-02	-3.420E-02	2.423E-03
20	-4.0	9.412E+01	8.576E+01	7.180E+05	
1.018E+00	-3.404E-01	2.176E+00	1.401E+01	-1.490E+01	2.191E+00
3.572E-02	-1.194E-02	7.633E-02	1.821E-02	-3.318E-02	2.847E-03
21	-5.0	9.439E+01	8.619E+01	7.191E+05	
1.079E+00	-4.195E-01	2.243E-02	9.181E+00	-1.475E+01	2.116E+00
3.766E-02	-1.444E-02	7.899E-04	1.187E-02	-3.270E-02	2.735E-03

Table C.15 Rotating WVT Alpha Sweep, 6 Blades, Run 1

WIND TUNNEL DATA ACQUISITION PROGRAM SUMMARY

TITLE: rotate2
AERO TARE FILE: official.ATRWEIGHT TARE FILE: rotate1.WTR
DATA FILE: rotate2.DAT DATE: 03-18-1997 TIME: 19:59:59
REF. AREA = 410.00 sq.in. REF. CHORD = 15.75 in. REF. SPAN = 27.00 in.
AR = 1.65 HMT = 0.00 in. VMT = 1.00 in.
FORCE BALANCE = 2 PRESSURE TRANSDUCER = 1 THERMISTOR = 1

RUN	ALPHA	VEL(fps)	TEMF(F)	RN	
FX-DRAG	FY-SIDEFORCE	FZ-Lift	MX-Roll	MY-Pitch	MZ-Yaw
CFX	CFY	CFZ	CMX	CMY	CMZ
1	15.0	9.354E+01	8.293E+01	7.203E+05	
5.125E+00	-8.604E-01	3.046E+01	7.654E+01	-4.164E+01	-1.734E+01
1.811E-01	-3.040E-02	1.076E+00	1.082E-01	-9.241E-02	-2.259E-02
2	14.0	9.344E+01	9.348E+01	7.182E+05	
4.622E+00	-8.406E-01	2.953E+01	7.708E+01	-3.854E+01	-1.622E+01
1.642E-01	-2.980E-02	1.047E+00	1.012E-01	-8.674E-02	-2.143E-02
3	13.0	9.332E+01	9.392E+01	7.162E+05	
4.076E+00	-8.162E-01	2.775E+01	7.557E+01	-2.497E+01	-1.477E+01
1.450E-01	-2.903E-02	9.871E-01	8.955E-02	-7.898E-02	-1.945E-02
4	12.0	9.366E+01	8.426E+01	7.181E+05	
3.874E+00	-7.956E-01	2.745E+01	7.894E+01	-3.318E+01	-1.379E+01
1.369E-01	-2.613E-02	9.699E-01	9.675E-02	-7.437E-02	-1.804E-02
5	11.0	9.349E+01	8.454E+01	7.161E+05	
3.571E+00	-7.014E-01	2.579E+01	7.690E+01	-3.132E+01	-1.279E+01
1.267E-01	-2.499E-02	9.147E-01	9.302E-02	-7.054E-02	-1.691E-02
6	10.0	9.372E+01	8.482E+01	7.173E+05	
3.179E+00	-6.649E-01	2.435E+01	6.970E+01	-2.886E+01	-1.076E+01
1.122E-01	-2.346E-02	8.597E-01	9.115E-02	-6.471E-02	-1.408E-02
7	9.0	9.359E+01	8.515E+01	7.154E+05	
2.723E+00	-6.429E-01	2.254E+01	6.581E+01	-2.759E+01	-9.556E+00
9.651E-02	-2.272E-02	7.987E-01	8.639E-02	-6.208E-02	-1.254E-02
8	8.0	9.372E+01	8.545E+01	7.157E+05	
2.502E+00	-5.946E-01	2.153E+01	6.284E+01	-2.635E+01	-7.574E+00
8.847E-02	-2.103E-02	7.614E-01	8.220E-02	-5.917E-02	-9.920E-03
9	7.0	9.370E+01	8.577E+01	7.149E+05	
2.314E+00	-5.286E-01	2.032E+01	5.986E+01	-2.547E+01	-6.445E+00
8.192E-02	-1.871E-02	7.191E-01	7.847E-02	-5.724E-02	-8.449E-03

Table C.15 Rotating WVT Alpha Sweep, 6 Blades, Run 1 (cont'd)

10	6.0	9.387E+01	9.599E+01	7.156E+05	
1.955E+00	-4.752E-01	1.774E+01	5.376E+01	-2.414E+01	-4.242E+00
6.897E-02	-1.677E-02	6.259E-01	7.025E-02	-5.409E-02	-5.543E-03
11	5.0	9.384E+01	8.621E+01	7.148E+05	
1.685E+00	-4.239E-01	1.557E+01	4.760E+01	-2.229E+01	-2.415E+00
5.951E-02	-1.497E-02	5.500E-01	6.227E-02	-5.000E-02	-3.160E-03
12	4.0	9.386E+01	9.675E+01	7.128E+05	
1.677E+00	-4.303E-01	1.551E+01	4.735E+01	-2.193E+01	-2.313E+00
5.927E-02	-1.521E-02	5.480E-01	6.197E-02	-4.921E-02	-2.027E-02
13	3.0	9.395E+01	9.693E+01	7.140E+05	
1.514E+00	-4.108E-01	1.413E+01	4.411E+01	-2.112E+01	-1.298E+00
5.349E-02	-1.449E-02	4.985E-01	5.764E-02	-4.732E-02	-1.695E-03
14	2.0	9.393E+01	8.718E+01	7.134E+05	
1.411E+00	-3.173E-01	1.017E+01	3.443E+01	-1.777E+01	3.964E-01
4.984E-02	-1.121E-02	3.591E-01	4.503E-02	-3.983E-02	5.184E-04
15	1.0	9.382E+01	8.736E+01	7.120E+05	
1.183E+00	-3.488E-01	9.963E+00	3.391E+01	-1.764E+01	1.040E+00
4.199E-02	-1.235E-02	3.492E-01	4.447E-02	-3.965E-02	1.364E-03
16	0.0	9.381E+01	8.757E+01	7.115E+05	
1.114E+00	-3.992E-01	8.595E+00	3.094E+01	-1.689E+01	1.374E+00
3.946E-02	-1.414E-02	3.045E-01	4.042E-02	-3.799E-02	1.813E-03
17	-1.0	9.371E+01	9.775E+01	7.102E+05	
1.043E+00	-3.814E-01	6.922E+00	2.650E+01	-1.581E+01	1.513E+00
3.704E-02	-1.355E-02	2.459E-01	3.494E-02	-3.564E-02	1.990E-03
18	-2.0	9.334E+01	9.791E+01	7.071E+05	
9.423E-01	-3.342E-01	5.396E+00	2.242E+01	-1.518E+01	1.749E+00
3.375E-02	-1.197E-02	1.933E-01	2.973E-02	-3.452E-02	2.319E-03
19	-3.0	9.342E+01	8.910E+01	7.074E+05	
1.121E+00	-4.523E-01	3.772E+00	1.821E+01	-1.475E+01	2.001E+00
4.009E-02	-1.617E-02	1.349E-01	2.411E-02	-3.348E-02	2.650E-03
20	-4.0	9.347E+01	8.828E+01	7.072E+05	
1.036E+00	-3.978E-01	2.179E+00	1.445E+01	-1.419E+01	2.077E+00
3.701E-02	-1.422E-02	7.788E-02	1.913E-02	-3.219E-02	2.749E-03
21	-5.0	9.314E+01	8.843E+01	7.044E+05	
1.039E+00	-3.930E-01	7.921E-01	1.094E+01	-1.415E+01	1.853E+00
3.741E-02	-1.415E-02	2.315E-02	1.459E-02	-3.234E-02	2.471E-03

Table C.16 Rotating WVT Alpha Sweep, 6 Blades, Run 2

WIND TUNNEL DATA ACQUISITION PROGRAM SUMMARY

TITLE: rotate3
AERO TARE FILE: official.ATRWEIGHT TARE FILE: rotate1.WTR
DATA FILE: rotate3.DAT DATE: 03-18-1997 TIME: 20:36:46
REF. AREA = 410.00 sq.in. REF. CHORD = 15.75 in. REF. SPAN = 27.00 in.
AR = 1.65 HMT = 0.00 in. VMT = 1.00 in.
FORCE BALANCE = 2 PRESSURE TRANSDUCER = 1 THERMISTOR = 1

RUN	ALPHA	VEL(fps)	TEMP(F)	RN	
FX-DRAG	FY-SIDEFORCE	FZ-Lift	MX-Roll	MY-Pitch	MZ-Yaw
CFX	CFY	CFZ	CMX	CMY	CMZ
1	15.0	9.404E+01	8.457E+01	7.202E+05	
5.011E+00	-9.162E-01	3.051E+01	7.668E+01	-4.122E+01	-1.721E+01
1.757E-01	-3.212E-02	1.070E+00	9.958E-02	-9.177E-02	-2.235E-02
2	14.	9.421E+01	8.543E+01	7.195E+05	
4.498E+00	-7.154E-01	2.974E+01	7.685E+01	-3.836E+01	-1.653E+01
1.574E-01	-2.504E-02	1.041E+00	9.960E-02	-9.522E-02	-2.181E-02
3	13.0	9.419E+01	8.612E+01	7.178E+05	
4.420E+00	-8.387E-01	2.965E+01	7.629E+01	-3.590E+01	-1.587E+01
1.549E-01	-2.939E-02	1.004E+00	9.902E-02	-7.989E-02	-2.059E-02
4	12.0	9.434E+01	8.644E+01	7.181E+05	
3.950E+00	-8.914E-01	2.762E+01	7.524E+01	-3.299E+01	-1.493E+01
1.391E-01	-3.116E-02	9.656E-01	9.743E-02	-7.323E-02	-1.940E-02
5	11.0	9.430E+01	8.672E+01	7.172E+05	
3.718E+00	-8.216E-01	2.619E+01	7.295E+01	-3.042E+01	-1.249E+01
1.302E-01	-2.975E-02	9.169E-01	9.458E-02	-6.805E-02	-1.619E-02
6	10.0	9.440E+01	8.705E+01	7.172E+05	
2.982E+00	-6.765E-01	2.462E+01	7.017E+01	-2.907E+01	-1.035E+01
1.042E-01	-2.365E-02	8.606E-01	9.084E-02	-6.452E-02	-1.340E-02
7	9.0	9.450E+01	8.735E+01	7.172E+05	
2.935E+00	-6.474E-01	2.310E+01	6.682E+01	-2.737E+01	-7.203E-01
1.02 E-01	-2.26 E-02	9.065E-01	8.629E-02	-6.066E-02	-1.271E-02
8	9.0	9.439E+01	8.757E+01	7.159E+05	
2.932E+00	-6.242E-01	2.183E+01	6.341E+01	-2.721E+01	-7.200E+00
9.911E-02	-2.185E-02	7.638E-01	8.218E-02	-5.045E-02	-9.465E-03
9	7.0	9.407E+01	8.795E+01	7.129E+05	
2.135E+00	-5.048E-01	1.960E+01	5.855E+01	-2.569E+01	-5.090E+00
7.527E-02	-1.779E-02	6.911E-01	7.644E-02	-5.749E-02	-6.545E-03

Table C.16 Rotating WVT Alpha Sweep, 6 Blades, Run 2 (cont'd)

10	6.0	9.423E+01	8.807E+01	7.135E+05	
1.885E+00	-4.979E-01	1.734E+01	5.221E+01	-2.364E+01	-3.563E+00
6.625E-02	-1.750E-02	6.095E-01	6.796E-02	-5.276E-02	-4.637E-03
11	5.0	9.439E+01	8.824E+01	7.142E+05	
1.647E+00	-4.138E-01	1.531E+01	4.697E+01	-2.193E+01	-1.994E+00
5.773E-02	-1.450E-02	5.367E-01	6.097E-02	-4.881E-02	-2.589E-03
12	4.0	9.432E+01	8.841E+01	7.134E+05	
1.503E+00	-4.303E-01	1.381E+01	4.218E+01	-2.076E+01	-1.194E+00
5.275E-02	-1.686E-02	4.848E-01	5.483E-02	-4.626E-02	-1.552E-03
13	3.0	9.431E+01	8.861E+01	7.129E+05	
1.366E+00	-4.310E-01	1.228E+01	3.942E+01	-1.946E+01	-3.294E-01
4.796E-02	-1.514E-02	4.314E-01	5.127E-02	-4.339E-02	-4.285E-04
14	2.0	9.440E+01	8.911E+01	7.123E+05	
1.365E+00	-3.967E-01	1.229E+01	3.945E+01	-1.950E+01	-1.341E-01
4.759E-02	-1.392E-02	4.310E-01	5.127E-02	-4.344E-02	-1.743E-04
15	1.0	9.414E+01	8.927E+01	7.100E+05	
1.107E+00	-2.570E-01	8.472E+00	3.016E+01	-1.694E+01	1.212E+00
3.909E-02	-1.260E-02	2.990E-01	3.942E-02	-3.796E-02	1.535E-03
16	0.0	9.416E+01	8.945E+01	7.098E+05	
1.082E+00	-4.006E-01	7.152E+00	2.622E+01	-1.605E+01	1.419E+00
3.819E-02	-1.414E-02	2.524E-01	3.427E-02	-3.594E-02	2.115E-03
17	-1.0	9.405E+01	8.959E+01	7.084E+05	
1.040E+00	-4.061E-01	6.449E+00	2.487E+01	-1.573E+01	1.698E+00
3.681E-02	-1.437E-02	2.222E-01	3.259E-02	-3.532E-02	2.225E-03
18	-2.0	9.368E+01	8.971E+01	7.055E+05	
1.022E+00	-3.942E-01	5.109E+00	2.145E+01	-1.509E+01	1.991E+00
3.644E-02	-1.371E-02	1.822E-01	2.823E-02	-3.417E-02	2.630E-03
19	-3.0	9.289E+01	8.984E+01	7.049E+05	
1.075E+00	-4.424E-01	3.644E+00	1.766E+01	-1.494E+01	2.291E+00
3.819E-02	-1.571E-02	1.294E-01	2.224E-02	-3.270E-02	3.014E-03
20	-4.0	9.362E+01	8.999E+01	7.044E+05	
1.030E+00	-4.105E-01	2.297E+00	1.460E+01	-1.451E+01	2.192E+00
3.679E-02	-1.467E-02	8.210E-02	1.932E-02	-3.292E-02	2.989E-03
21	-5.0	9.370E+01	9.010E+01	7.048E+05	
1.042E+00	-4.382E-01	9.255E-01	1.060E+01	-1.411E+01	1.937E+00
3.719E-02	-1.542E-02	2.945E-02	1.400E-02	-3.196E-02	2.559E-03

Table C.17 Rotating WVT Alpha Sweep, 6 Blades, Run 3

WIND TUNNEL DATA ACQUISITION PROGRAM SUMMARY

TITLE: rotate4
AERO TARE FILE: official.ATRWEIGHT TARE FILE: rotate1.WTR
DATA FILE: rotate4.DAT DATE: 03-18-1997 TIME: 21:17:49
REF. AREA = 410.00 sq.in. REF. CHORD = 15.75 in. REF. SPAN = 27.00 in.
AR = 1.65 HMT = 0.00 in. VMT = 1.00 in.
FORCE BALANCE = 2 PRESSURE TRANSDUCER = 1 THERMISTOR = 1

RUN	ALPHA	VEL(fps)	TEMP(F)	RN	
FX-DRAG	FY-SIDEFORCE	FZ-Lift	MX-Roll	MY-Pitch	MZ-Yaw
CFX	CFY	CFZ	CMX	CMY	CMZ
1	15.0	9.431E+01	8.539E+01	7.203E+05	
5.360E+00	-9.601E-01	3.079E+01	-7.683E+01	-4.138E+01	-1.901E+01
1.872E-01	-3.353E-02	1.075E+00	9.936E-02	-9.174E-02	-2.329E-02
2	14.0	9.412E+01	8.575E+01	7.181E+05	
4.618E+00	-7.935E-01	2.689E+01	7.441E+01	-3.899E+01	-1.622E+01
1.620E-01	-2.783E-02	1.049E+00	9.954E-02	-8.695E-02	-2.107E-02
3	13.0	9.414E+01	8.608E+01	7.174E+05	
4.30?E+00	-8.490E-01	2.854E+01	7.602E+01	-3.550E+01	-1.509E+01
1.513E-01	-2.976E-02	1.002E+00	9.890E-02	-7.931E-02	-1.961E-02
4	12.0	9.413E+01	8.620E+01	7.169E+05	
3.764E+00	-7.070E-01	2.715E+01	7.409E+01	-3.293E+01	-1.298E+01
1.321E-01	-2.482E-02	9.532E-01	9.634E-02	-7.340E-02	-1.682E-02
5	11.0	9.437E+01	8.660E+01	7.120E+05	
3.566E+00	-8.073E-01	2.602E+01	7.223E+01	-3.055E+01	-1.263E+01
1.246E-01	-2.821E-02	9.093E-01	9.361E-02	-6.779E-02	-1.634E-02
6	10.0	9.410E+01	8.697E+01	7.153E+05	
3.217E+00	-7.492E-01	2.491E+01	6.973E+01	-2.949E+01	-1.156E+01
1.131E-01	-2.635E-02	8.762E-01	9.083E-02	-6.586E-02	-1.504E-02
7	9.0	9.409E+01	8.718E+01	7.141E+05	
2.748E+00	-6.509E-01	2.292E+01	6.583E+01	-2.724E+01	-8.456E+00
9.699E-02	-2.295E-02	8.081E-01	8.596E-02	-6.093E-02	-1.114E-02
8	8.0	9.397E+01	8.742E+01	7.124E+05	
2.657E+00	-5.176E-01	2.227E+01	6.245E+01	-2.752E+01	-7.798E+00
9.394E-02	-2.184E-02	7.973E-01	8.179E-02	-5.191E-02	-1.021E-02
9	7.0	9.407E+01	8.765E+01	7.122E+05	
2.580E+00	-5.476E-01	2.067E+01	5.915E+01	-2.658E+01	-7.559E+00
9.093E-02	-1.930E-02	7.286E-01	7.952E-02	-5.947E-02	-9.966E-02

Table C.17 Rotating WVT Alpha Sweep, 6 Blades, Run 3 (cont'd)

10	6.0	9.382E+01	8.799E+01	7.106E+05	
1.889E+00	-4.876E-01	1.781E+01	5.171E+01	-2.363E+01	-3.753E+00
6.695E-02	-1.728E-02	6.314E-01	6.790E-02	-5.318E-02	-4.927E-03
11	5.0	9.286E+01	8.816E+01	7.105E+05	
1.634E+00	-4.467E-01	1.575E+01	4.689E+01	-2.226E+01	-2.349E+00
5.788E-02	-1.583E-02	5.578E-01	5.[illegible]E-02	-5.007E-02	-3.083E-03
12	4.0	9.406E+01	8.833E+01	7.116E+05	
1.429E+00	-4.137E-01	1.326E+01	4.098E+01	-2.024E+01	-6.276E-01
5.044E-02	-1.460E-02	4.679E-01	5.357E-02	-4.535E-02	-8.204E-04
13	3.0	9.412E+01	8.850E+01	7.117E+05	
1.427E+00	-4.341E-01	1.225E+01	4.108E+01	-2.019E+01	-5.839E-01
5.[illegible]E-02	-1.530E-02	4.671E-01	5.364E-02	-4.520E-02	-7.624E-04
14	2.0	9.404E+01	8.871E+01	7.[illegible]E+05	
1.353E+00	-4.169E-01	1.199E+01	3.910E+01	-1.[illegible]19E-01	1.[illegible]63E-01
4.782E-02	-1.472E-02	4.235E-01	4.985E-02	-4.305E-02	1.790E-04
15	1.0	9.410E+01	8.898E+01	7.106E+05	
1.198E+00	-4.108E-01	1.057E+01	3.450E+01	-1.825E+01	7.592E-01
4.227E-02	-1.450E-02	3.732E-01	4.509E-02	-4.090E-02	9.924E-04
16	0.0	9.399E+01	8.906E+01	7.094E+05	
9.839E-01	-4.772E-01	8.964E+00	3.022E+01	-1.637E+01	1.190E+00
3.492E-02	-1.689E-02	3.173E-01	3.[illegible]61E-02	-3.679E-02	1.560E-03
17	-1.0	9.396E+[illegible]	8.[illegible]33E+01	7.089E+05	
1.015E+00	-4.076E-01	6.492E+00	2.433E+01	-1.574E+01	1.771E+00
3.596E-02	-1.444E-02	2.300E-01	3.192E-02	-3.541E-02	2.323E-03
18	-2.0	9.391E+01	8.[illegible]37E+01	7.081E+05	
1.060E+00	-4.056E-01	5.651E+00	2.244E+01	-1.497E+01	1.816E+00
3.759E-02	-1.439E-02	2.004E-01	2.949E-02	-3.370E-02	2.398E-03
19	-3.0	9.367E+01	8.[illegible]2E+01	7.060E+05	
1.164E+00	-3.990E-01	3.730E+00	1.722E+01	-1.438E+01	2.180E+00
4.150E-02	-1.423E-02	1.330E-01	2.274E-02	-3.256E-02	2.879E-03
20	-4.0	9.355E+01	8.960E+01	7.048E+05	
1.049E+00	-4.674E-01	2.488E+00	1.448E+01	-1.438E+01	2.190E+00
3.749E-02	-1.671E-02	8.682E-02	1.917E-02	-3.265E-02	2.901E-03
21	-5.0	9.326E+01	9.975E+01	7.023E+05	
1.098E+00	-4.162E-01	8.836E-01	1.006E+01	-1.421E+01	1.902E+00
3.952E-02	-1.498E-02	3.180E-02	1.341E-02	-3.249E-02	2.543E-03